To the Graduate Council:

I am submitting herewith a thesis written by Hae Ryong Kwon entitled “Study of the Structure and Function of CXC Chemokine Receptor 2.” I have examined the final electronic copy of this thesis for form and content and recommend that it be accepted in partial fulfillment of the requirements for the degree of Master of Science, with a major in Life Sciences.

Tim Sparer

Major Professor

We have read this thesis
and recommend its acceptance:

Jeffrey Becker

Daniel Roberts

Accepted for the Council:

Carolyn R. Hodges

Vice Provost and Dean of the
Graduate School

(Original signatures are on file with official student records.)

STUDY OF THE STRUCTURE AND FUNCTION OF CXC CHEMOKINE RECEPTOR 2

A Thesis

Presented for the

Master of Science

Degree

The University of Tennessee, Knoxville

Hae Ryong Kwon

December 2010

DEDICATION

I dedicate this thesis to my fiancé, Hyejune Park who equally shared all the emotional burdens with me through this process. There is no doubt in my mind that without your love and prayer I could not have done this. Most importantly, I dedicate this thesis to my mother and sister, Kyung-Ja Choi and Sung-Ah Kwon for their endless patient and prayer. I also dedicate this thesis to my father, Hee-Dae Kwon, who has been resting in peace.

ACKNOWLEDGEMENT

I would like to thank my advisor, Dr. Timothy Sparer. He inspired me with his endless enthusiasm, knowledge and scientific insight. I am thankful that he was so patient and supportive during the times I was struggling with my projects. I am honored to have worked for you. I also would like to thank my committee members: Dr. Jeffrey Becker and Dr. Daniel Roberts for their critical reviews and guidance during my studies.

Furthermore, I also extend gratitude to Dr. Tom Masi for his advice and scientific insight for my research. Additionally, I would like to thank my Korean friends, Dr. Giljun Park, Dr. Hee-Jung Kim, and Dr. Jinho Heo for your player and support for me. I also thank Courtney Copeland and Holly Saito for all the fun in Dr. Sparer's lab.

ABSTRACT

It has been shown that the amino terminus and second extracellular loop (EC2) of CXCR2 are crucial for ligand binding and receptor activation. The lack of an ionic lock motif in the third intracellular loop of CXCR2 focuses an investigation of the mechanism by which these two extracellular regions contribute to receptor recognition and activation.

The first objective of this investigation was to predict the structure of CXCR2 based on known structures of crystallized GPCRs. Rhodopsin, β_2-adrenergic receptor, CXCR4 were used for homology modeling of CXCR2 structure. Highly conserved motifs found in sequence alignments of the template GPCRs were helpful to generate CXCR2 models. We also studied solvent accessibility of residues in the EC2 of CXCR2 in the inactive state. Most of the residues in the EC2 were found to be solvent accessible in the inactive state, suggesting the residues might be involved in ligand recognition.

Second, we studied the role of charged residues in the EC2 of CXCR2 in ligand binding and receptor activation using constitutively active mutants (CAM) of CXCR2, D9K and D9R. Combinatorial mutations consisting of the CAM in the amino terminus and single mutations of charged residues in the EC2 were generated to study two concepts including “attraction” and “repulsion” models. The mutant receptors were used to test their effects on cell surface expression, ligand binding, receptor activation through PLC-β3, and cellular transformation.

All the mutations in the repulsion model result in CXCR2 receptors that are unable to bind ligand, suggesting that each of the Arg residues in the EC2 are important for ligand recognition. Interestingly, mutations in the attraction model partially inhibited receptor activation by the CAM D9K, suggesting that Glu198 and Asp199 residues in the EC2 are associated with receptor activation. Furthermore, a novel CAM, E198A/D199A, was identified in this study. These negatively charged residues are very close to a conserved disulfide bond linking the EC2 and the third transmembrane.

In this sense, these current discoveries concerning the structural basis of CXCR2 and interdisciplinary approaches would provide new insights to investigate unknown mechanisms of interaction with its cognate ligands and receptor activation.

Table of Contents

PART I GENERAL INTRODUCTION 1

Chapter 1 G protein-coupled receptors 2

An overview 2

Classification of GPCRs 3

Tertiary structure of GPCRs 6

Ligand binding and receptor activation 13

Signal transduction of GPCRs 14

Chapter 2 CXC Chemokine Receptor 2 (CXCR2) and Cognate Chemokines 21

Chemokines and cognate chemokine receptors 21

Interaction of CXCR2 and its cognate chemokines 23

Receptor activation and signal transduction of CXCR2 25

Statement of research aims 31

PART II PREDICTION OF THE TERTIARY STRUCTURE OF CXCR2 AND STUDY OF THE CONFORMATION OF THE SECOND EXTRACELLULAR LOOP OF THE RECEPTOR IN AN INACTIVE STATE 33

Chapter 1 Abstract 34

Chapter 2 Introduction 36

Chapter 3 Materials and Methods 39

Cell line and medium 39

Cysteine-scanning mutagenesis 39

Expression of the CXCR2 receptor in HEK293 cells 40

MTSEA-biotin labeling and flow cytometry analysis 40

Homology modeling of human CXCR2 41
Prediction of secondary structure of GPCRs 42
Chapter 4 Results 44
Structural similarity and differences between homology modeled CXCR2 and crystal structures of GPCRs 44
Secondary structure of the second extracellular loop of CXCR2 54
Solvent accessibility of residues on the second extracellular loop of CXCR2 in the inactive state 58
Chapter 5 Discussion 61
PART III INVOLVEMENT OF THE SECOND EXTRACELLULAR LOOP OF CXCR2 IN LIGAND RECOGNITION AND RECEPTOR ACTIVATION 65
Chapter 1 Abstract 66
Chapter 2 Introduction 68
Chapter 3 Materials and Methods 74
Cell lines and media 74
Site-directed mutagenesis and transfection 74
Ligand binding assay 75
Immunostaining of phospho-PLC-β3 75
Loss of contact inhibition (foci formation) assay 76
Chapter 4 Results 77
Charged residues in the second extracellular loop of CXCR2 are required for ligand recognition 77
Involvement of the amino terminus and second extracellular loop of CXCR2 in ligand recognition 78

Constitutively inactive mutants CXCR2 induced by charge-reversal complementary mutations (derived from repulsion model) 80

Negatively charged residues in EC2 of CXCR2 are highly associated with receptor activation of CXCR2 (derived from attraction model) 81

A novel constitutively active mutant with double alanine mutations in CXCR2 82

Chapter 5 Discussion 87

PART IV CONCLUSIONS 91

REFERENCES 96

VITA 107

LIST OF TABLES

Table 1. GPCR as drug targets.....5

Table 2. Chemokine receptor and their cognate chemokine families in humans 22

Table 3. Primers for cysteine-scanning mutagenesis on different regions of CXCR2 43

Table 4. CXCL8-binding and surface expression of wild-type CXCR2 and mutant receptors.....79

LIST OF FIGURES

Figure 1. Comparison of GPCR structures. 10

Figure 2. Crystal structure of the chemokine receptor CXCR4 and its structural similarity with other crystal GPCRs. 12

Figure 3. Molecular model of the M_3 muscarinic acetylcholine receptor (M3R)-$G\alpha_q$ complex. 15

Figure 4. Diversity of G-protein-coupled receptor signaling. 19

Figure 5. Characterized IL-8 signaling pathways. 27

Figure 6. Computational modeling of the EC2 of rhodopsin, CXCR2, CXCR1, and the receptor mutants $B_{D199V}A$, B_{D199N}, and $A_{V190D}B$. 30

Figure 7. Sequence alignment of CXCR2 and bovine rhodopsin. 46

Figure 8. Sequence alignment of CXCR2 and β_2AR. 47

Figure 9. Sequence alignment of CXCR2 and CXCR4. 48

Figure 10. Homology modeled CXCR2 structures based on the crystal structures of bovine rhodopsin, human β_2AR, and human CXCR4. 49

Figure 11. Superposition and structural similarity of homology modeled CXCR2 structures with other GPCRs. 50

Figure 12. Prediction of ligand binding sites in β2AR-based and CXCR4-based CXCR2 structure. 52

Figure 13. Prediction of secondary structure of the second extracellular loop of CXCR2 56

Figure 14. Solvent accessibility maps of the single cysteine mutants of CXCR2. 60
Figure 15. Models of receptor activation of CXCR2 73
Figure 16. Phosphorylation of PLC-β3 in wild-type and mutant CXCR2 receptors. 83
Figure 17. Foci formation assay with NIH3T3 transfectants stably expressing charge-reversal complementary mutant receptors derived from the repulsion model. 84
Figure 18. Foci formation assay with NIH3T3 transfectants stably expressing combinatorial mutant receptors derived from the attraction model. 85
Figure 19. Foci formation assay in the presence of inhibitors of intracellular signaling. 86

PART I

GENERAL INTRODUCTION

Chapter 1 G protein-coupled receptors

An overview

G protein-coupled receptors (GPCRs) are the largest family of membrane-bound receptors found in eukaryotes including yeast and mammals. There are 1,000 genes in the human genome that encode GPCRs and comprise diverse groups of receptors for ligands such as hormones, neurotransmitters, chemokines, and calcium ions. GPCRs can be sensory receptors for various odorants, bitter and sweet taste, and photons of light (*1, 2*). Furthermore, GPCRs regulate a variety of biological pathways inside cells and are an ideal target for the development of effective drugs to treat human conditons/disorders (Table 1) (*3*).

The main structural feature of GPCRs is the conservation of three intracellular and extracellular loops connecting seven transmembrane domains. Localization of GPCRs on the cell surface allows for the transfer of extracellular stimuli into intracellular biochemical responses. Upon ligand binding, GPCRs undergo conformational changes to activate intracellular signaling cascades (*4*). The change initiates the activation of heterotrimeric G proteins. This protein complex includes G alpha (Gα), G beta (Gβ), and G gamma (Gγ) subunits and upon activation leads to the release of guanosine diphosphate (GDP) and the concomitant binding of guanosine triphosphate (GTP). Upon exchange, the Gα protein disassembles from the Gβγ dimer. The released G protein can regulate

the stimulation or inhibition of secondary messenger molecules including adenylate cyclase, guanylyl cyclase, phospholipases, or ion channels. Phosphorylation of the cytoplasmic domains of GPCRs by GPCR kinases and arrestins are involved in receptor desensitization and internalization (*5, 6*).

Resolution of GPCR structures has been solved in the past few years. Although there are many limitations to structural resolution such as heterologous expression systems, purification of GPCRs, and their large molecular size, five crystal structures of GPCRs have been successfully elucidated including bovine rhodopsin, human β_2 adrenergic (β_2AR), avian β_1AR, human A_{2A} adenosine receptor, opsin, and human CXC chemokine receptor 4 (CXCR4) (*7, 8*). Furthermore, structural information derived from mutagenesis, biochemical, biophysical, and computational modeling approaches have added to our understanding of the conformational changes in GPCRs (*2, 9-11*). These studies have provided new insights into GPCR structure and activation.

Classification of GPCRs

All GPCRs share the same structural basis of seven transmembranes connected via three extracellular and intracellular loops, an amino terminus, and carboxy terminus. However, few sequences are conserved among the different GPCRs, which are commonly classified into six families (http://gpcr.org/).

The families of class A, B, and C are grouped on the basis of sequence similarity (*2*). Class A is the largest family of GPCRs and is considered

rhodopsin-like receptors. This family comprises receptors for various ligands including peptides and small molecules (*12*). Distinct regions were identified as highly conserved residues such as the (D/E)R(Y/W) motif at the bottom of transmembrane (TM) 3 and the NPXXY motif in TM7 that play critical roles in receptor structure and function (*13-15*). Class B, also called secretin-like receptors, is composed of the receptors for gastrointestinal peptide hormone family, corticotropin-releasing hormone, calcitonin and parathyroid hormone (*2*). In this class of receptors, the amino terminus and extracellular loops are highly associated with ligand binding, whereas there is no evidence for the involvement of transmembrane helices. However this is not based on the crystal structure as no class B receptor structures have been solved to date (*16*). This family of receptors is characterized by forming tight network structures of disulfide bonds with several cysteine residues localized on the amino terminus. Class C is known as metabotropic glutamate receptors. Their very large amino terminus (300-600 amino acids) is involved in ligand recognition. Two distinct lobes of the amino terminus of these receptors are used to bind ligand in a “Venus flytrap” manner (*1, 17*). Class D and E are minor families containing STE2 and STE3 yeast pheromone receptors, respectively. Class F is composed of cyclic adenosine monophosphate (cAMP) and archaebacterial opsin receptors.

Table 1. GPCR as drug targets.

Receptor	Drugs and some key indications
AT_1 angiotensin II receptor	Antagonists (e.g. losartan) in the treatment of essential hypertension or congestive heart failure
α_{1A}-adrenergic receptor	Antagonists (e.g. tamsulosin) to treat micturition (bladder emptying) disorders associated with enlarged prostate glands
β_1-adrenergic receptor	Antagonists (e.g. propranolol, atenolol, metoprolol, carvedilol) to treat essential hypertension or congestive heart failure
β_2-adrenergic receptor	Agonists (e.g. terbutaline, salbutamol, formoterol, salmeterol) for treatment of obstructive airway disease or premature labor
D_2 dopamine receptor	Antagonists (e.g. haloperidol and clozapine) to treat schizophrenia Agonists (e.g. levodopa) for the treatment of Parkinson's disease
D_3 dopamine receptor	Antagonists (e.g. haloperidol) in the treatment of schizophrenia
5-HT_{2A} receptor	Antagonists (e.g. clozapine) to treat schizophrenia Indirect agonists (e.g. fluvoxamine) for the treatment of depression
5-HT_{2C} receptor	Antagonists (e.g. clozapine) to treat schizophrenia

Table modified from Insel et al. (*3*))

Tertiary structure of GPCRs

Studies focusing on the structure of GPCRs are very important to understand their function and for drug development against GPCR mutants that cause disease (*7, 18*). During the past several years, remarkable progress has been made in the structural biology of GPCRs. This is due to specialized methods to resolve their protein structures including X-ray crystallography, electron microscopy or diffraction, nuclear magnetic resonance (NMR) spectroscopy, and molecular modeling (*14, 19-21*). Currently, Six GPCRs in the inactive state (in the absence of ligand) have been crystallized including human β_2 adrenergic receptor (β_2AR), avian β_1AR, human A_{2A} adenosine receptor, CXC chemokine receptor 4 (CXCR4), as well as bovine rhodopsin and opsin (*8, 13, 22-26*). The high-resolution structural analysis has provided the molecular basis to address the structure and function of GPCRs (*7*) (Fig. 1). In order to obtain stability and conformational homogeneity for GPCR crystallization, various modifications have been tried with antibodies, fusion proteins, agonists, stabilizing mutants, and special crystallization environments.

The first GPCR crystallized was bovine rhodopsin, composed of the protein opsin and 11-*cis*-retinal (*13*). Fifteen bovine rhopdosins (or opsins) have now been crystallized and published (*14*). There are significant structural differences in the third intracellular loop (IC3) between the crystal structures, suggesting that this part is important for movement in order for transducin (or $G\alpha_q$ for squid rhodopsin) to couple to the receptor. Although there is the conservation

of common structural features of the GPCRs, bovine rhodopsin has irregular transmembrane helices, especially with respect to bending at Pro residues and kinking around Gly-Gly residues (*13, 27*). The presence of Pro267, a highly conserved residue in TM6, causes a significant distortion suggesting that the proline may function as a toggle switch to transfer motions from the extracellular surface to the cytoplasmic surface (*28*). The proline in other GPCRs like β_2AR may also be a crucial residue for receptor function. Rhodopsin and β_2AR have a conserved Pro in TM6 that is important for receptor activation (*29, 30*). Two adjacent Gly residues (Gly89 and Gly90 of rhodopsin) that are conserved in many GPCRs induce a π-helix (*i*+5→*i* hydrogen bonding) in TM2 (*31, 32*). The amino terminus and three extracellular loops are moved towards each other to make a compact structure forming the chromophore-binding pocket (*22, 33*). In the amino terminus of rhodopsin, post-translational modifications were found on several distinct residues including glycosylations of Asn2 and Asn15 and acetylation of Met1 (*34, 35*). Thus, pairs of β-sheets almost parallel to the membrane are localized on the amino terminus.

The crystal structures of class A GPCRs show a highly conserved disulfide bond linking the Cys residue on the second extracellular loop (EC2) between TM4 and TM5 and a Cys on the front region of TM3. Rhodopsin has two short β-sheets associated with the ligand-binding pocket on its EC2 (*13*). The EC2 of rhodopsin, but not EC1 and EC3, is folded deeply into the helix bundles, whereas the EC2 of β_2AR and β_1AR are exposed to the solvent and contain a

short α-helix structure tied by intra- and inter-disulfide bonds to create a cavity for ligand binding (*22, 24*). The EC2 is crucial for the formation of the ligand binding pocket has also been observed in other class B GPCRs including complement factor 5a receptor (C5aR) as well as other class A GPCRs (*36, 37*).

One of highly conserved motifs, (D/E)R(Y/W), is positioned in the second intracellular loop (IC2) of all the crystal structures. The tripeptide motif on the boundary of TM3 forms an 'ionic lock' with Glu on TM6 and has been shown that this linkage is crucial for maintaining the receptors in an inactive state (*38*). The ionic lock was observed on the crystal structure of rhodopsin, but not β_2AR and β_1AR. However, the fact that mutation of the ionic lock in β_2AR increases constitutive activity supports the formation of the linkage in the receptor (*39*). Disruption of the ionic lock in β_2AR is accomplished by the contact of the Arg (R) residue of the (D/E)R(Y/W) motif and T4 lysozyme fused to IC3 (*22, 40*). On the other hand, it is unclear why an inverse agonist bound to β_1AR showed disruption of the linkage (*24*). Interestingly, in rhodopsin, the tripeptide Val137-Val138-Val139 is located next to the highly conserved (D/E)R(Y/W) motif and might keep rhodopsin in the inactive state (*33*).

The crystal structures of rhodopsin and β_2AR have been used to create homology models for other GPCRs that have not been solved (*32, 41, 42*). These model predictions are based on the fact that GPCRs have highly conserved motifs and structural conservation, even though their primary sequences are

quite divergent (*43*). One study compared all the transmembrane proteins of the different GPCRs to one another (*14*).

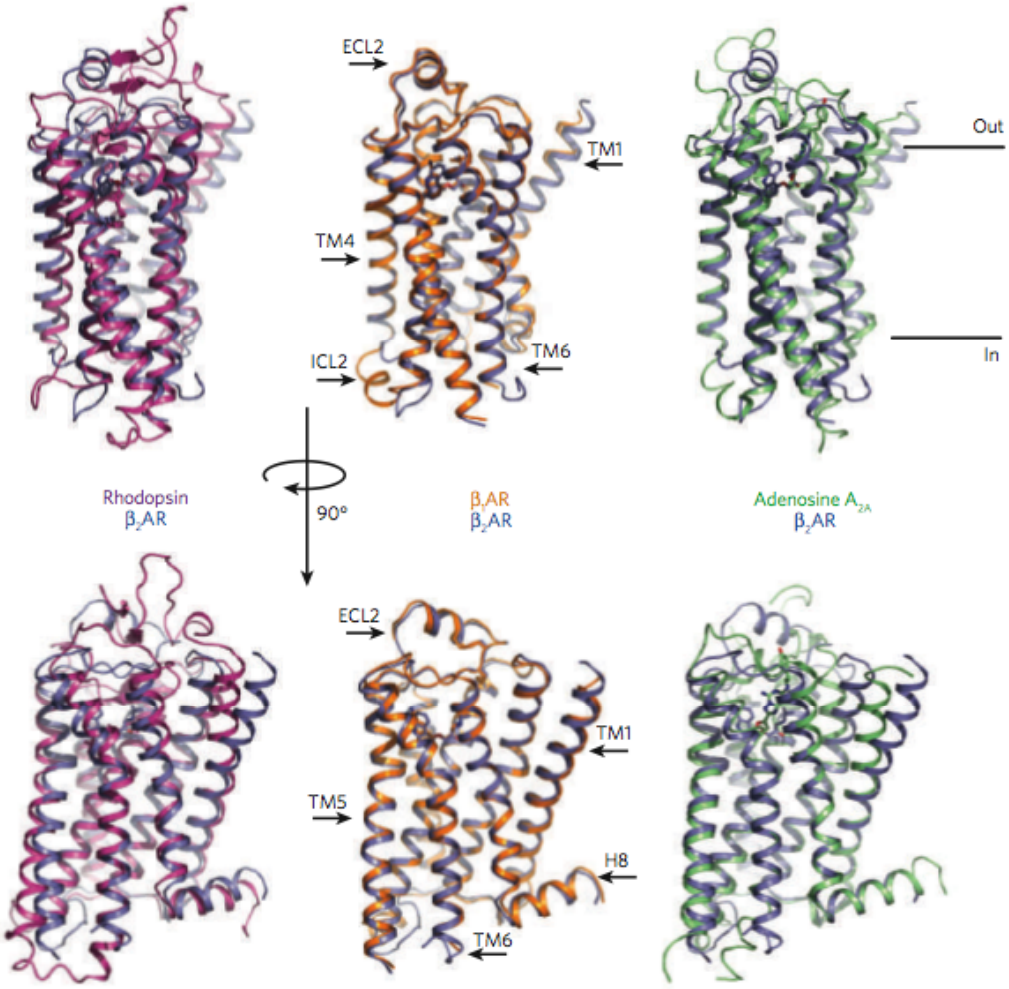

Figure 1. Comparison of GPCR structures.

Bovine rhodopsin (purple), avian β_1AR (orange) and human A_{2A} adenosine receptor (green) are each superimposed on the human β_2AR structure (blue). The extracellular loop2 (EC2), intracellular loop (IC2), cytoplasmic helix 8 (H8) and transmembrane (TM) segments are labeled on one of the structures. Figure from Rosenbaum et al (*7*).

This study showed that all the rhodopsin structures superposed well, except for squid rhodopsin. Interestingly, the β_2AR and β_1AR superpose poorly on each other, whereas they fit quite well with rhodopsin. Additional studies using homology modeling suggests which crystallized GPCR is a better template for predicting the structures of the other uncrystallized GPCRs (*44*). This study showed that current crystal structures of GPCRs are not sufficient for homology modeling and drug design, because only 3 subfamilies including rhodopsin, adenosine, and adrenergic receptor have crystal structures. However, it was suggested that multiple-template homology modeling using all crystallized GPCR structures could improve the current templates for dynamic simulations like ligand docking.

Recently the crystal structure of a chemokine receptor that belongs to class A GPCRs family was resolved (*8*) (Fig. 2). The CXCR4 structure provides new insights into its interaction with ligand, CXCL12, but also with human immunodeficiency virus (HIV) glycoprotein gp120. Furthermore, this new structures will aid in modeling the structure and function of other chemokine receptors, even though each has distinct characteristics in its interaction with their cognate ligands.

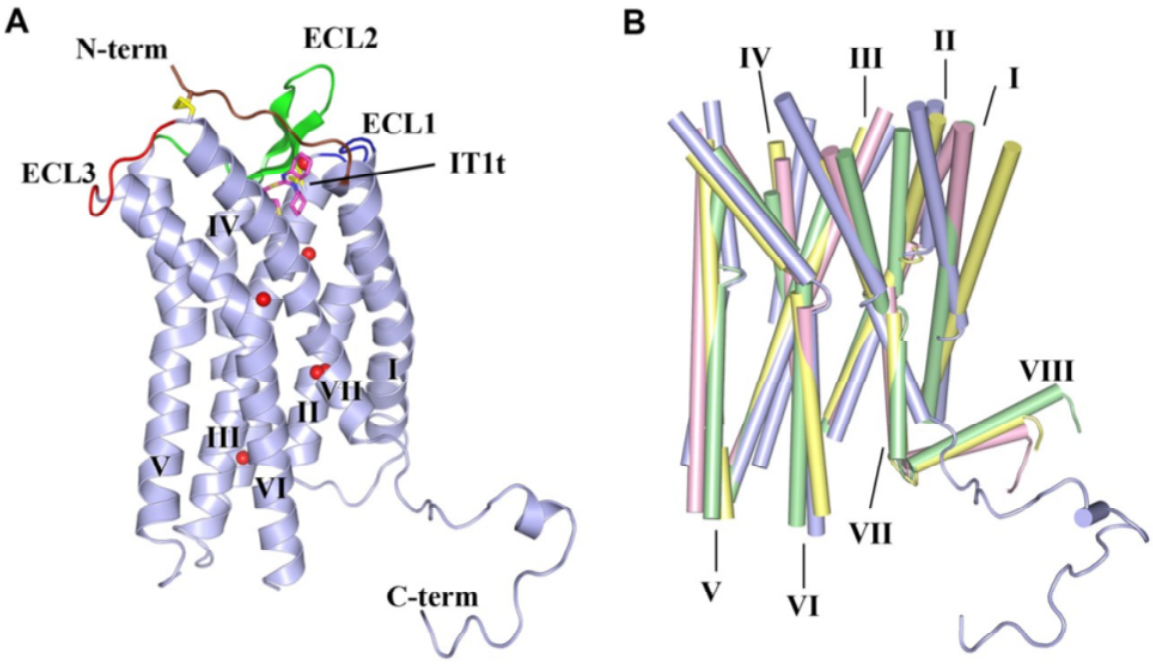

Figure 2. Crystal structure of the chemokine receptor CXCR4 and its structural similarity with other crystal GPCRs.

Overall fold of the CXCR4-IT1t complex and comparison with other GPCR structures. (**A**) Overall fold of the CXCR4-2–IT1t. The receptor is colored blue. The amino terminus, first extracellular loop (EC1), EC2, and EC3 are highlighted in brown, blue, green, and red, respectively. The compound IT1t is shown in a magenta stick representation. The disulfide bonds are yellow. Conserved water molecules are shown as red spheres. (**B**) Comparison of transmembrane helices for CXCR4 (blue); β_2AR (PDB ID: 2RH1; yellow); A_{2A}AR (PDB ID: 3EML; green); and rhodopsin (PDB ID: 1U19; pink). Figure from Wu et al (*8*).

Ligand binding and receptor activation

Numerous studies of GPCRs aim to understanding the mechanism of ligand binding and receptor activation using biological, biochemical, and biophysical approaches (*45*). Various methods were used to identify the binding domains including site-directed and random mutagenesis, receptor chimeras, competition with synthesized peptides, and addition of probes. For bioinformatical approaches, this experimental data was applied to improve ligand-docking model (*46*).

Despite the variation in the mechanism of ligand binding, there are some similarities between the interaction of ligands and receptors. Small ligands (photon, biogenic amines and nucleosides) bind within transmembrane regions, whereas large molecules like peptides and proteins bind to extracellular loops (*45*). Peptide ligands show direct interaction of both amino-terminus and extracellular loops (*4*). However, some peptide ligands can interact with transmembrane domains as well as extracellular loops (*47*).

Initially, a simple model was used to explain how agonist binding induces a conformational change. The model was called the “two-state model” with an equilibrium between the inactive conformation (R) and active conformation (R*) (*48*). However, more recently crystal structures and biophysical studies led to the creation of new model known as the “multi-state” model (*7, 49*). Upon ligand binding, GPCRs become activated and undergo a conformational change, resulting in G protein activation. The conformational changes leads to the

rearrangement of the interhelical interactions on transmembranes including TM3, TM6 and TM7. The extracellular domains and the flexible third intracellular loop are involved in this rearrangement. The recognition sites such as the second intracellular loop (IC2) including (D/E)R(Y/W) motif close to TM3 are exposed to activate signaling partners including heterotrimeric G proteins and arrestins (*50, 51*) (Fig. 3). A highly conserved Pro residue on TM6 allows the rigid transmembrane helices to move as part of the conformational change (*29*).

Post-translational modifications on cytoplasmic domains of GPCRs are involved in receptor desensitization and internalization (*5, 6*). GPCR kinases and arrestins are involved in these modifications. In the cases of rhodopsin and β_2AR, there are residues for different post-translational modifications on their cytoplasmic loops, including palmitoylation at Cys, phosphorylation at Ser, and ubiquitinylation at Lys (*35, 52*).

Signal transduction of GPCRs

The cytoplasmic domains of GPCRs interact with proteins that are responsible for initiating intracellular signaling cascades (*53*) (Fig. 4). Heterotrimeric G proteins are predominantly used as the first intracellular modulators of GPCR signaling (*54*). To date, 23 Gα protein subtypes have been identified and are classified into 4 different groups such as $G\alpha_{i/o}$, $G\alpha_s$, $G\alpha_{q/11}$, and $G\alpha_{12/13}$. There are also 6 Gβ and 11 Gγ proteins (*55*).

Figure 3. Molecular model of the M_3 muscarinic acetylcholine receptor (M3R)-Gα_q complex.

(a) Side view of the complex between the inactive state of the M3R and the Gq heterotrimer. The M3R is shown in red, Gα_q in yellow, Gβ in gray and Gγ in pink. **(b)** Enlargement of the M3R-Gαq interface. M3R residues are shown in blue, Gα_q residues in orange. The interaction between R31C in the αN helix of Gα_q and I173C in the i2 loop of the M3R provided a key contact site for the docking process. The C terminus of Gα_q points toward the intracellular core of the receptor, between the IC2 and helix 8 (H8). The finding that the C-terminal residues of Gα_q can interact with multiple M3R residues in the IC2 loop (leu173 and Arg176) and the N-terminal portion of H8 (Thr549, Thr552 and Thr556) suggests that the extreme C terminus of Gα_q is conformationally highly flexible. Agonist-induced M3R activation promotes the formation of cross-links between the extreme C terminus of Gα_q and the cytoplasmic end of TM6 (A488C) (gray arrow) and the N-terminal segment of H8 (T549C and T552C) of the M3R. Moreover, in the activated state of the receptor, a residue in the α4-β6 loop of Gα_q (D321C) could be cross-linked to the N-terminal portion of H8 (K548C, T549C and T552C) (gray arrow). Figure from Hu et al (*51*).

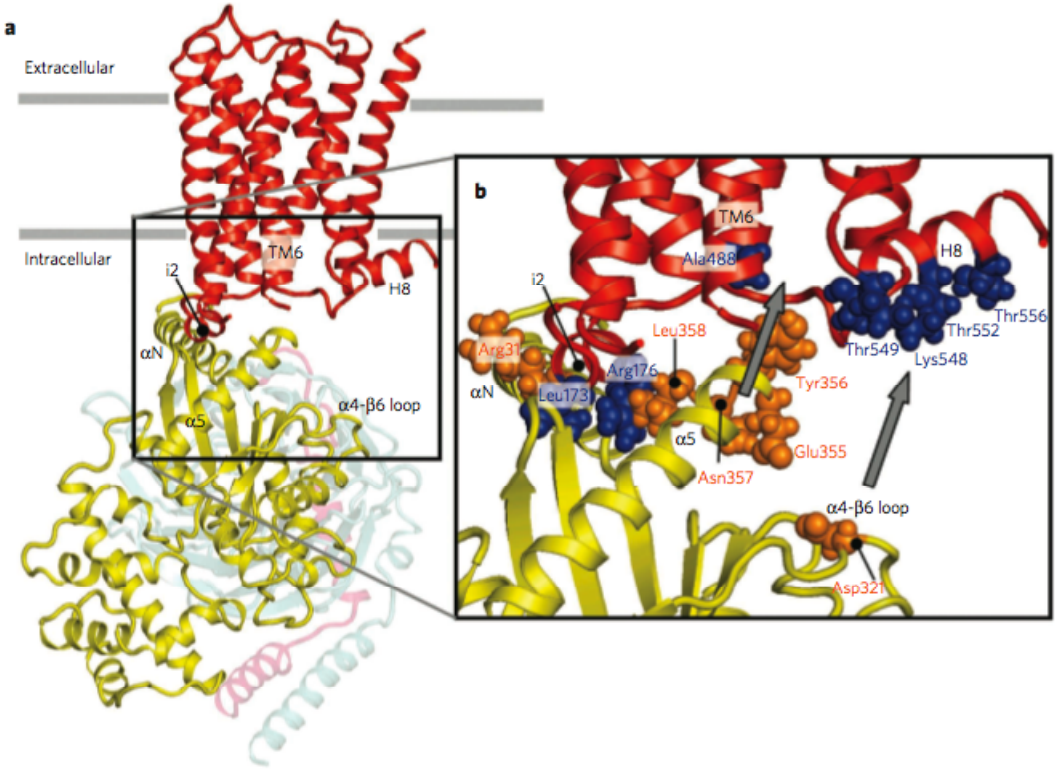
a
Extracellular
Intracellular
TM6
i2
H8
αN
α5
α4-β6 loop
b
TM6
Ala488
H8
i2
Leu358
Thr556
Arg31
Thr552
Thr549
Lys548
Arg176
Tyr356
αN
Leu173
α5
Glu355
Asn357
α4-β6 loop
Asp321

The expression pattern and combination of the heterotrimeric G proteins is cell type-dependent, indicating that GPCRs can interact with certain G proteins that are available in a given cell or localize closely to the receptors. Although it has been shown that second intracellular loop (IC2), IC3, and cytoplasmic terminus function as key regions for interaction with G protein coupling, no consensus motif has been identified (*56*).

Activation of the three G proteins leads to exchange of guanosine diphosphate (GDP) and guanosine triphosphate (GTP), followed by dissociation of Gα protein and Gβγ dimer. The released G proteins can regulate the stimulation or inhibition of secondary messenger molecules including adenylate cyclase, guanylyl cyclase, phospholipases, or ion channels.

Each family of G proteins has distinct characteristics (*2*). The $G\alpha_s$ family functions as a stimulator of adenylyl cyclase to increase cyclic adenosine monophosphate (cAMP) levels. Whereas, $G\alpha_{i/o}$ proteins play a role in the inactivation of adenylyl cyclase, resulting in a decrease of cAMP levels. Furthermore, almost all the proteins that belong to $G\alpha_{i/o}$ family are pertussis toxin-sensitive (PTX). $G\alpha_{q/11}$ including $G\alpha_{14}$, $G\alpha_{15}$, and $G\alpha_{16}$ can bind phospholipases C-β (PLC-β) (*57*). Proteins of the $G\alpha_{12/13}$ family are ubituitously expressed and localized (*58*). This family can activate small G proteins (Rho and Ras family), Src family tyrosine kinase, and phospholipase D (PLD). Interestingly, when $G\alpha_{12/13}$ mutants are in a constitutively active form, cellular transformation is induced in a Rho signaling-dependent manner (*59*). Gβ and Gγ proteins have

been shown to function as a heterodimer. This complex induces adenylyl cyclase, PLC-β, and phosphoinositide-3 kinase (PI3K) (*60, 61*).

Agonist-occupied GPCRs induce not only signal transduction cascades but also activation of various intracellular regulatory molecules. The G protein-coupled receptor kinases (GRKs) are serine/threonine kinases. GRKs catalyze phosphorylation of GPCRs and recruit arrestins to the phosphorylated GPCR for receptor desensitization and internalization (*62, 63*). After activation, the regulators of G protein signaling (RGS) proteins are used to return the GTP-bound Gα proteins to their basal state (Gα) via GTP hydrolysis. This results in the reassociation of the heterotrimeric G proteins and inactivation of the GPCR (*64*). Interestingly, arrestins function not only in GPCR desensitization and internalization but also as a G protein-independent signal transducer (*65, 66*).

Figure 4. Diversity of G-protein-coupled receptor signaling.

Various ligands use GPCRs to stimulate membrane, cytoplasmic and nuclear targets. GPCRs interact with heterotrimeric G proteins composed of α, β and γ subunits that are GDP bound in the resting state. Agonist binding triggers a conformational change in the receptor, which catalyses the dissociation of GDP from the α subunit followed by GTP-binding to Gα and the dissociation of Gα from Gβγ subunits. The α subunits of G proteins are divided into four subfamilies: $G\alpha_s$, $G\alpha_i$, $G\alpha_q$ and $G\alpha_{12}$, and a single GPCR can couple to either one or more families of Gα proteins. Each G protein activates several downstream effectors. Typically $G\alpha_s$ stimulates adenylyl cyclase and increases levels of cyclic AMP (cAMP), whereas $G\alpha_i$ inhibits adenylyl cyclase and lowers cAMP levels, and members of the Gαq family bind to and activate phospholipase C (PLC), which cleaves phosphatidylinositol bisphosphate (PIP2) into diacylglycerol and inositol triphosphate (IP3). The Gβ subunits and Gγ subunits function as a dimer to activate many signaling molecules, including phospholipases, ion channels and lipid kinases. Besides the regulation of these classical second-messenger generating systems, Gβγ subunits and Gα subunits such as $G\alpha_{12}$ and $G\alpha_q$ can also control the activity of key intracellular signal-transducing molecules, including small GTP-binding proteins of the Ras and Rho families and members of the mitogen-activated protein kinase (MAPK) family of serine-threonine kinases, including extracellular signal-regulated kinase (ERK), c-jun N-terminal kinase (JNK), p38 and ERK5, through an intricate network of signaling events that has yet to be fully elucidated. Ultimately, the integration of the functional activity of the G-protein-regulated signaling networks controls many cellular functions and the aberrant activity of G proteins and their downstream target molecules can contribute to cancer progression and metastasis. 5-HT, 5-hydroxytryptamine; ECM, extracellular matrix; GABA, gamma-aminobutyric acid; GEF, guanine nucleotide exchange factor; GRK, G protein receptor kinase; LPA, lysophosphatidic acid; PI3K, phophatidylinositol 3- kninase; PKA and PKC, protein kinase A and C; S1P sphingosine-1-phosphate. Figure from Dorsam and Gutkind (*53*).

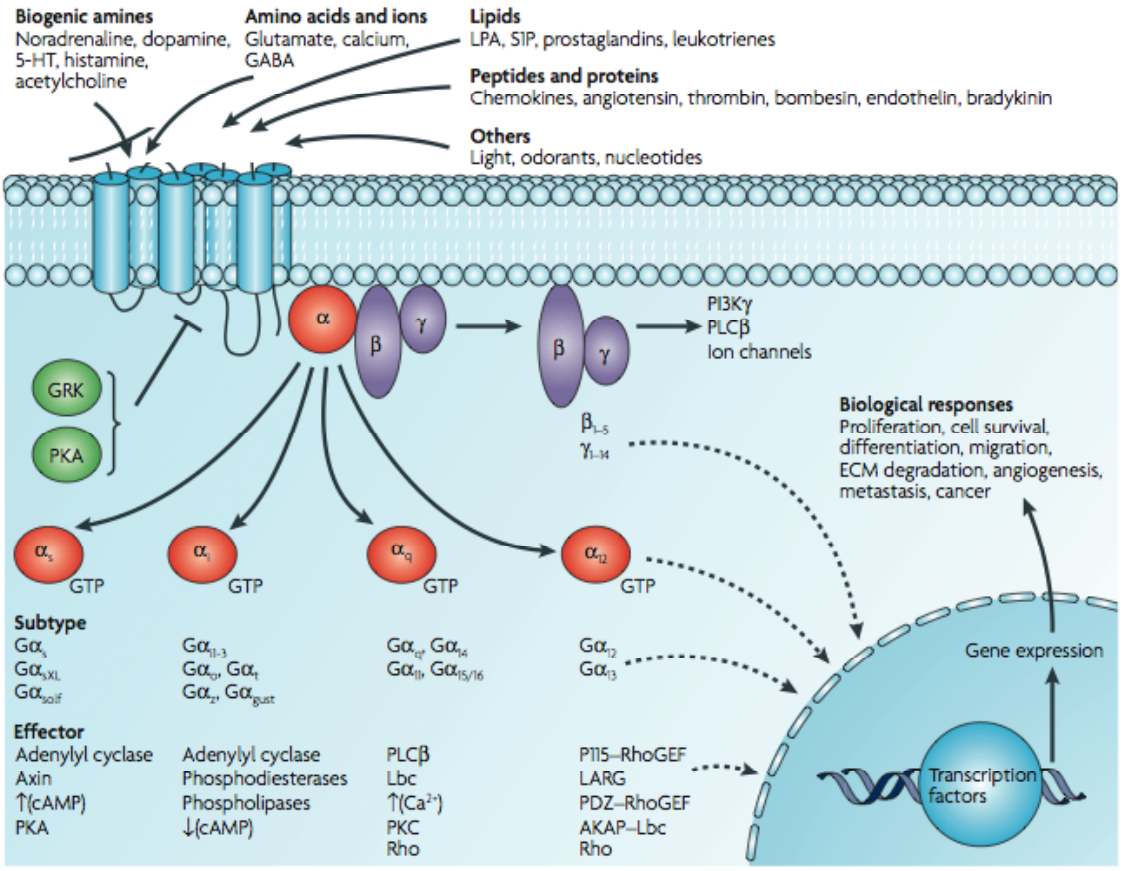
Biogenic amines
Noradrenaline, dopamine, 5-HT, histamine, acetylcholine
Amino acids and ions
Glutamate, calcium, GABA
Lipids
LPA, S1P, prostaglandins, leukotrienes
Peptides and proteins
Chemokines, angiotensin, thrombin, bombesin, endothelin, bradykinin
Others
Light, odorants, nucleotides
α
β
γ
PI3Kγ
PLCβ
Ion channels
GRK
PKA
β1–5
γ1–14
Biological responses
Proliferation, cell survival, differentiation, migration, ECM degradation, angiogenesis, metastasis, cancer
GTP
GTP
GTP
GTP
Subtype
Gαs
GαsXL
Gαolf
Gαi1-3
Gαo, Gαt
Gαz, Gαgust
Gαq, Gα14
Gα11, Gα15/16
Gα12
Gα13
Effector
Adenylyl cyclase
Axin
↑(cAMP)
PKA
Adenylyl cyclase
Phosphodiesterases
Phospholipases
↓(cAMP)
PLCβ
Lbc
↑(Ca2+)
PKC
Rho
P115–RhoGEF
LARG
PDZ–RhoGEF
AKAP–Lbc
Rho
Gene expression
Transcription factors

Chapter 2 CXC Chemokine Receptor 2 (CXCR2) and Cognate Chemokines

Chemokines and cognate chemokine receptors

Chemokines are a family of small cytokines, or cell-signaling molecules, that regulate inflammation through GPCRs expressed on leukocytes (*67*). In higher vertebrates, over 50 different chemokines have been identified (*68*). These proteins induce various biological and biochemical activities such as cell migration, cell adhesion, and exocytosis (*69*). There are four families of chemokines including C, CC, CXC, and CX3C. The chemokines of C or CC subfamily have a single Cys residue or two contiguous Cys residues on the amino terminus of the protein, respectively. CXC or CX3C subfamilies contain one or three amino acids between the two cysteine residues. The CXC chemokines are classified into two subfamilies: the glutamate-leucine-arginine (ELR) and non-ELR families. Generally, the ELR CXC chemokines promote angiogenesis while the CXC chemokines that lack the ELR motif inhibit angiogenesis (*70*). However, the non-ELR chemokine CXCL12 (SDF-1) induces angiogenesis, which may relate to its ability to induce cancer metastasis (*71*).

In the early 1990s, two CXC chemokine receptors for CXCL8 (IL-8) were the first identified chemokine receptors. Now there are 19 chemokines receptors including 7 members for CXC, 11 for CC, 1 for C and 1 for CX3C type (*72-76*).

Table 2. Chemokine receptor and their cognate chemokine families in humans

Receptor	Swissprot	Ligand(s)	Main function
CXC chemokine receptors			
CXCR1	P25024	CXCL1 (Groα), CXCL6 (GCP-2), CXCL8 (IL-8)	Neutrophil migration; innate immunity; acute inflammation
CXCR2	P25025	CXCL1 (Groα), CXCL2 (Groβ), CXCL3 (Groγ), CXCL5 (ENA-78), CXCL6 (GCP-2), CXCL7 (NAP-2), CXCL8 (IL-8)	Neutrophil migration; innate immunity; acute inflammation; angiogenesis
CXCR3	P49682	CXCL9 (Mig), CXCL10 (IP-10), CXCL11 (I-TAC)	T cell migration; adaptive immunity; Th1 inflammation
CXCR4	P30991	CXCL12 (SDF-1 α/β)	B cell lymphopoiesis; bone marrow myelopoiesis; central nervous system and vascular development; HIV infection
CXCR5	P32302	CXCL13 (BLC, BCA-1)	B cell trafficking; lymphoid development
CXCR6	O00574	CXCL16	T cell migration
CXCR7	P25106	CXCL11 (I-TAC), CXCL12 (SDF-1 α/β)	Dendritic and B cells; HIV infection
CC chemokine receptors			
CCR1	P32246	CCL3 (MIP-1α, LD78α), CCL5 (RANTES), CCL7 (MCP-3), CCL8 (MCP-2), CCL13 (MCP-4), CCL14 (HCC-1), CCL15 (HCC-2), CCL16 (HCC-4), CCL23 (MPIF-1)	T cell and monocyte migration; innate and adaptive immunity; inflammation
CCR2	P41597	CCL2 (MCP-1), CCL7 (MCP-3), CCL8 (MCP-2), CCL13 (MCP-4), CCL16 (HCC-4),	T cell and monocyte migration; innate and adaptive immunity; Th1 inflammation
CCR3	P51677	CCL5 (RANTES), CCL7 (MCP-3), CCL8 (MCP-2), CCL11 (Eotaxin), CCL13 (MCP-4), CCL15 (HCC-2), CCL24 (Eotaxin 2), CCL26 (Eotaxin 3), CCL28 (MEC)	Eosinophil, basophil, and T cell migration; allergic inflammation
CCR4	P51679	CCL17 (TARC), CCL22 (MDC),	T cell and monocyte migration; allergic inflammation
CCR5	P51681	CCL3 (MIP-1α, LD78α), CCL4 (MIP-1β), CCL5 (RANTES), CCL8 (MCP-2), CCL16 (HCC-4)	T cell and monocyte migration; innate and adaptive immunity; HIV infection
CCR6	P51684	CCL20 (MIP3α)	Dendritic cell migration
CCR7	P32248	CCL19 (MIP3β), CCL21 (SLC),	T cell and dendritic cell migration; lymphoid development; primary immune response
CCR8	P51685	CCL1 (I-309)	T cell trafficking
CCR9	P51686	CCL25 (TECK)	T cell homing to gut
CCR10	P46092	CCL27 (CTACK, ILC), CCL28 (MEC)	T cell homing to skin
CCR11	Q9NPB9	CCL19 (MIP3β), CCL21 (SLC), CCL25 (TECK)	Expressed abundantly in the heart
CX3C chemokine receptor			
CX3CR1	P49238	CX3CL1 (Fractalkine)	3T cell and NK cell trafficking and adhesion; innate and adaptive immunity; Th1 inflammation
C chemokine receptor			
XCR1	P46094	XCL1 (Lymphotactin, SCM-1α)	T cell trafficking

Table modified from Murphy et al. (*74*), chemokine/chemokine receptor nomenclature (*75*), and Zlotnik et al (*76*).

The binding of chemokine ligands to their receptors is very promiscuous except for that of CXCL12 (SDF-1) and CXCR4.

Interaction of CXCR2 and its cognate chemokines

Most chemokine receptors can be activated by more than one chemokine (*77*). CXC chemokine receptor 2 (CXCR2) binds multiple CXC chemokines including CXCL1 (Growth related oncogene-α (GRO-α)), CXCL2 (GRO-β), CXCL3 (GRO-γ), CXCL5 (epithelial neutrophil-activating protein 78 (ENA78)), CXCL6 (granulocyte chemotactic protein 2 (GCP2)), CXCL7 (neutrophil-activating peptide 2 (NAP2)), and CXCL8 (*78, 79*). Although CXCR1 and CXCR2 show over 75% amino acid identity, only CXCL6 and CXCL8 activate CXCR1, suggesting that the two chemokine receptors have different mechanisms for chemokine ligand binding (*80*). There are three divergent regions between the two receptors including the amino terminus, EC2, and cytoplasmic terminus, however studies for ligand binding has been focused on the amino terminus and EC2 (*81, 82*). Studies using chimeric CXCR1/2 receptors showed that CXCL1, CXCL7, and CXCL8 bind to overlapping but distinct regions of CXCR2 (*83, 84*). The amino terminus and EC2 of CXCR2 are critical regions for binding CXCL1 and CXCL7, whereas only EC2 is involved in CXCL8 ligand binding. However, use of synthetic peptides corresponding to the amino terminus and extracellular loops of CXCR2, the amino terminus, but not the EC2, was also identified as a binding motif for CXCL8 (*85*). Additionally, site-directed mutagenesis of the amino terminus and EC1 of CXCR2 showed that specific charged residues on

the amino terminus of CXCR2 are critical for CXCL1 (Asp9, Glu12, Lys108 and Lys120 of CXCR2) and CXCL8 (Glu7, Asp9 and Glu12 of CXCR2) binding (*86*). Site-directed mutagenesis and chimeric receptors of CXCR1/2 including the amino terminus, TM4, EC2, TM5, EC3, and TM7 showed that the amino terminus of CXCR1 and EC2 of CXCR2 are important for CXCL8 binding, while the amino terminus of CXCR2 is involved in CXCL1 binding (*87*). A recent study using a random phage-epitope library showed certain synthetic epitopes inhibited binding of CXCL8 (or antibody) to CXCR1/2 and blocked chemotaxis of human neutrophils (*88*). The consensus sequences of the synthetic epitopes were identical with residues on amino terminus of CXCR1/2 (Trp10-Asp11-Phe12 for CXCR1 and Asp13-Phe14-Trp15 for CXCR2), indicating that amino terminus of the receptors is important for ligand binding. Although some of the information about ligand binding is not consistent, the amino terminus and/or the EC2 are critical for binding to its cognate chemokines. Additionally, amino acid substitutions showed that the Cys residues of CXCR2 are highly associated with CXCL8 ligand binding, but not surface expression, including Cys119, Cys196, and Cys286 in the extracellular loops and Cys308 in TM7 (*89*).

The amino terminus of CXCL8 is important for high affinity and binding specificity (*90*). Site-directed mutagenesis of CXCL8, two binding sites for CXCR1 and CXCR2 were predicted (*91*). In the study, two residues, Tyr13 and Lys15, in the amino terminus of CXCL8 were identified as important sites for CXCR1 binding. Both Glu4-Leu5-Arg6 (ELR) motif and Tyr13-Ser14-Lys15 are

exposed to the surface and localize on opposite ends on the same face of the ligand. The fact that the distance between the two regions is 23 angstroms (2.3 nm) suggests that the two sites of CXCL8 can span the distance between the amino terminus and third extracellular loop of CXCR1/2. Additionally, substitutions of residues of bovine CXCL8 were used to identify analogues with high affinity (K11R) or antagonist activity (K11R/G31P) (*92, 93*). The human/bovine chimeric hbG31P (bovine CXCL8(3-44)K11R/G31P-hCXCL8(45-72)) preserved antagonist activity, indicating that the analogue can be used as potential antagonist for human CXCL8 and its receptors (*94*).

CXCR2 normally expressed on neutrophils contains two *N*-glycosylation sites (*95*). There are three possible residues for *N*-glycosylation at Asn17, Asn186, and Asn197. Because of the proximity of the Asn residues and transmembranes, Asn17 and Asn197 are probably the most likely candidates for glycosylation. Asn186 is closer to the transmembrane domain and probably cannot handle the *N*-linked sugar moieties. *N*-glycosylation on the extracellular domains of CXCR2 is not involved in ligand binding but contributes to the maintenance of the receptors expressed on the cell surface (*73, 84, 95*).

Receptor activation and signal transduction of CXCR2

CXCR2 is expressed on a various tumor cells including breast cancer, head and neck cancer, melanoma, pancreatic, and ovarian cancer (*96-100*). CXCL8 can activate both CXCR1 and CXCR2 receptors and has been

characterized as a mediator of cancer progression. Activation of these receptors promote the expression of genes highly associated with cell survival, proliferation, angiogenesis, and invasion (*78, 101*) (Fig. 5).

Antagonists have been used to understand the mechanism of CXCR1 and CXCR2 activation. Competition binding with CXCL1 and CXCL8 and a small molecule antagonist, SB225002, to CXCR2 mutants was used to show how these chemokines activate the receptor (*87*). The antagonist binds to the transmembrane helices within CXCR2, but not to the ligand binding sites, and causes an allosteric change that blocks to binding of CXCL1 and CXCL8. Currently, two different antagonists were used to understand the difference between CXCR1 and CXCR2 in antagonism (*102*). It has been shown that the EC2 of the receptors does not play a crucial role in compound antagonism, and a single amino acid (Lys320 for CXCR2 and Asn311 for CXCR1) of the receptor is important to allosteric binding.

Viral oncogene ORF74 encoded by Kaposi's sarcoma-associated herpesvirus (human herpesvirus 8), also called KSHV-GPCR, is the closest homologue to CXCR2 (*103*). KSHV-GPCR constitutively activates AP-1, CREB, NFAT, and MAPK via $G\alpha_i$ or $G\alpha_q$, and NF-κB through only $G\alpha_q$. This is true in different cell lines including COS-7, primary effusion lymphoma (PEL), and endothelial cells (*104-107*). Currently, studies of M33 from murine cytomegalovirus (MCMV) and US28 of human cytomegalovirus (HCMV), both viral GPCR homologues,

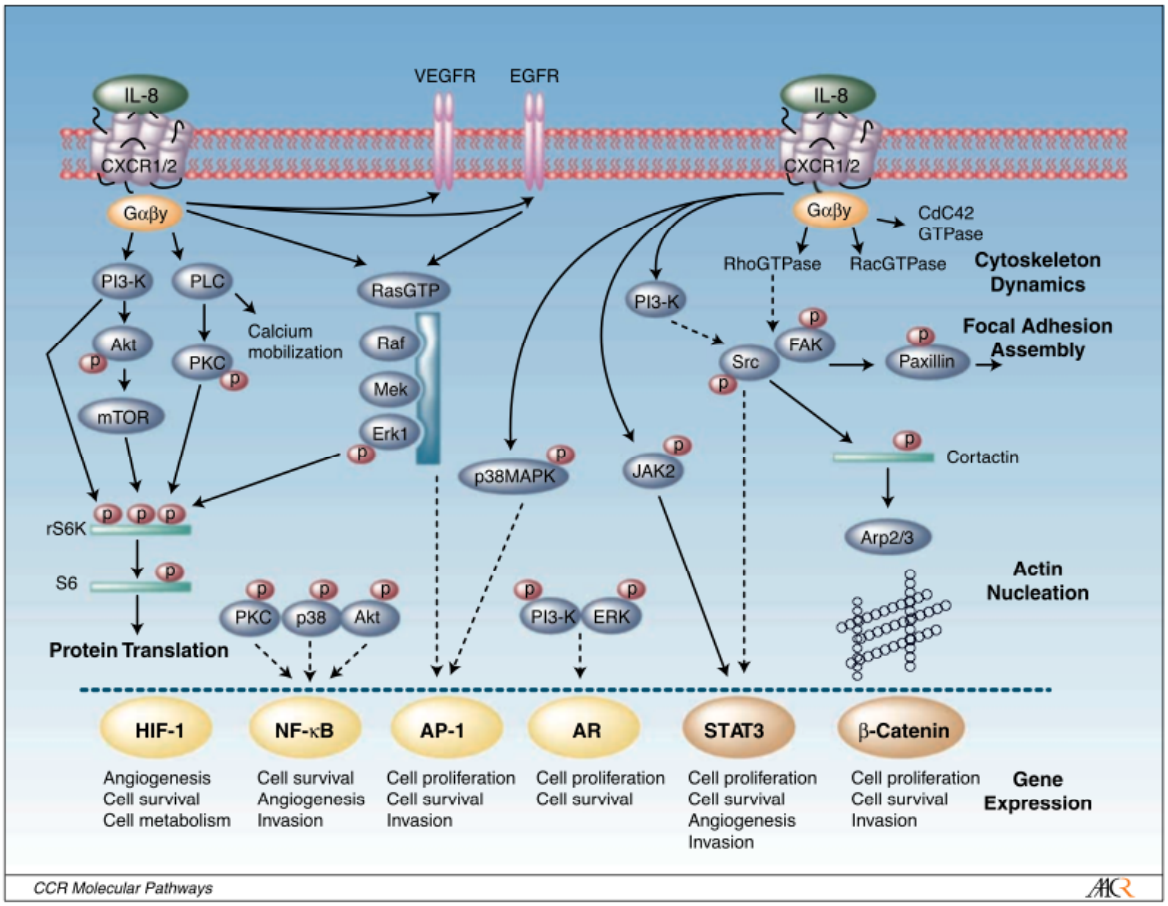

Figure 5. Characterized IL-8 signaling pathways.

A schematic diagram illustrating the range of signaling pathways that are activated after stimulation of CXCR1 and/or CXCR2 receptors with IL-8. After activation of heterotrimeric small G proteins, IL-8 signaling promotes activation of the primary effectors phosphatidyl-inositol-3-kinase or phospholipase C, promoting the activation of Akt, PKC, calcium mobilization and/or MAPK signaling cascades. These signaling pathways have been shown to promote protein translation (left) and regulate the activity of a range of transcription factors (bottom). *Solid gold lines*, transcription factors whose activity has been shown to be positively regulated by IL-8 signaling using various reporter assays. In the case of signal transducers and activators of transcription 3 (STAT3) and h-catenin, IL-8 signaling has been shown to promote nuclear translocation of these factors; however, transcriptional activation of either factor remains to be shown. *Dashed lines*, the putative pathways through which IL-8 signaling regulates transcription factor activity. In addition, IL-8 signaling activates members of the RhoGTPase family and activates a number of nonreceptor tyrosine kinases (e.g., Src family kinases and FAK) that regulate the architecture of the cell cytoskeleton and its interaction with the surrounding extracellular environment. Figure from Waugh and Wilson (*101*).

have been shown to activate the $G\alpha_q$ protein and induce phopholipase C-β (PLC-β) activity, followed by stimulation of CREB and NF-κB signals (*108-111*). Additionally, M33 can induce CREB and NF-κB stimulation via a PLC-β independent manner (*112*). On the other hand, another GPCR homolog, UL33, of HCMV enhances CREB transcriptional activities by the G_s pathway not the $G_{q/11}$ pathway (*113*).

It has been shown that CXCR2 can couple to different G proteins in different cell lines, including $G\alpha_i$, $G\alpha_{12}$, $G\alpha_{13}$, $G\alpha_{14}$, $G\alpha_{15}$, $G\alpha_{16}$, and $G\beta\gamma$ subunits (*114-116*). CXCR2 can interact with non-G proteins like vasodilator-stimulated phosphoprotein (VASP) to activate downstream signaling (*117*). It is suggested that multiple signaling cascades can be activated in a G-protein-dependent and -independent manner.

A point mutation of Asp143 (to Val, the same as KSHV-GPCR) of the highly conserved (D/E)R(Y/W) motif in CXCR2 leads to constitutive activation of the receptor and cellular transformation similar to KSHV-GPCR (*118*). Transformation was totally inhibited using AG490, a specific kinase inhibitor for JAK2-STAT3 signaling (*119*). Constitutive activation of KSHV-GPCR and CXCR2 mutant D143V is highly associated with STAT3 phosphorylation. Another motif related to CXCR2 activation was identified in the cytoplasmic terminus (*120*). Mutation of the LLKIL motif inhibited chemotaxis via disruption of Akt, Rac1, and Cdc42 recruitment. Interestingly, EC2 as well as the carboxy terminus of CXCR2 is important for activation and regulation of the receptor (*84*). Mutation of Asp199

(to Val) on EC2 delayed internalization of the receptor, whereas Asp199 substitution with Asn restored internalization. Homology modeling of CXCR2 based on rhodopsin showed that Asp199 functions to stabilize the receptor conformation using hydrogen bonds between several residues on EC2 (Fig. 6).

A current study of CXCR2 expressed on ovarian cancer cells reported that cancer growth is regulated by MAPK and NF-κB pathways (*121*). Additionally, it was shown that CXCL1 binding to CXCR2 but not CXCR1 induced transactivation of the epidermal growth factor receptor (EGFR) via the chemokine receptor, followed by proliferation of ovarian cancer cells (*122*).

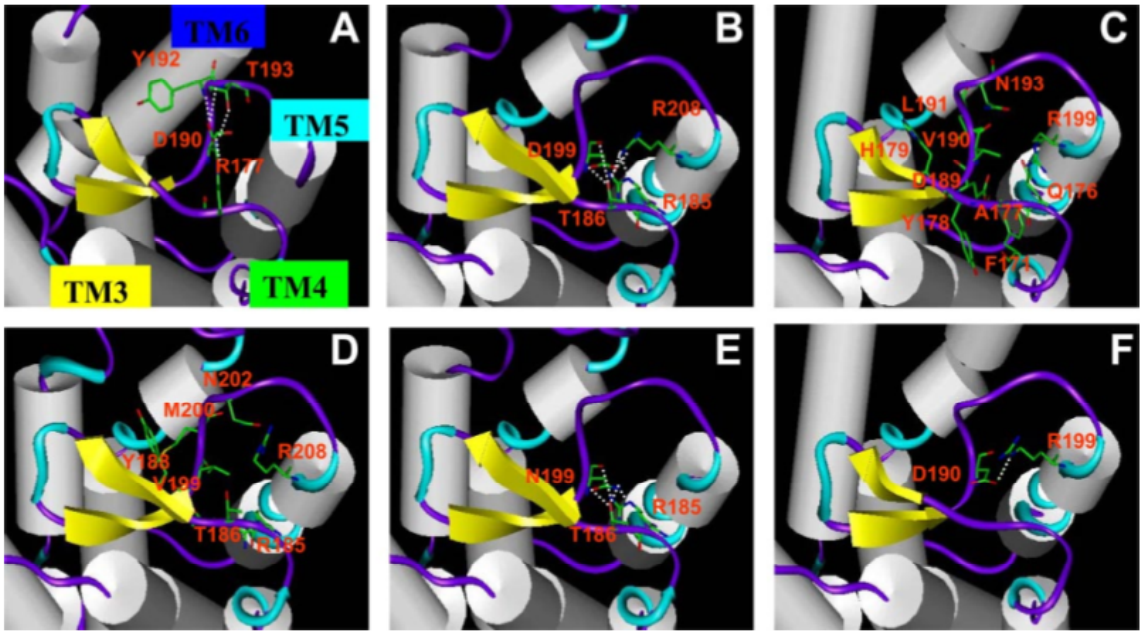

Figure 6. Computational modeling of the EC2 of rhodopsin, CXCR2, CXCR1, and the receptor mutants $B_{D199V}A$, B_{D199N}, and $A_{V190D}B$.

Shown are receptor interactions involving Asp190 of rhodopsin (A) and its corresponding residues Asp199 of the EC2 of CXCR2 (B), Val190 of CXCR1 (C), Val199 of $B_{D199V}A$ (D), Asn199 of B_{D199N} (E), and Asp190 of $A_{V190D}B$ (F). The protein secondary structural elements are displayed as follows: α-helix, white; β-sheet, yellow; turn, cyan; and random coil, purple. The color coding of receptor residue atoms is as follows: green, carbon; red, orange; and blue, nitrogen. H-bond-forming residues (in stick depiction) in association with Asp190 in rhodopsin (Tyr192, Thr193, and Arg177) (A), Asp199 in CXCR2 (Thr186, Arg208, and Arg185) (B), Asn199 in B_{D199N} (Thr186 and Arg185) (E), and Asp190 in $A_{V190D}B$ (Arg199) (F) are shown by white dotted lines. No H-bond was formed in CXCR1 (C) and $B_{D199V}A$ (D). The residues within 3.0 Å of Val190 (CXCR1) or Val199 ($B_{D199V}A$) are represented. Figure from Nasser et al (*84*).

Statement of research aims

Most chemokine receptors can be activated by more than one chemokine (*77*). CXC chemokine receptor 2 (CXCR2) binds multiple CXC chemokines including CXCL1 (GRO-α), CXCL2 (GRO-β), CXCL3 (GRO-γ), CXCL5 (ENA78), CXCL6 (GCP2), CXCL7 (NAP2), and CXCL8 (*78, 79*). Although CXCR1 and CXCR2 show over 75% amino acid identity, only CXCL6 and CXCL8 activate CXCR1, suggesting that the two chemokine receptors have different mechanisms for ligand binding (*80*). In previous studies with multiple chimeric receptors, it was shown that CXCR1 and CXCR2 have distinct mechanisms of ligand binding and receptor activation (*80, 81, 83-88*). The studies suggested that divergent regions including the amino terminus and second extracellular loop between the receptors are crucial in construction of selectivity determinants for different cellular responses. However, the mechanism of ligand binding and receptor activation is still unknown.

First, in our study, CXCR2 structure is predicted on the basis of crystal GPCR structures including rhodopsin, β_2AR by homology modeling, and CXCR4. The topology of the EC2 region of CXCR2 in the inactive state is determined by using substituted cysteine accessibility method (SCAM).

Second, we studied the role of charged residues in EC2 of CXCR2 in ligand binding and receptor activation. Two concepts, “attraction” and “repulsion” models, were designed to investigate the mechanism of CXCR2 activation (Fig. 14). To end that, we constructed combinatorial mutation sets consisting of

constitutively active mutants (CAM) Asp9 in the amino terminus and substitutions in EC2. These mutant receptors were generated by site-directed mutagenesis and transfected into mouse fibroblast NIH3T3 cell lines. The NIH3T3 cells stably expressing wild-type CXCR2 and mutant receptors were used to investigate cell surface expression of the receptor, ligand-binding, and receptor activation through phospholipase C-β3 (PLC-β3).

PART II

PREDICTION OF THE TERTIARY STRUCTURE OF CXCR2 AND STUDY OF THE CONFORMATION OF THE SECOND EXTRACELLULAR LOOP OF THE RECEPTOR IN AN INACTIVE STATE

Chapter 1 Abstract

The first objective of this investigation was to predict the structure of CXCR2 based on known structures of crystallized GPCRs. Bovine rhodopsin, human β_2-adrenergic receptor, and human CXCR4 were used for homology modeling of CXCR2 structure. Highly conserved motifs ((D/E)R(Y/W), NPXXY, toggle switch, and disulfide bonds) found in sequence alignments of the template GPCRs were helpful to generate CXCR2 models. Using Cα RMSDs, structural alignments of the seven transmembrane domains showed the individual models tend to be similar to their templates. Based on the sequence alignments and RMSD values, the CXCR4-based model shows a very similar structure to CXCR2. The second extracellular loop of the homology modeled CXCR2 provided two β-strands like CXCR4 and the prediction is very similar with results obtained from web-based prediction programs. Superimposition of the second extracellular loop of CXCR4 and CXCR4-based CXCR2, showed the second extracellular loop of CXCR2 is structurally very similar with that of CXCR4 with below 2.0 Å RMSD.

Furthermore, we studied solvent accessibility of residues in the second extracellular loop of CXCR2, a key region for ligand binding and receptor activation, in the inactive state of the receptor. MTSEA-biotin accessibility of substituted cysteine residues in second extracellular loop was measured by immunostaining of FITC-streptavidin using flow cytometric analysis. The

normalization of the accessibility was determined by surface expression levels of the substituted cysteine mutant receptors. Most of residues in the second extracellular loop were found to be solvent accessible in the inactive state of CXCR2, indicating that the residues might be involved in ligand binding. Most of the charged residues in second extracellular loop also have solvent accessibility. However, five amino acids ^{204}TANWR^{208} showed no solvent accessibility, pointing to possible interaction with the amino terminus or other extracellular loops. Our finding of ligand binding sites for CXCR2 also indicated that most of the residues in the second extracellular loop could form a ligand binding pocket to contact CXCL8.

In this sense, these current discoveries about structural basis of CXCR2 and interdisciplinary approaches would provide new insights to investigate unknown mechanisms of interaction with its cognate ligands and receptor activation.

Chapter 2 Introduction

CXCR2, also called IL-8RB, was initially identified as a chemokine receptor expressed on neutrophils (*123*). CXCR2 is a member of the rhodopsin-like subfamily (class A) of G protein-coupled receptors, and has the closest homology to CXCR1, with 77% amino acid identity (*72, 73, 123*). Multiple chemokines can bind CXCR2 including CXCL1 (Growth related oncogene-α (GRO-α)), CXCL2 (GRO-β), CXCL3 (GRO-γ), CXCL5 (epithelial neutrophil-activating protein 78 (ENA78)), CXCL6 (granulocyte chemotactic protein 2 (GCP2)), CXCL7 (neutrophil-activating peptide 2 (NAP2)), and CXCL8 (*78, 79*). The function of CXCR2 has been studied in a variety of immune cells such as neutrophils and macrophages, indicating that the receptor plays a critical role in immune response and inflammation (*121*). Furthermore, it has been shown that CXCR2 receptors are also expressed on various cancer cells including breast cancer, head and neck cancer, melanoma, pancreatic, and ovarian cancer (*96-100*).

In previous studies utilizing chimeric receptors, it has been shown that CXCR1 and CXCR2 have distinct mechanisms of ligand binding and receptor activation (*80, 81, 83-88*). The studies suggested that divergent regions including the amino terminus and second extracellular loop between the receptors are crucial in construction of selectivity determinants for different cellular responses. The CXCL8, a chemokine ligand that binds to both CXCR1 and CXCR2, has

been used to study which part of the ligand is important to bind the receptors (*90, 91*). Both the Glu4-Leu5-Arg6 (ELR) motif and Tyr13-Ser14-Lys15 on the amino terminus of CXCL8 might initially interact with the amino terminus and third extracellular loop of the receptors. However, a current study suggested another model that the N-loop (His18 to Phe21) of CXCL8 binds the amino terminus of the cognate receptors and then the ELR motif of the ligand interacts with the second extracellular loop of the receptors (*124*). Although there are different possible mechanisms of the interaction of CXCL8 and its cognate receptors, the fact that extracellular parts of CXCR1 and CXCR2 are crucial for ligand binding and receptor activation has been conserved.

Six GPCRs in the inactive state have been crystallized including human β_2 adrenergic receptor (β_2AR), avian β_1AR, human A_{2A} adenosine receptor, CXC chemokine receptor 4 (CXCR4) as well as bovine rhodopsin and opsin (*8, 13, 22-26*). The high-resolution structural analysis has provided a crucial molecular basis to address structure and function of GPCRs (*7*). Previously, the crystal structures of rhodopsin and β_2AR have been used to predict structures of GPCRs that are not structurally solved (*32, 41, 42*). The prediction is based on the fact that GPCRs have highly conserved motifs and structural conservation, even though their primary sequences are quite divergent (*43*). However, the limited crystallized structures are not sufficient for homology modeling and drug design of structurally unknown GPCRs (*44*). Recently, a novel crystal structure of chemokine receptor CXCR4 has been solved belonging to class A GPCRs (*8*).

The CXCR4 structure is expected to be the best template to homology model other chemokine receptors including CXCR1 and CXCR2.

In GPCRs, the second extracellular loops in particular show highly variable length and non-conserved amino acid sequences (*43*). The function of EC2 in different GPCRs has been shown to negatively regulate receptor activation. In C5aR and rhodopsin receptors, the EC2 region plays a critical role in stabilization of the inactive conformation of GPCRs (*36, 37, 125*). Another example has been observed in the melanocortin receptor with the fact that a short length of EC2 and the absence of a conserved disulfide bond allow the receptor to induce a high basal activity (*126*). However, in the M_3 muscarinic acetylcholine receptor (M3R), it has been shown that multiple residues on EC2 are important in stabilizing the active state of the receptor (*127*).

In our study, a CXCR2 structure is predicted on the basis of crystal GPCR structures including rhodopsin, β_2AR, and CXCR4 by using homology modeling. Furthermore, the accessibily of residues in the EC2 region of CXCR2 in the inactive state is determined by using substituted cysteine accessibility method (SCAM).

Chapter 3 Materials and Methods

Cell line and medium

Human embryonic kidney (HEK) 293 cells were cultured with Dulbecco's modified eagle medium (DMEM) containing 10% newborn calf serum (NCS), 1X non-essential amino acids (NEAA), and 1X penicillin/streptomycin.

Cysteine-scanning mutagenesis

The *CXCR2* gene cloned into pRc/CMV vector was used as a template for site-directed mutagenesis. Forward and reverse primers were manually designed for single cysteine substitution of all the residues (from Phe183 to Lue214) in the EC2 of CXCR2 (Table 3). PCR mutagenesis was performed with a modification of the QuickChange® method (Stratagene). 1X PCR mixture (50 µl) contains 300-400 ng of template plasmid including wild-type *CXCR2* gene, 0.5 U Taq polymerase (Takara, Japan), 1X Taq polymerase buffer, 2 µl deoxynucleotide mixture, 10 pmoles each primer, and nuclease-free H_2O. Cycling conditions were a cycle of 98 ℃ for 3 min, 35 cycles of 98 ℃ for 30 sec, 55 ℃ for 30 sec, and 72 ℃ for 10 min, and a cycle of 72 ℃ for 20 min. Dpn I digestion treatment was performed, followed by cleaning via a PCR purification kit. All mutations were conformed by sequencing analysis (Molecular biology resource facility, University of Tennessee, Knoxville).

Expression of the CXCR2 receptor in HEK293 cells

Plasmid DNAs of wild-type CXCR2 and mutant receptors were transiently transfected into HEK293 cells. The transfections were performed with Lipofectamine 2000 reagent according to the manufacturer's instructions. 4.0 x 10^5 HEK293 cells were seeded in 60 mm dishes one day before transfection. 4 μg of plasmid DNA and 4 μl of Lipofectamine 2000 were individually diluted into 250 μl fresh DMEM, incubated for 5 min at room temperature, and mixed together followed by incubation for 30 min at room temperature. The mixtures and 1 ml fresh DMEM were added to each 60 mm dish and incubated for 4 hr at 37 ℃. The mixtures was substituted with new medium including 10% newborn calf serum (NCS), followed by cultivation for 48 hr at 37 ℃.

MTSEA-biotin labeling and flow cytometry analysis

2-[(biotinoyl)amino]ethyl methanethiosulfonate (MTSEA-biotin) labeling was performed as previously described (*9*) with the following modifications. MTSEA-biotin was dissolved in dimethyl sulfoxide (DMSO) and prepared as a 20 mM stock. A final concentration of 0.1 mM MTSEA-biotin in 1X PBS was used for MTSEA-labeling. Cells expressing the wild-type CXCR2 and mutant receptors were harvested by using cell scrapers (BD Falcon^{TM}, NJ) with 2 ml 1X PBS. After

centrifugation, 200 µl MTSEA-biotin was added to the cells for 2 min at room temperature, followed by washing with 4ml 1X PBS.

In order to determine cell surface expression of CXCR2, 25 µl of 1% goat serum in 1X PBS was used for blocking non-specific antibody binding for 15 min at room temperature. 10 µl of an anti-CXCR2-specific monoclonal antibody, phycoerythrin (PE)-conjugated mouse monoclonal anti-human IL-8 receptor B (R&D systems, MN), was added to the cells for 1 hr at RT in the dark. After washing with 4 ml 1X PBS, 200 µl strepavidin-fluorescein isothiocyanate (FITC) (1:200 dilution) (BD Biosciences, CA) was added to the cells for 1 hr at RT in the dark, followed by an additional washing. Fixation of the cells was performed with 200 µl 4% paraformaldehyde (PFA). A BD FACSCalibur^{TM} (BD Sciences) was used to obtain flow cytometry data from the immunostained samples. The flow cytometry data were analyzed by FlowJo 8.7 software (Tree Star Inc., OR).

Homology modeling of human CXCR2

To construct a homology modeled CXCR2, published crystal structures of bovine rhodopsin (Protein Data Bank (PDB) code: 1U19), β_2AR (PDB code: 2RH1), and CXCR4 (PDB code: 3ODU) were used as templates. Homology modeling was performed in Molecular Operating Environment (MOE 2008.10) of chemical computing group (Montreal, Canada). Sequence alignments of CXCR2 and the three templates were performed using BLOSUM30 matrix, a gap open penalty of 10.0 and a gap extension penalty of 0.05. The results of alignments

was evaluated by using the highly conserved residues on class A GPCR family, including the (D/E)R(Y/W) motif in TM3, the Cys residues on the boundary of EC1 and TM3 and within the EC2 that form disulfide bridges and the NPXXY motif in TM7. The formation of disulfide bridges was induced by automatic search option. The backbone atoms on transmembrane regions were kept fixed and remaining residues are refined by energy-minimization with assisted model building with energy refinement (Amber)-99 force fields. Root mean square deviation (RMSD) was calculated to evaluate structural similarity and differences between homology modeled CXCR2 and templates. Furthermore, Site Finder in MOE software was used to search possible binding sites for ligands.

Prediction of secondary structure of GPCRs

Structures of the second extracellular loops were predicted by two web-based programs, the self-optimized prediction method (SOPMA) of the network protein sequence analysis (NPS@) (*128*) and the web server for protein surface accessibility and secondary structure predictions (NetSurfP ver. 1.1) of center for biological sequence analysis (CBS) (*129*).

Table 3. Primers for cysteine-scanning mutagenesis on different regions of CXCR2

Region	Name	Forward primer	Reverse primer
N-ter	D9C	5'- CATGGAGAGTtgtAGCTTTGAAGATTTCTGGAAAGGTG-3'	5'- CAAAGCTacaACTCTCCATGTTAAAATC-3'
IC1	G79C	5'-GTCtgcCGCTCCGTCACTGATGTCTACCTGCTG-3'	5'-GTGACGGAGCGgcaGACCCTGCTGTATAAGATGAC-3'
TM4	L182C	5'-GTCTTAtgcTTCCGAAGGACCGTCTACTC-3'	5'-CGGTCCTTCGGAAgcaTAAGACAGGCAGGGC-3'
	F183C	5'-CTTACTTtgcCGAAGGACCGTCTACTCATC-3'	5'-CGGTCCTTCGgcaAAGTAAGACAGGCAGGGC-3'
EC2	R184C	5'-CTTTTCtgcAGGACCGTCTACTCATCCAATG-3'	5'-CGGTCCTgcaGAAAAGTAAGACAGGCAGGGC-3'
	R185C	5'-CGAtgcACCGTCTACTCATCCAATGTTAGC-3'	5'-GTAGACGGTgcaTCGGAAAAGTAAGACAGGC-3'
	T186C	5'-CGAAGGtgcGTCTACTCATCCAATGTTAGC-3'	5'-GAGTAGACgcaCCTTCGGAAAAGTAAGACAGGC-3'
	V187C	5'-GAAGGACCtgcTACTCATCCAATGTTAGCCCAGC-3'	5'-CATTGGATGAGTAgcaGGTCCTTCGGAAAAG-3'
	Y188C	5'-CGTCtgcTCATCCAATGTTAGCCCAGCCTGC-3'	5'-CATTGGATGAgcaGACGGTCCTTCGGAAAAG-3'
	S189C	5'-CTACtgcTCCAATGTTAGCCCAGCCTGCTATG-3'	5'-CATTGGAgcaGTAGACGGTCCTTCGGAAAAG-3'
	S190C	5'-CTCAtgcAATGTTAGCCCAGCCTGCTATGAG-3'	5'-GCTAACATTgcaTGAGTAGACGGTCCTTCGGAAAAG-3'
	N191C	5'-CATCCtgcGTTAGCCCAGCCTGCTATGAGGAC-3'	5'-GCTAACgcaGGATGAGTAGACGGTCCTTCGAAAAG-3'
	V192C	5'-CAATtgcAGCCCAGCCTGCTATGAGGACATG-3'	5'-GCTGGGCTgcaATTGGATGAGTAGACGGTCCTTCG-3'
	S193C	5'-CAATGTTtgcCCAGCCTGCTATGAGGACATG-3'	5'-GCTGGgcaAACATTGGATGAGTAGACGGTCCTTCG-3'
	P194C	5'-GTTAGCtgcGCCTGCTATGAGGACATGGGCAAC-3'	5'-CATAGCAGGCgcaGCTAACATTGGATGAGTAGACG-3'
	A195C	5'-GCCCAtgcTGCTATGAGGACATGGGCAAC-3'	5'-CATAGCAgcaTGGGCTAACATTGGATGAGTAGACG-3'
	Y197C	5'-CTGCtgcGAGGACATGGGCAACAATACAGCAAAC-3'	5'-CATGTCCTCgcaGCAGGCTGGGCTAACATTGGATG-3'
	E198C	5'- GCCTGCTATtgtGACATGGGCAACAATACAGC-3'	5'- GTTGCCCATGTCacaATAGCAGGCTGGGCTAAC-3'
	D199C	5'- CTATGAGtgtATGGGCAACAATACAGCAAAC-3'	5'- GTTGCCCATacaCTCATAGCAGGCTGGGCTAAC-3'
	M200C	5'-GAGGACtgcGGCAACAATACAGCAAACTGGC-3'	5'-GTTGCCgcaGTCCTCATAGCAGGCTGGGCTAAC-3'
	G201C	5'-CATGtgcAACAATACAGCAAACTGGCGGATGC-3'	5'-GCTGTATTGTTgcaCATGTCCTCATAGCAGGC-3'
	N202C	5'-CATGGGCtgcAATACAGCAAACTGGCGGATGC-3'	5'-GCTGTATTgcaGCCCATGTCCTCATAGCAGGC-3'
	N203C	5'-CAACtgcACAGCAAACTGGCGGATGCTG-3'	5'-GCTGTgcaGTTGCCCATGTCCTCATAGCAGGC-3'
	T204C	5'-CAACAATtgcGCAAACTGGCGGATGCTGTTAC-3'	5'-GCCAGTTTGCgcaATTGTTGCCCATGTCCTC-3'
	A205C	5'-CAACAATACAtgcAACTGGCGGATGCTGTTAC-3'	5'-GCCAGTTgcaTGTATTGTTGCCCATGTCCTC-3'
	N206C	5'-CAGCAtgcTGGCGGATGCTGTTACGGATCCTG-3'	5'-GCATCCGCCAgcaTGCTGTATTGTTGCCCATG-3'
	W207C	5'-GCAAACtgcCGGATGCTGTTACGGATCCTG-3'	5'-CAGCATCCGgcaGTTTGCTGTATTGTTGC-3'
	R208C	5'-GCAAACTGGtgcATGCTGTTACGGATCCTGCCCCAG-3'	5'-CAGCATgcaCCAGTTTGCTGTATTGTTGCCCATGTC-3'
	M209C	5'-CTGGCGGtgcCTGTTACGGATCCTGCCCCAG-3'	5'-GTAACAGgcaCCGCCAGTTTGCTGTATTGTTG-3'
	L210C	5'-CGGATGtgcTTACGGATCCTGCCCCAGTC-3'	5'-GATCCGTAAgcaCATCCGCCAGTTTGCTGTATTG-3'
	L211C	5'-GCTGtgcCGGATCCTGCCCCAGTCCTTTGGC-3'	5'-CAGGATCCGgcaCAGCATCCGCCAGTTTGCTG-3'
	R212C	5'-GCTGTTAtgcATCCTGCCCCAGTCCTTTGGC-3'	5'-CAGGATgcaTAACAGCATCCGCCAGTTTGCTG-3'
	I213C	5'-GTTACGGtgcCTGCCCCAGTCCTTTGGCTTCATCG-3'	5'-CTGGGGCAGgcaCCGTAACAGCATCCGCCAGTTTG-3'
	L214C	5'-CGGATCtgcCCCCAGTCCTTTGGCTTCATCG-3'	5'-CTGGGGgcaGATCCGTAACAGCATCCGCCAG-3'

Uppercase sequences in the forward and reverse primers above indicate original nucleotides of CXCR2 and red lowercase sequences are for the site-direct cysteine amino acid mutation.

Chapter 4 Results

Structural similarity and differences between homology modeled CXCR2 and crystal structures of GPCRs

Sequence alignment and homology modeling for CXCR2 were performed with bovine rhodopsin, β_2AR, and CXCR4 in MOE software. Sequence alignments with rhodopsin and β_2AR showed low identity in the alignment (18.1% for rhodopsin, 24.2% for β_2AR), whereas CXCR4 provided relatively high identity (33.3%) to CXCR2 (Fig. 7, 8, 9). In all the cases, the (D/E)R(Y/W) and NPXXY motifs are conserved in their primary sequences. The modeling produced a rhodopsin-based CXCR2 model (bRho-CXCR2), a β_2AR-based model (b2AR-CXCR2), and a CXCR4-based model (CXCR4-CXCR2) (Fig. 10). All three models contain the highly conserved disulfide bond of GPCRs however the CXCR4-based model has one more disulfide bond linking amino terminus and third extracellular loop. Like their templates, bRho-CXCR2 and CXCR4-CXCR2 produced two β-strands in its second extracellular loop, whereas b2AR-CXCR2 showed only one α-helix.

To evaluate structural similarity of homology modeled CXCR2 structures and crystal structures of GPCRs, superposition of the structures were performed and RMSD values of seven transmembrane helices were measured (Fig. 11). Zero at RMSD means they are identical in conformation. The bRho-CXCR2

showed the lowest value (1.64 Å) in the comparison with rhodopsin, the b2AR-CXCR2 was the most identical to β_2AR (2.02 Å), and CXCR4-CXCR2 was very similar to CXCR4 (0.78 Å). Interestingly, the RMSD from CXCR4-CXCR2 versus CXCR4 was the lowest among comparison of the models with their own templates. The highest RMSD value (2.93 Å) was derived from the comparison of b2AR-CXCR2 and CXCR4. Furthermore, Site Finder was used to predict ligand binding sites of b2AR-CXCR2 and CXCR4-CXCR2 (Fig. 12). The prediction indicates that residues in all the extracellular loops are highly associated with ligand binding. Residues in some of transmembranes domains showed the involvement in ligand binding as well.

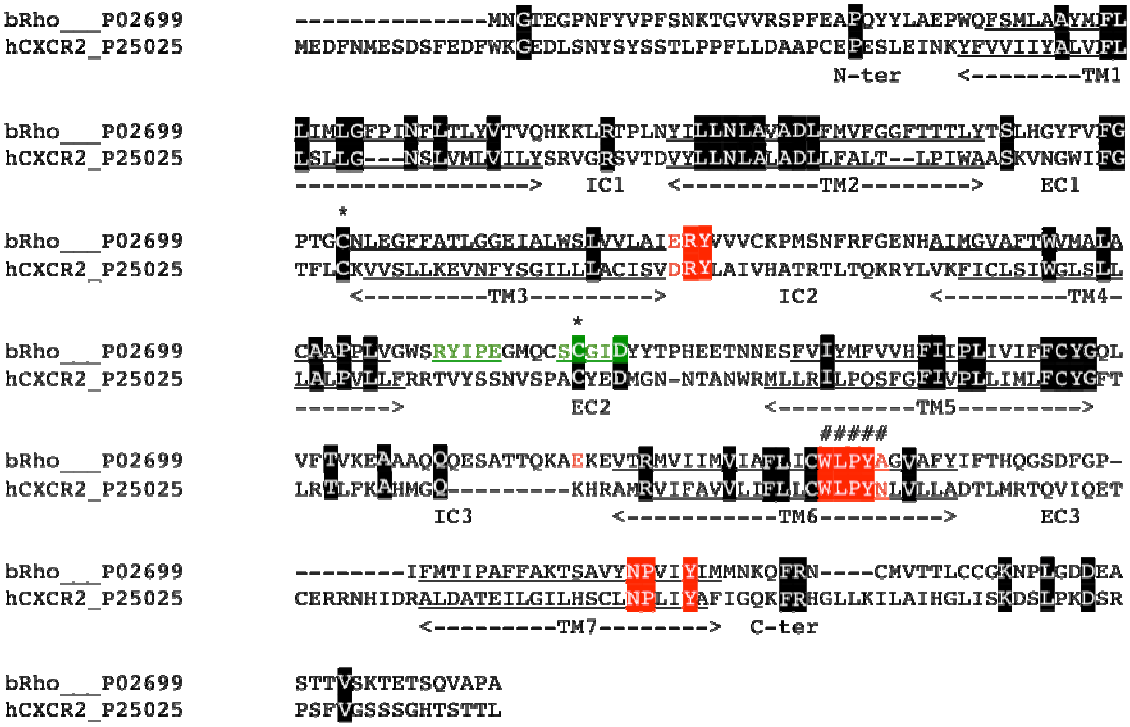

Figure 7. Sequence alignment of CXCR2 and bovine rhodopsin.

Identical residues are represented with color boxes. CXCR2 shows 18.1% (65/360 amino acids) identity with rhodopsin. Both have the highly conserved (D/E)R(Y/W), NPXXY motif, and rotamer toggle switch (#) (red texts and boxes), whereas only bovine rhodopsin has a Glu residue in its IC3 forming an ionic lock between TM3 and TM6. In the EC2 of rhodopsin, there are two β-strand structures (Green). Asterisks indicate the Cys residues that form a conserved disulfide bond in GPCRs. Each motif of rhodopsin and CXCR2 were based on crystal structure of rhodopsin (PDB code: 1U19) and prediction of universal protein resource (Uniprot, www.uniprot.org), respectively.

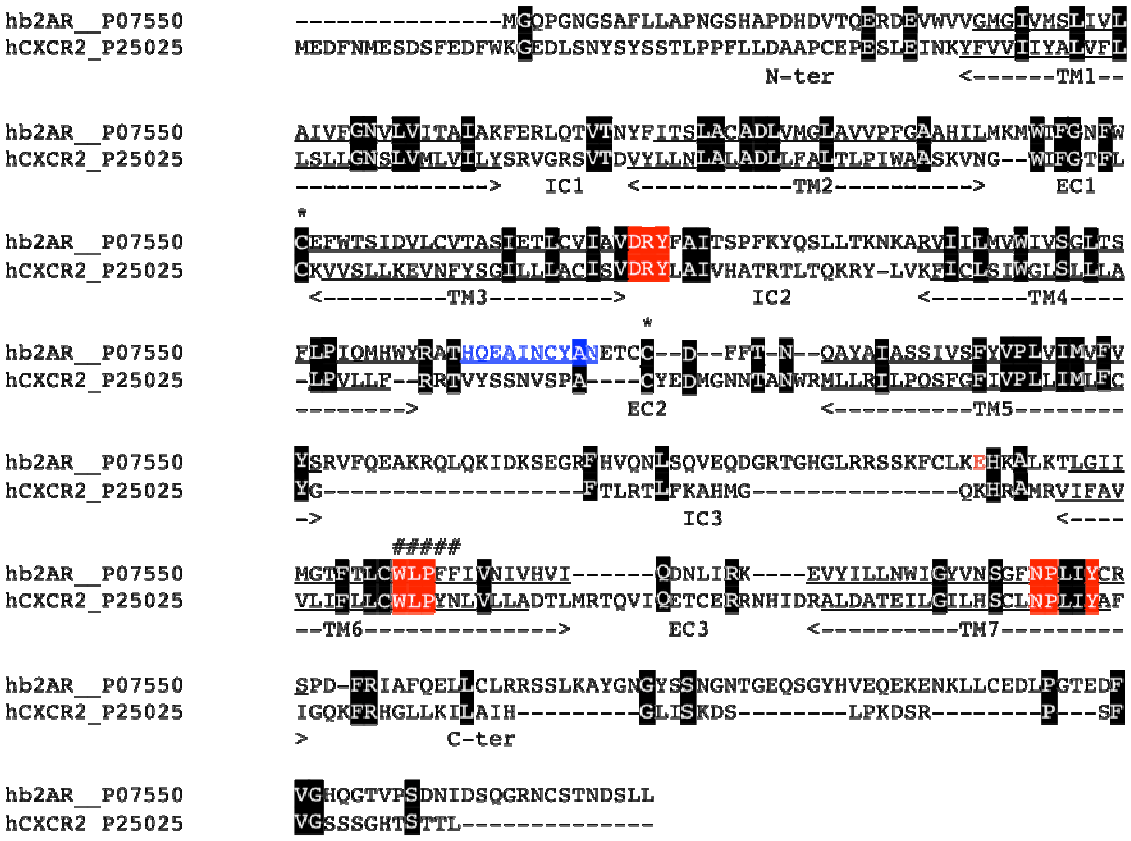

Figure 8. Sequence alignment of CXCR2 and β_2AR.

Identical residues are represented with color boxes. CXCR2 shows 24.2% (87/360 amino acids) identity with β_2AR. Both share the highly conserved (D/E)R(Y/W), NPXXY motif, and rotamer toggle switch (#) (red texts and boxes), whereas a Glu residue in its IC3 forming an ionic lock between TM3 and TM6 only conserved in β_2AR. In the EC2 of β_2AR, there are two α-helices structures (blue). Asterisks indicate the Cys residues that form a conserved disulfide bond in GPCRs. Each motif of β_2AR and CXCR2 were based on crystal structure of β_2AR (PDB code: 2RH1) and prediction of universal protein resource (Uniprot, www.uniprot.org), respectively.

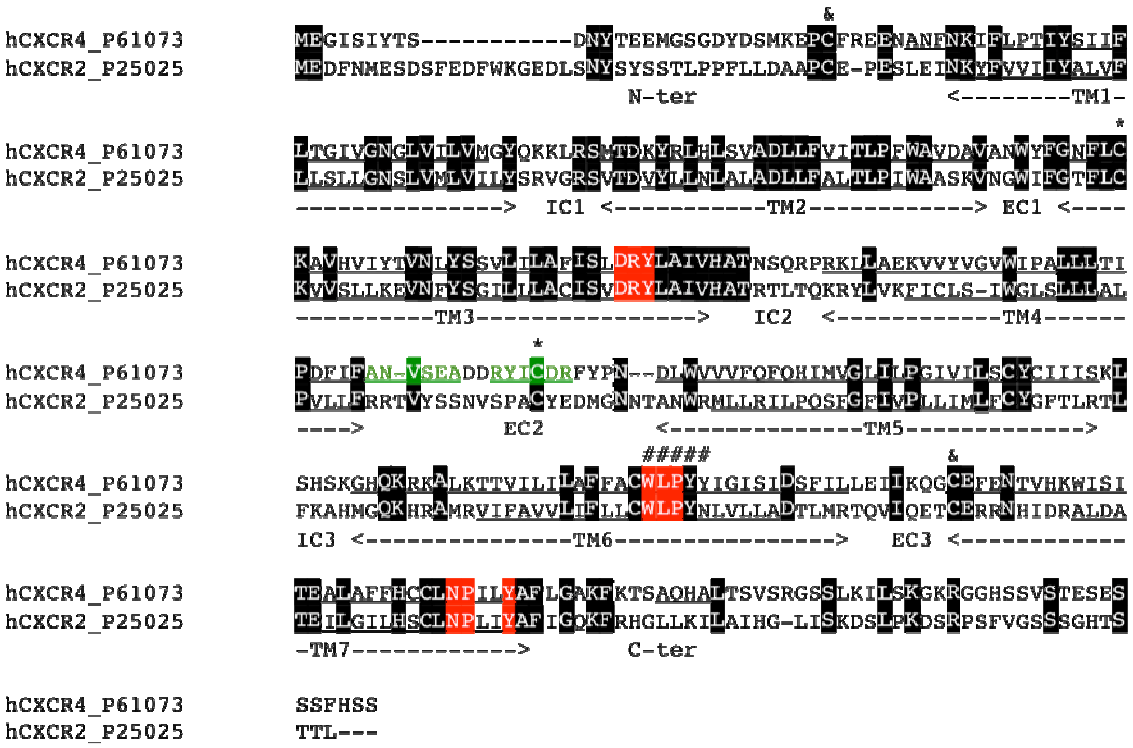

Figure 9. Sequence alignment of CXCR2 and CXCR4.

Identical residues are represented with color boxes. CXCR2 shows 33.3% (120/360 amino acids) identity with CXCR4. Their EC2s shared few amino acids (16% identity, 4/25 amino acids). Both share the highly conserved (D/E)R(Y/W), NPXXY motif, and rotamer toggle switch (#) (red boxes). However, CXCR2 and CXCR4 has no a Glu residue in its IC3 forming an ionic lock between TM3 and TM6 conserved in rhodopsin and β_2AR. In the EC2 of CXCR4, there are two β-strand structures (green). There are two disulfide bonds (* and &) in the GPCRs. Each motif of CXCR4 and CXCR2 were based on crystal structure of CXCR4 (PDB code: 3ODU) and prediction of universal protein resource (Uniprot, www.uniprot.org), respectively.

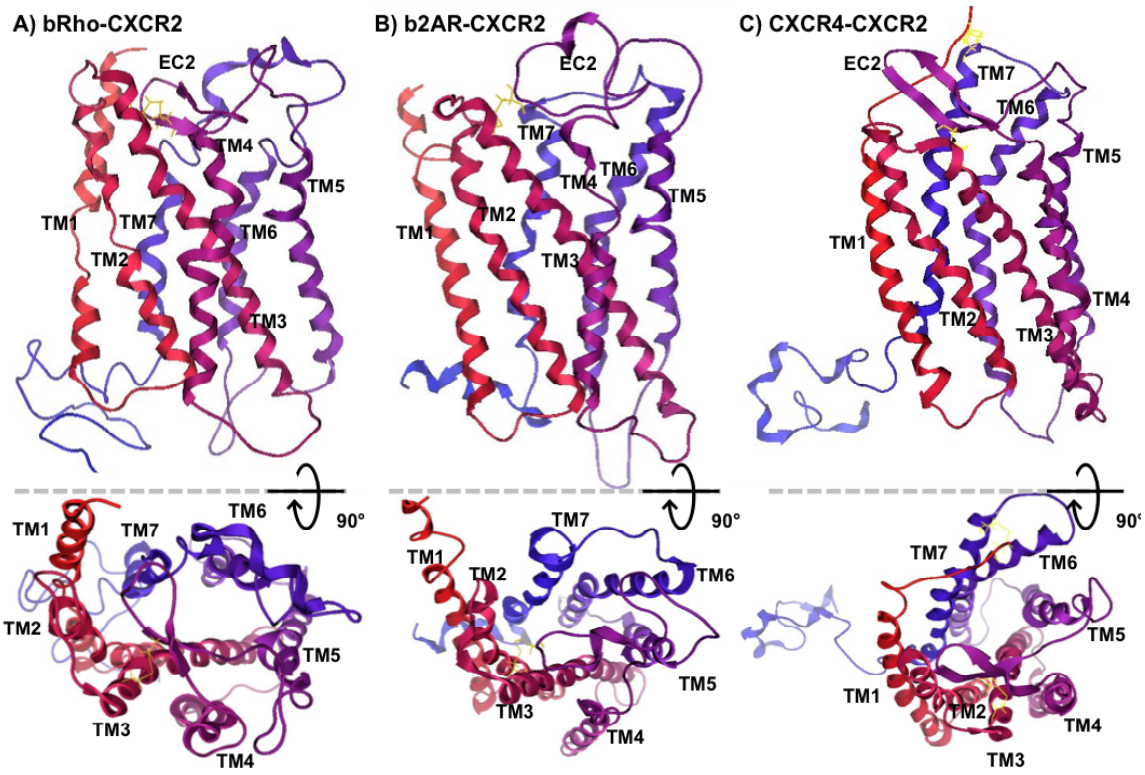

Figure 10. Homology modeled CXCR2 structures based on the crystal structures of bovine rhodopsin, human β_2AR, and human CXCR4.

Three homology models for CXCR2 based on three crystallized GPCRs: (A) rhodopsin-based CXCR2 structure (B) β_2AR-based CXCR2 structure (C) CXCR4-based CXCR2 structure. The homology models share a conserved disulfide bond linking TM3 and EC2, but only CXCR4 and CXCR2 have one more disulfide bond linking amino terminus and EC3 (yellow).

Figure 11. Superposition and structural similarity of homology modeled CXCR2 structures with other GPCRs.

(A) Transmembranes domains of the rhodopsin-based CXCR2 model (red) were superimposed with the crystal structure of rhodopsin (gray). Most of the residues in the transmembranes showed below pairwise root mean squared deviations (RMSD) 2.0 Å, except for Gly65 (orange) in TM1 (3 amino acids gap in sequence alignment) and Phe97 to W104 (purple) in TM2 (2 amino acids gap in sequence alignment). (B) Superposition of transmembranes of the β_2AR-based CXCR2 model (green) and its template, β_2AR (gray) was performed. Most of the residues in the transmembranes showed below RMSD 2.0 Å, except for Lys48 (orange) to Val52 in TM1 and Ala177 to Phe183 (purple) in TM4 (1 amino acid gap in sequence alignment). (C) Seven transmembranes of the CXCR4-based CXCR2 (purple) were superposed with the CXCR4 crystal structure (gray). None of the residues in transmembranes are over RMSD 2.0 Å. (D) The RMSDs were measured with the seven transmembrane helices of crystallized GPCRs and homology models of CXCR2. Transmembranes regions were determined by multiple sequence alignment with their primary sequences.

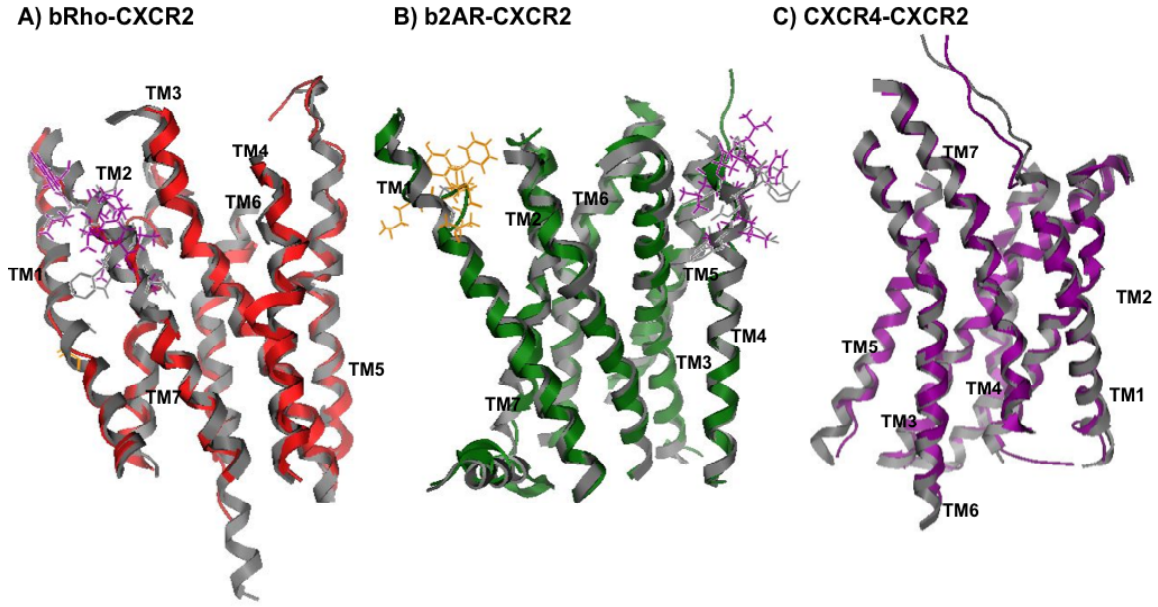

D) Cα root mean square deviation (RMSD) for seven transmembranes

	bRho	β_1AR	β_2AR	A_{2A}AR	CXCR4	bRho-CXCR2	b2AR-CXCR2	CXCR4-CXCR2
bRho (1U19)		2.40	2.43	2.79	2.50	**1.64**	2.85	2.54
β_1AR (2VT4)			**0.36**	1.84	2.05	2.32	**2.07**	1.92
β_2AR (2RH1)				1.85	2.12	2.32	**2.02**	1.98
A_{2A}AR (3EML)					2.52	2.87	2.69	2.43
CXCR4 (3ODU)						2.46	2.93	**0.78**
CXCR2 models: bRho-CXCR2							2.78	2.50
CXCR2 models: b2AR-CXCR2								2.81
CXCR2 models: CXCR4-CXCR2								

RMSD (Å): 3.0, 2.5, 2.0, 1.5, 1.0, 0.5

Figure 12. Prediction of ligand binding sites in β2AR-based and CXCR4-based CXCR2 structure.

The Site Finder in Molecular Operation Environment (MOE) software was used to search for potential ligand binding sites in β_2AR-based CXCR2 (A) and CXCR4-based CXCR2 models (B). Spheres indicate possible contact sites for ligand binding (red = hydrophilic, white = hydrophoblic). **(A)** In the β_2AR-based CXCR2, most of the residues in the predicted binding site are localized in the extracellular loops, including Lys108, Val109, Asn110, Gly111, and Trp112 in the first extracellular loop, Arg184, Arg185, Cys196, Tyr197, Glu198, Asp199, Met200, and Thr204 in the second extracellular loop (yellow), and Glu284, Thr285, Cys286, Arg289, Asn290, Asp293, and Leu296 in the third extracellular loop. Furthermore, some transmembranes residues were predicted as binding sites, including Phe97, Thr100, Ile103, Trp104, and Ser107 in the second transmembrane, Cys119, Val122, Ser123, Lys126, Glu127, and Phe130 in the third transmembrane, and Phe218, Trp264, Tyr267, and Leu271 in the fifth transmembrane. **(B)** CXCR4-based CXCR2 also has many residues in extracellular domains as potential ligand binding sites; Glu40, Pro41, Glu42, and Lys48 in the amino terminus, Trp104, Ser107, Lys108, Val109, Asn110, Gly111, and Trp112 in the first extracellular loop, and Arg184, Arg185, Thr186, Tyr188, Ser190, Asn191, Val192, Ser193, Pro194, Ala195, Cys196, Tyr197, Glu198, Asp199, Arg208, Leu211, and Arg212 in the second extracellular loop. Furthermore, several residues in the transmembrane domains were predicted as ligand binding sites: Tyr55 in the first transmembrane, Phe97 and Leu101 in the second transmembrane, Val122, Ser123, Lys126, Glu127, and Phe130 in the third transmembrane, Val180 in the fourth transmembrane, Pro215 and Gln216 in the fifth transmembrane, Tyr267, Leu271, Asp274, and Arg278 in the sixth transmembrane, and Arg289, Ile292, Asp293, Arg294, Leu296, Asp297, Glu300, Ile301, and Ile304 in the seventh transmembrane.

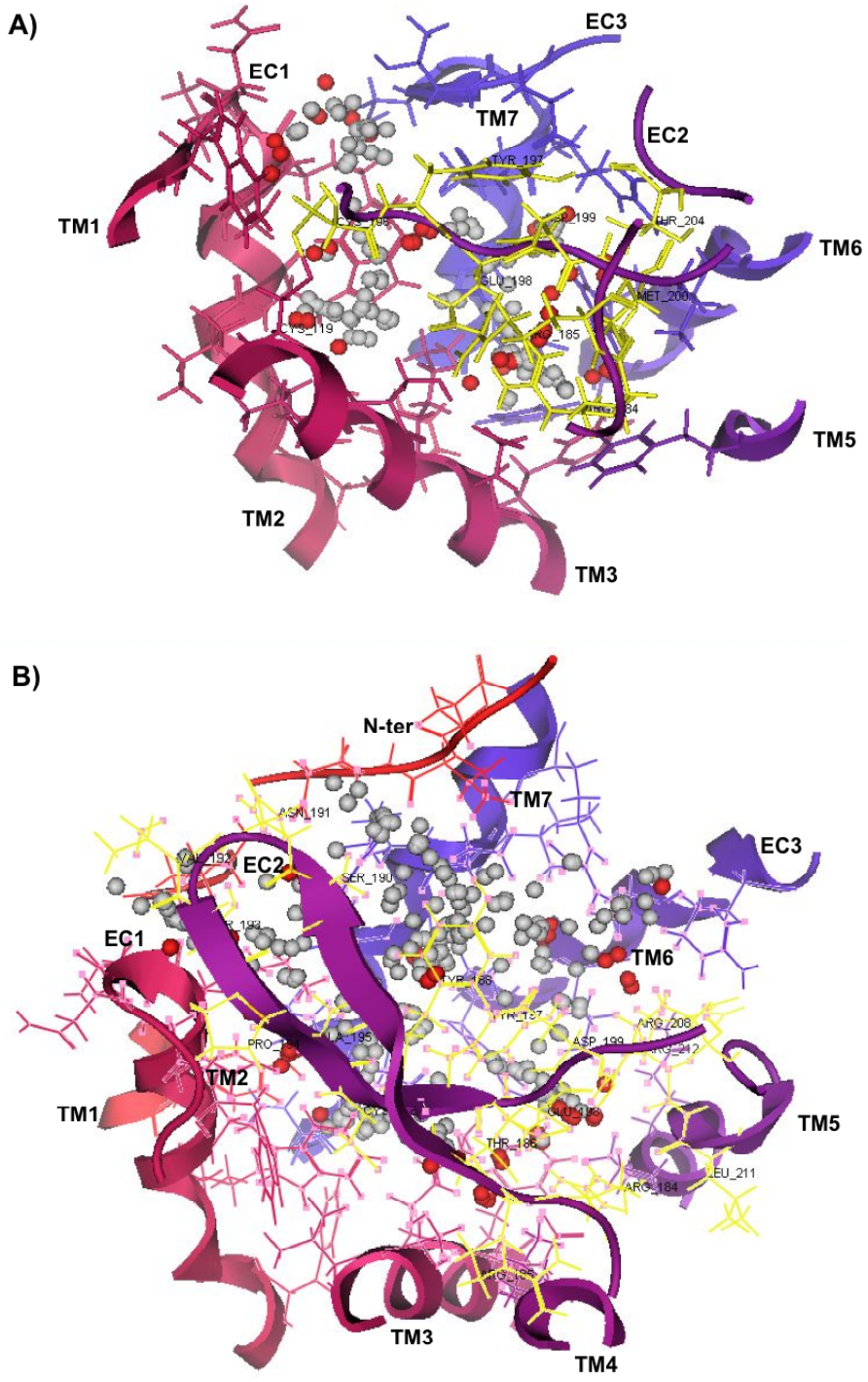
A)
EC1
EC3
TM7
EC2
TM1
TM6
TM5
TM2
TM3
B)
N-ter
TM7
EC3
EC2
EC1
TM6
TM2
TM1
TM5
TM3
TM4

Secondary structure of the second extracellular loop of CXCR2

Structures of the second extracellular loops of different GPCRs including bovine rhodopsin (bRho), human β_2-AR (beta2AR), CXCR4, and CXCR2 were predicted by SOPMA of NPS@ and NetSurfP (ver. 1.1) (Fig. 13). The predictions for bovine rhodopsin, β_2-adrenergic receptor, and CXCR4 were compared with their crystal structures to evaluate the accuracy of their predictions. In rhodopsin, the prediction of the NetSurfP was very similar with its crystal structure with the accuracy of a kind of secondary structure, number of secondary structures and position of the structures. The α-helix in EC2 of β_2-AR was predicted by NPS@SOPMA, although the sequence length of the predicted helix was very short. In CXCR4, both methods showed two β-strands like its crystal structure.

Based on the accuracy of two methods for secondary structure prediction, the secondary structure EC2 of CXCR2 was predicted and aligned with that of CXCR4-based CXCR2 (CXCR4-CXCR2). Like the CXCR4-based CXCR2 model, two methods provided showed two β-strands. Especially, structure predictions for amino acids surrounding Cys196, a highly conserved cysteine forming disulfide bind with Cys119, were very similar with each other (in NSP@SOPMA, NetSurfP, and homology modeling). Furthermore, the predictions showed beginning of the fifth transmembrane of CXCR2, which is important for defining the boundary of the second extracellular loop of CXCR2.

The second extracellular loop of the CXCR4-based CXCR2 model was superimposed with that of the CXCR4crystal structure. The superimposition

showed the second extracellular loop of CXCR2 is structurally very similar with that of CXCR4 (below 2.0 Å RMSD per residue, 0.6 Å RMSD in total), with an exception of Asn203 of CXCR2 (Asp193 of CXCR4) (over 2.0 Å RMSD per residue).

Figure 13. Prediction of secondary structure of the second extracellular loop of CXCR2

A) Structures of the second extracellular loops of several GPCRs including bovine rhodopsin (bRho), β_2-adrenergic receptor (beta2AR), CXCR4, and CXCR2 were predicted by using NPS@SOPMA and NetSurfP (ver. 1.1). The predictions for bovine rhodopsin, β_2-adrenergic receptor, and CXCR4 were also compared with their crystal structures. The predicted secondary structure of the EC2 of CXCR2 was aligned with that of CXCR4-based CXCR2 (CXCR4-CXCR2). Color code was used to show secondary structures: h = α-helix, e = β-strand, t = turn, and c = coil. Cys residues that form a conserved disulfide bond were indicated with specific signs (* for rhodopsin, β_2AR, CXCR4, and CXCR2, # for intra disulfide bond in only β_2AR). **B)** The structures of the second extracellular loops of CXCR4 and CXCR4-based CXCR2 model were superimposed with each other. All of the residues in the EC2 of CXCR2 except for Asp203 (over 2.0 Å RMSD, compared with Asp193 of CXCR4) were structurally very similar to CXCR4. Two cysteine residues (Cys119 and Cys196) forming a conserved disulfide bond were represented.

A)

```
                                  *
bRho          174 GWSRYIPEGMQCSCGIDYYTPHEETNNES 202
NPS@SOPMA         ecccccctttccccceeecccccccccch
NetSurfP          hhceeeccccceeeeeecccccchhhhh
Crystal           ccceeeeecccceeeeecccccccccccc

                             #     #*
Beta2AR       175 RATHQEAINCYANETCCDFFTN 195
NPS@SOPMA         ccchhcccccccccceeehc
NetSurfP          hccccccceeeecccccccc
Crystal           cchhhhhhhhhhccccccccc

                                  *
CXCR4         175 ANVSEADDRYICDRFYPN 192
NPS@SOPMA         eecccccccccceeeccc
NetSurfP          hhceccccceeeeecccc
Crystal           eeeeeeccceeeeeeccc

                                  *
CXCR2         184 RRTVYSSNVSPACYEDMGNNTANWRMLLR 212
NPS@SOPMA         ecccccccccceeeeccccccchhhhhhh
NetSurfP          hheeecccccceeeeeccccchhhhhhhh
CXCR4-CXCR2       cceeeeettceeeeecccccctthhhhh
(Homology model)
```

B)

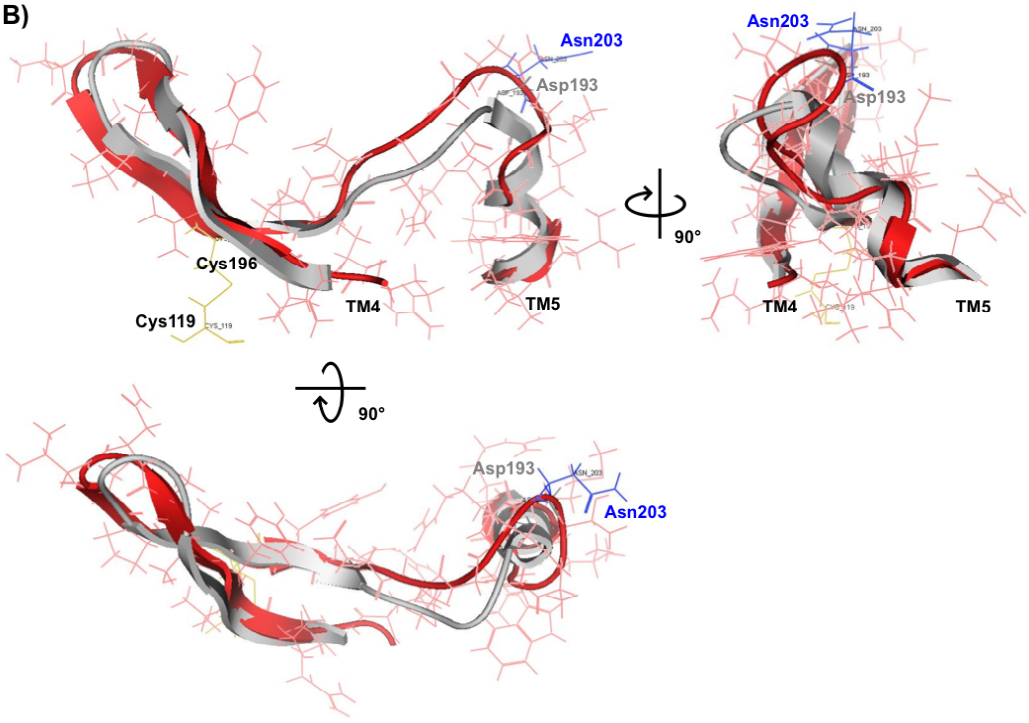

Solvent accessibility of residues on the second extracellular loop of CXCR2 in the inactive state

Wild-type CXCR2 and single cysteine mutant receptors were transiently transfected into HEK293 cells. After 48 h of cultivation, whole cells were harvested and exposed to MTSEA-biotin for labeling of water-accessible cysteine residues. Cell surface-expressed CXCR2 receptors and MTSEA-biotin labeled receptors were immunostained with an anti-CXCR2 antibody and streptavidin-FITC, respectively. Flow cytometry was used to show solvent accessibility of individual CXCR2 receptors mutants. Accessibility values of wild-type CXCR2 and single cysteine mutant receptors were calculated from the mean fluorescence intensity (MFI) of FITC (detects accessibility of an additional Cys residue) divided by MFI of PE (detects total cell surface expression level of CXCR2 receptors). The relative accessibility values were derived from accessibility values of the mutant receptors fold over that of wild-type. A representative graph was drawn for the relative accessibility values (Fig. 14).

The experiment reveals that residue D9C in the amino terminus of CXCR2, is solvent exposed, whereas residue G79C in the first intracellular loop is not water accessible. L182C and F183C which are predicted to be in the fourth transmambrane (TM4) showed similar or less solvent accessibility compared with that of wild-type CXCR2. Residues of the second extracellular loop are divided into two groups by their location relative to residue Cys196 that is critical for a highly conserved disulfide bond found in class A GPCRs. The front group is from

R184C to A195C and the rear group is from Y197C to L214C. Although there is fluctuation between accessibility values, all of the residues in the front group of EC2 are solvent exposed. Interestingly, in the rear group of EC2, Y197C next to Cys196 and the penta-amino acids, T204 to R208, showed similar water accessibility with wild-type CXCR2 and the rest of the rear group are solvent exposed. The solvent accessibility of I213C close to the fifth transmembrane (TM5) was the highest in our experiment.

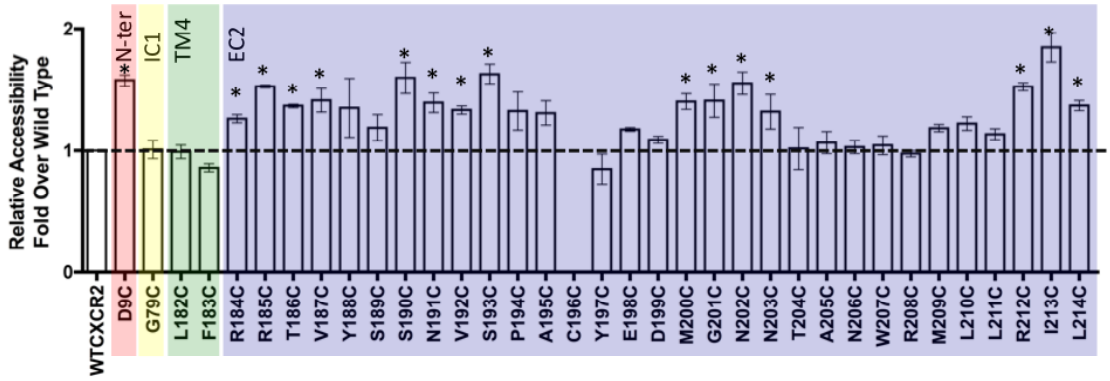

Figure 14. Solvent accessibility maps of the single cysteine mutants of CXCR2.

Each color box indicates different regions of mutant CXCR2 with a cysteine substitution. Red box represents the D9C mutant receptor in the amino terminus, yellow is G79C with a single mutation in the first intracellular loop (IC1), green contains two fourth transmembrane (TM4) mutants (L182C and F183C), and blue has all the mutants for the residues in the second extracellular loop (EC2). Statistical analysis was calculated by student t-test with statistical significance (*) set at $P<0.05$.

Chapter 5 Discussion

Crystal structures of GPCRs have been used to predict structures of other GPCRs that have not been solved (*32, 41, 42*). Homology modeling for CXCR2 using the crystallized bovine rhodopsin have been attempted to explain experiments of receptor stabilization and antagonism (*32, 41, 42, 84, 102*). However, their observations about the predicted CXCR2 models focused on some limited regions of interested (e.g. second extracellular loop and seventh transmembrane). Furthermore, their homology modeled CXCR2 structures were not evaluated through the comparison with more recent crystal structures of other GPCRs.

In this study, we performed homology modeling for CXCR2 by using three crystallized GPCRs, rhodopsin, β_2AR and CXCR4. Sequence alignments between them showed conservation of highly conserved motifs (e.g. (D/E)R(Y/W), NPXXY, and toggle switch), pointing to the possibility of using the three crystal structures as templates for the homology modeling (Fig. 7, 8, 9). Furthermore, the motifs and alignments were used to compare locations and length of transmembrane helices for evaluation of homology modeled CXCR2. The highly conserved disulfide bond linking TM3 and EC2 was automatically generated during the homology modeling process in all the models, but only the CXCR4-based CXCR2 model has one more disulfide bond linking the amino terminus and EC3. The homology modeled structures are intended to show

structural similarity with their templates. Especially since the secondary structures in the second extracellular loops were the same as their original templates (e.g. β-strands of rhodopsin and α-helix of β_2AR) (Fig. 10) and their RMSD values also represented the intention (Fig. 11). However, we made use of β_2AR and CXCR4 as a template for homology modeling, even though they have some structural modifications that interrupt modeling for other GPCRs (e.g. fusion with T4 lysozyme in the third intracellular loop in both structures, and an intra-disulfide bond in the second extracellular loop found only in β_2AR). Even though all three crystallized GPCR stuctures were used as templates and showed significant structural conservation in transmembrane domains, CXCR4 might be the best template for CXCR2 based on high identity (33.3%) in sequence alignment and the lowest RMSD values (0.78Å) in structure superposition (Fig. 9,10). Furthermore, two secondary structure prediction programs, NPS@SOPMA and NetSurfP were used to predict the secondary structure of the second extracellular loop of CXCR2. In three GPCRs including rhodopsin, β_2AR, and CXCR4, the programs showed highly accurate results in the comparison of crystal structures and their predictions. The prediction of the programs suggested that the second extracellular of CXCR2 has two β-strands like rhodopsin and CXCR4. Similarly, the CXCR4-based CXCR2 model suggested two β-strands, even though CXCR2 and CXCR4 have very low identity between the residues in their second extracellular loops. Interestingly, the superimposition of CXCR4-based CXCR2 and CXCR4 suggested that the

structure of the second extracellular loop of the CXCR2 model might be very similar with CXCR4 (Fig. 13).

We also studied the topology of residues in the EC2 of CXCR2 by using substituted-cysteine accessibility method (SCAM), due to the importance of this region in ligand binding and potential receptor activation. Unlike the common SCAM process with immunoblotting (*9, 130*), flow cytometric analysis was performed to amplify signals of FITC-streptavidin bound MTSEA-biotin. Furthermore, cell surface expression levels of mutant receptors that are needed to normalize MTSEA-biotin accessibility were measured at the same time through immunostaining with a specific antibody against CXCR2. The refined approach was evaluated by the accessibility of several mutant receptors including D9C (amino terminus), G79C (IC1), L182C (TM4), and F183C (TM4).

Our SCAM results indicate that most of the residues in EC2 are water-accessible in the inactive state of CXCR2 (in the absence of ligand) (Fig. 14). Especially, all the charged residues (R184C, R185C, E198C, D199C, and R212C) in EC2 except for R208C are exposed to solvent. Because charged residues on the extracellular loops were considered as key residues to form a binding pocket, ligands of CXCR2 could contact the exposed residues followed by receptor activation. In the study to find CXCL8 binding sites to homology modeled CXCR2 structures, most of the residues in EC2 including the charged residues were predicted as potential key residues (Fig. 12). In EC2, five sequential amino acids ^{204}TANWR^{208} were predicted as non-accessible residues.

These residues might be involved in the interaction with the amino terminus or other extracellular loops. Since the CXCR2 models lack an amino terminus, there are limitations to studying the mechanisms for ligand binding and receptor activation. Thus our interdisciplinary approaches and observations would be very helpful to plan new approaches to discover unknown mechanisms about CXCR2.

PART III

INVOLVEMENT OF THE SECOND EXTRACELLULAR LOOP OF CXCR2 IN LIGAND RECOGNITION AND RECEPTOR ACTIVATION

Chapter 1 Abstract

It has been shown that the amino terminus and second extracellular loop of CXCR2 are crucial for ligand binding and receptor activation. The lack of an ionic lock motif (a Glu residue) in the third intracellular loop in CXCR2 focuses an investigation of two extracellular regions in CXCR2 involved in receptor recognition and activation. Using constitutively active mutants, D9K and D9R, in CXCR2, the potential role of charged residues in the second extracellular loop of CXCR2 was investigated.

Combinatorial mutations consisting of the constitutively active mutants in the amino terminus and single mutations of charged residues in the second extracellular loop were generated to study two concepts including “attraction” and “repulsion” models. The mutant receptors were used to test their effects on cell surface expression, ligand binding, receptor activation through PLC-β3, and cellular transformation. All the mutations in the repulsion model result in CXCR2 receptors that are unable to bind ligand, indicating that all the Arg residues (Arg184, Arg185, Arg208, and Arg212) in the second extracellular loop are important for ligand recognition. Although charge-reversal complementary mutations in the repulsion model were expected to retain structural constraints of CXCR2, none of the mutant receptors function as wild-type CXCR2 in the inactive and active states. Interestingly, mutations in the attraction model partially inhibited receptor activation of constitutively active mutant D9K, suggesting that Glu198 and Asp199 residues in the second extracellular loop are highly

associated with receptor activation. Furthermore, a novel constitutively active mutant E198A/D199A was identified in this study. These negatively charged residues are very close to a disulfide bond (Cys119-Cys196) linking the second extracellular loop and the third transmembrane. The unique location suggests that the neutralization (with Ala residues) of the residues might be needed to control TM3 promote slight breakdown of structural constraint of the constitutively activated CXCR2 with D9K mutation.

These observations are helpful to understand how the extracellular regions of CXCR2 interact with its cognate ligands and transfer signals intracellularly.

Chapter 2 Introduction

GPCRs respond to a variety of ligands that are classified into agonist and antagonist. GPCRs can also induce constitutive activation in the absence of external ligands. Single point mutations of GPCRs as well as some wild-type GPCRs have been shown to lead to constitutively activity (*131*). Moreover, the constitutively active mutants of GPCRs have been used as important pharmacological targets for the development of potent drugs against mutant GPCR-mediated diseases (*132*).

In class A GPCRs, it has been shown that the highly conserved (D/E)R(Y/W) motif in TM3 is important for interaction with D/E residue at the boundary of IC3 and TM6 (*38*). The interaction, also called the 'ionic lock', is crucial to stabilize the inactive conformation of GPCR receptors. Mutations of these residues result in an increase of constitutive activity (*39, 133*). Furthermore, breakage of the ionic lock is linked to turning on the 'toggle switch' in TM6, with the change of configuration of a conserved Pro residue surrounding aromatic residues in TM6 (*38*). These mechanisms for receptor activation are conserved in both rhodopsin and β_2AR have been well studied. However, in most (~80%) of class A GPCRs, residues for the ionic lock or toggle switch are not present (*133*).

Currently, novel mechanisms for receptor activation have been found. The first example is a model with ionic locks on the extracellular surface (*134*). Free fatty acid receptor 1 (FFAR1) does not contain residues for both an ionic lock and

toggle switch similar to rhodopsin and β_2AR. FFAR1 contains a Lys instead of a Glu in TM6 (for an ionic lock) and a Val and Asn rather than the aromatic residues in TM6 (for a toggle switch). Interestingly, homology modeling of FFAR1 showed two ionic locks between two Glu residues on EC2 and two Arg residues on distinct transmembranes including TM5 and TM7. Single alanine mutations for the two Glu on EC2 induced constitutive activation of the receptor in the absence of ligand, indicating that the EC2 of the receptor can participate in receptor activation. Furthermore, a random mutagenesis study of residues on EC2 of the complement factor 5a receptor (C5aR), a class B GPCR, showed that multiple residues in EC2 are highly associated with receptor stabilization in the inactive state (*36*).

A second example is the role of conserved Cys residues in the amino terminus and third extracellular loop (EC3) of chemokine receptors (*135*). CXCR4 was used as a model to substitute a Ser pair, aromatic pair (Phe), or salt bridge pair (Arg/Asp) for the conserved Cys residues. The mutation with a Ser pair in a constitutively active mutant (CAM) CXCR4 (N119S) disrupted the receptor activation, whereas the other substitutions with the Phe or Arg/Asp pair in the CAM CXCR4 showed little effect on the constitutively activity of the receptor. The result suggested that the disufide bond derived from the conserved Cys in the amino terminus and EC3 of chemokine receptors is important for receptor activation and signaling.

CXCR2 shares the highly conserved (D/E)R(Y/W) motif like other GPCRs in class A. A point mutation of Asp143 (to Val, the same with KSHV-GPCR) of

the motif on CXCR2 leads to constitutive activation of the receptor and cellular transformation similar to KSHV-GPCR (*118*). However, like FFAR1 (Lys219), CXCR2 has Lys246 instead of D/E residue in TM6 to interact with Arg of the (D/E)R(Y/W) motif for an ionic lock, whereas aromatic residues (Trp264 and Tyr267 in TM6 of CXCR2) for a toggle switch are conserved in TM6. This suggests that CXCR2 is different in the mechanism for receptor activation compared to rhodopsin and β_2AR. In a previous study of the role of EC2 in activation and regulation of the receptor, it has been shown that mutation of Asp199 (to Val) in EC2 delayed the internalization of the receptor, whereas substitution with Asn restored the internalization speed (*84*). With homology modeling of CXCR2 based on rhodopsin, the study suggested that Asp199 functions to stabilize the receptor conformation using hydrogen bonds between several residues (Arg185, Thr186, and Arg208) in EC2. Currently, it has been shown that single point mutations of Asp9 in the amino terminus of CXCR2 leads to constitutive activation to promote cellular transformation activity in cells stably expressing the mutant receptors (Park et al., unpublished). The study also demonstrated that different constitutive active mutants show signal specificity. Taken together, these observations suggest that both the amino terminus and EC2 of CXCR2 are crucial in receptor activation.

Viral oncogene ORF74 encoded by Kaposi's sarcoma-associated herpesvirus (human herpesvirus 8), also called KSHV-GPCR, is the closest homolog to CXCR2 (*103*). KSHV-GPCR constitutively activates AP-1, CREB, NFAT, and MAPK via $G\alpha_i$ or $G\alpha_q$, and NF-κB through only $G\alpha_q$ subtype in

different cell lines including COS-7, primary effusion lymphoma (PEL), and endothelial cells (*104-107*). Currently, studies of M33 of murine cytomegalovirus (MCMV) and US28 of human cytomegalovirus (HCMV), viral GPCR homologs, have been shown that $G\alpha_q$ protein is activated to induce phopholipase C-β (PLC-β) activity, followed by stimulation of CREB and NF-κB signals (*108-111*). Additionally, M33 can induce CREB and NF-κB stimulation via a PLC-β independent manner (*112*). On the other hand, another GPCR homolog UL33 of HCMV enhances CREB transcriptional activities by G_s pathway not $G_{q/11}$ pathway (*113*).

As stated previously, a point mutation of Asp143 to Val in the highly conserved (D/E)R(Y/W) motif in CXCR2 leads to constitutive activation and cellular transformation (*118*). The transforming capacities were totally inhibited by using AG490, a specific kinase inhibitor of JAK2-STAT3 signaling (*119*). It has been demonstrated that the constitutive activity of KSHV-GPCR and CXCR2 mutant D143V is highly associated with STAT3 phosphorylation. A current study of CXCR2 expressed in ovarian cancer cells reported that cancer growth is regulated by the MAPK and NF-κB pathways (*121*). Additionally, it was shown that the chemokine CXCL1 binding to CXCR2 but not CXCR1 induces transactivation of epidermal growth factor receptor (EGFR) via the chemokine receptor, followed by proliferation of ovarian cancer cells (*122*).

In this study, we investigated a role of charged residues in EC2 of CXCR2 in ligand binding and receptor activation. Two concepts, “attraction” and “repulsion” models were designed to investigate the mechanism of CXCR2

activation (Fig. 15). To end that, we constructed combinatorial mutation sets consisting of constitutively active mutants (CAM) Asp9 in the amino terminus and substitutions in EC2. These mutant receptors were generated by site-directed mutagenesis and transfected into mouse fibroblast NIH3T3 cell lines. The NIH3T3 cells stably expressing wild-type CXCR2 and mutant receptors were used to investigate cell surface expression of the receptor, ligand-binding, and receptor activation through phospholipase C-β3 (PLC-β3).

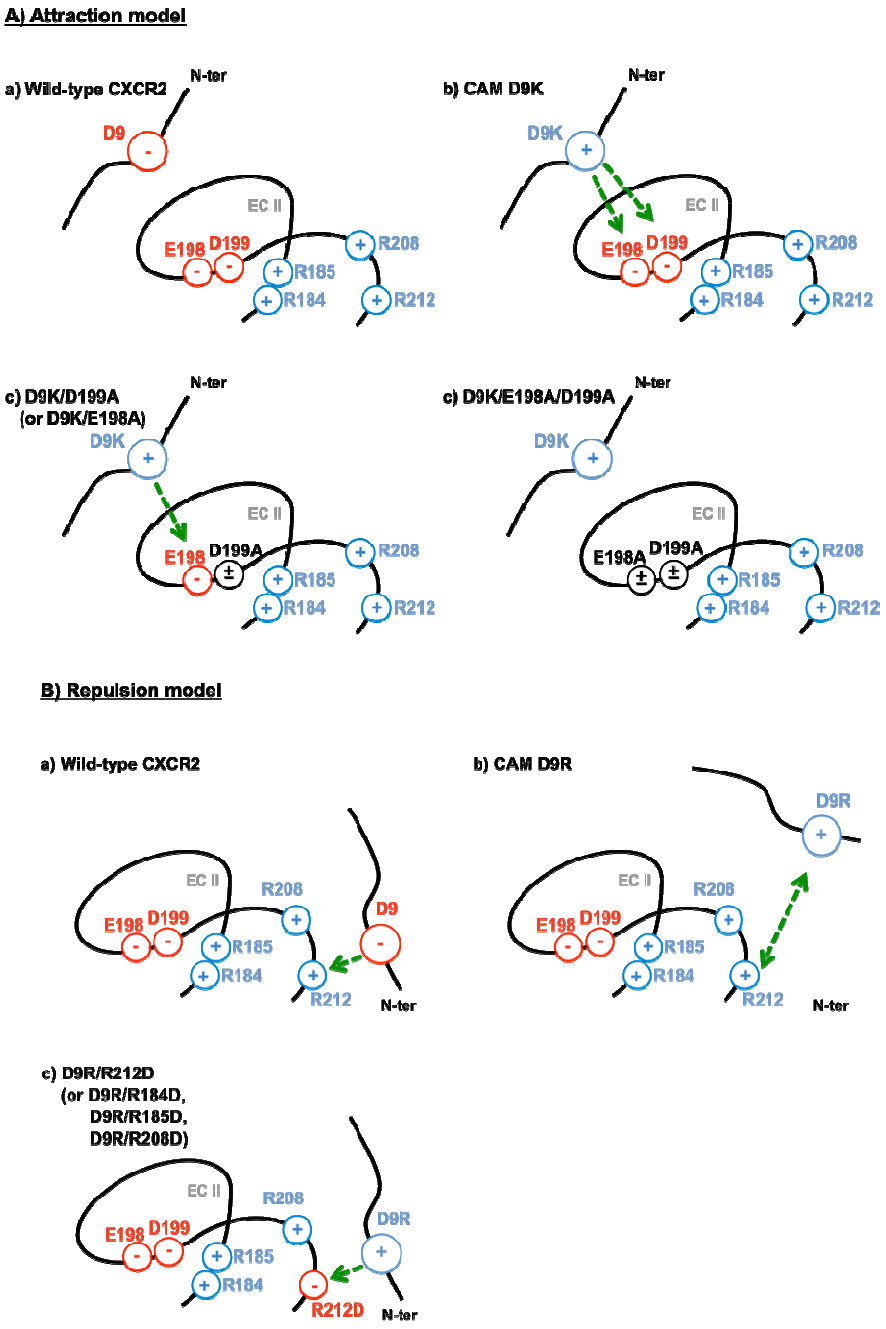

Figure 15. Models of receptor activation of CXCR2

This study used two models, attraction model (A) and repulsion model (B) to understand the mechanism of receptor activation of CXCR2.

CHAPTER 3 MATERIALS AND METHODS

Cell lines and media

NIH3T3 mouse fibroblast cells were cultured with DMEM containing 10% fetal clone 3 (FC3), 1X NEAA, and 1X penicillin/streptomycin. Transfectant NIH3T3 cells stably expressing wild-type CXCR2 or mutant receptors were maintained in the medium with 800 μg/ml G418, also known as Geneticin.

Site-directed mutagenesis and transfection

The *CXCR2* gene cloned in pRc/CMV vector was used as a template for site-directed mutagenesis. Forward and reverse primers were manually designed for charged residues on EC2 of CXCR2 (Table 4). PCR mutagenesis was performed with a modification of the QuickChange® method (Stratagene). Dpn I digestion treatment was performed, followed by cleaning via a PCR purification kit. All mutations were conformed by sequencing analysis (Molecular biology resource facility, University of Tennessee, Knoxville).

Plasmid DNAs of wild-type CXCR2 and mutant receptors were used to transfect NIH3T3 cells. The transfections were performed with Lipofectamine 2000 reagent according to the manufacturer's instructions. 4.0×10^5 NIH3T3 cells were seeded in 6-well plates one day before transfection. 2 μg of plasmid DNA and 4 μl of Lipofectamine 2000 were individually diluted into 250 μl fresh DMEM, incubated for 5 min at room temperature, and mixed together followed by

incubation for 30 min at room temperature. The mixtures and 500 μl fresh DMEM were added to each well and incubated for 4 hr at 37 ℃. The mixtures were substituted to new medium including 10% FC3, followed by cultivation for 48 hr at 37 ℃. Transfectant NIH3T3 cells stably expressing wild-type CXCR2 and mutant receptors were selected using the medium with 800 μg/ml G418. Single clonal cell lines were derived from the transfectants. An anti-CXCR2-specific monoclonal antibody, phycoerythrin (PE)-conjugated mouse monoclonal anti-human IL-8 receptor B (R&D systems, MN), and flow cytometry were used to confirm the cell surface expression level of CXCR2 on the clonal cell lines.

Ligand binding assay

Competition ligand binding assays were performed as previously described (*136*). Wild-type CXCR2 and mutant receptors were transiently transfected into COS-7 cells. After 48 hr, binding was performed on whole cells for 3 hr at 4 ℃ using radio-labeled ^{125}I-CXCL8 ligand in binding buffer (50 mM HEPES, pH 7.4, 1 mM $CaCl_2$, 5 mM $MgCl_2$, and 0.5% bovine serum albumin) and increasing amounts of unlabeled CXCL8. Washing was performed four times with binding buffer with 0.5 M NaCl at 4 ℃.

Immunostaining of phospho-PLC-β3

The single clonal cell lines stably expressing wild-type CXCR2 or mutant receptors were used to measure serine phosphorylation (for Ser537) of PLC-β3.

4.0 x 10^5 cells were seeded in 60 mm dishes with the medium containing 10% FC3 and after one day the medium is substituted to fresh DMEM without serum. After 18-20 hr the cells were harvested with 2 ml 1X PBS using cell scraper, centrifuged at 400 *g*, and fixed with 100 µl fixation buffer BD Cytofix^{TM} for 15 min (BD Biosciences). The fixed cells were permeabilized with BD^{TM} Phosflow Perm Buffer III (BD Biosciences) for 30 min on ice. A rabbit polyclonal antibody, p-PLC-β3 (Santa Cruz Biotechnology, Inc., CA) (1:50 dilution) was added to the permeabilized cells for 1 hr at room temperature in dark. Alexa Fluor 488 goat anti-rabbit IgG antibody (Invitrogen, CA) (1:50,000) was used as secondary antibody to immunostain the cells for 1 hr at RT in dark. There was a washing with 4ml 1X PBS between each step. BD FACSCalibur^{TM} (BD Sciences) was used to obtain flow cytometry data from the immunostained samples. The flow cytometry data were analyzed by FlowJo 8.7 software (Tree Star Inc., OR).

Loss of contact inhibition (foci formation) assay

The foci formation assay was performed by previously described (*118*). 1.0 x 10^5 untransfected NIH3T3 cells were cultured in each well of a 6-well plate. After one day, 100 stable transfectants were seeded on top of the untransfected cells and maintained with serum-reduced medium containing 2% FC3. The cells were grown with or without inhibitors including PTX, U-73122, or AG490. Foci were counted after 2 weeks.

Chapter 4 Results

Charged residues in the second extracellular loop of CXCR2 are required for ligand recognition

To study the role of charged residues in second extracellular loop of CXCR2, negatively charged residues including Glu198 and/or Asp199 and positively charged residues such as Arg184, Arg185, Arg208, and Arg212 were substituted to Ala residue to neutralize their charges. The positively charged residues were also mutated to Asp residues in the charge-reversal manner. Non-charged residues including Asn191, Asn202, and Asn203 were substituted to Ala as controls. The mutant constructs were generated by using site-directed mutagenesis and were conformed by sequence analysis.

The wild-type CXCR2 and mutant receptors were transfected into mouse fibroblast NIH3T3 cell lines followed by single clonal selection. With NIH3T3 cells stably expressing the wild-type CXCR2 and mutant receptors, cell surface expression of the receptors was investigated by immunostaining with a specific antibody for CXCR2 (Table 4). There was no detectable difference in cell surface expression between wild-type CXCR2 and mutant receptors.

To measure CXCL8-binding affinity to the wild-type CXCR2 and mutant receptors, the constructs were transiently transfected in COS-7 cell lines. Competition binding assays with radio-labeled ^{125}I-CXCL8 were performed to determine ligand binding affinity (IC_{50}) for each construct (Table 4). We found

that all the charged residues on EC2 of CXCR2, except for D199A, are involved in ligand binding. On the other hand, the mutations of Asn, an uncharged residue, in EC2 showed a similar level of binding affinity to the wild-type CXCR2 receptor.

Involvement of the amino terminus and second extracellular loop of CXCR2 in ligand recognition

The combinatorial mutations containing the CAM D9 residue in the amino terminus and mutations of charged residues in EC2 of CXCR2 were transiently transfected into COS-7 cell lines to measure CXCL8 binding affinity. Competition ligand binding with radio-labled ^{125}I-CXCL8 was performed for each construct (Table 4). Like the cases of the single mutations in EC2, all the combinatorial mutant receptors showed no binding to CXCL8. Interestingly, D9K/D199A showed no CXCL8 binding, whereas IC_{50} values of D9K and D199A individually are similar to wild-type CXCR2.

Table 4. CXCL8-binding and surface expression of wild-type CXCR2 and mutant receptors

Receptor construct		IC_{50} CXCL8 (nM)**	Surface expression***
Wild-type	CXCR2*	8.92±0.05	+
N-ter	D9K*	8.56±0.05	+
	D9R*	8.69±0.21	+
EC2	E198A	> 1000	+
	D199A	8.82±0.20	+
	E198A/D199A	> 1000	+
	R184A	N.D	+
	R185A	N.D	+
	R208A	N.D	+
	R212A	N.D	+
	R184A/R185A	N.D	+
	R184D	> 1000	+
	R185D	> 1000	+
	R208D	> 1000	+
	R212D	> 1000	+
	N191A	7.87±0.27	+
	N202A	8.78±0.09	+
	N203A	8.88±0.16	+
	N202A/N203A	8.75±0.09	+
N-ter and EC2	D9K/E198A	> 1000	+
	D9K/D199A	> 1000	+
	D9K/E198A/D199A	> 1000	+
	D9R/R184D	> 1000	+
	D9R/R185D	> 1000	+
	D9R/R208D	> 1000	+
	D9R/R212D	> 1000	+

*Data of wild-type CXCR2, D9K, and D9R were derived from Park et al., (Park et al., unpublished).
** N.D = not determined
>1000 = the CXCL8 binding constants of certain mutant receptors were undetectable up to 1 μM. The sign >1000 means 1000-fold greater than IC_{50} of CXCL8 binding towild-type CXCR2.
*** Surface expression was determined through immunostaining with an ant-CXCR2 antibody and flow cytometric analysis. The wild-type CXCR2 and mutant receptors showed the very similar expression level (+).

Constitutively inactive mutants CXCR2 induced by charge-reversal complementary mutations (derived from repulsion model)

Charge-reversal combinatorial mutant receptors consisting of CAM D9R and RxD mutations (R184D, R185D, R208D, and R212D) in EC2 were constructed to study whether the mutant receptors lead to constitutive activation like CAM D9R or change their structural constraints related to receptor function. Charge-reversal single mutations alone (R184D, R185D, R208D, and R212D) were used as controls. The NIH3T3 cells stably expressing the mutant receptors were used to investigate receptor activation by PLC-β3 signaling. The transfectants were immunostained with a specific PLC-β3 antibody to detect serine phosphorylation (Ser537 of PLC-β3). Flow cytometric analysis showed that CAM D9R induced significantly less phosphorylation than wild-type CXCR2 (Fig. 16). Both the charge-reversal single and combinatorial mutant receptors showed more phosphorylated PLC-β3 than wild-type CXCR2, suggesting the inactivation of PLC-β3.

To study whether the inactivation of PLC-β3 is involved in cellular transformation by the mutant receptors, foci formation assays were performed. None of the charge-reversal mutants formed foci, whereas CAM D9R significantly produced foci through constitutive activation (Fig. 17). Therefore, the charge-reversal single mutations as well as the combinatorial mutations lead to disruption of downstream signal transduction of CXCR2 through inhibition of PLC-β3 activity.

Negatively charged residues in EC2 of CXCR2 are highly associated with receptor activation of CXCR2 (derived from attraction model)

The combinatorial mutant receptors consisting of CAM D9K and substitution of negatively charged residues to Ala (E198A, D199A, E198A/D199A) were constructed. The mutant receptors were used to investigate whether the mutant receptors retained constitutive activation like CAM D9K or induce some change related to receptor function. The transfectants stably expressing the mutant receptors were used to study receptor activation by PLC-β3 signaling. Immunostaining and flow cytometric analysis with a specific PLC-β3 antibody were performed for determining serine phosphorylation (Ser537 of PLC-β3). In flow cytometric analysis, it was found that CAM D9K induced less PLC-β3 phosphorylation than wild-type CXCR2 (Fig. 16). The combinatorial mutations (D9K/E198A, D9K/D199A, D9K/E198A/D199A) and double mutation (E198A/D199A) showed PLC-β3 phosphorylation levels between CAM D9K and untransfected NIH3T3. Especially, D9K/D199A had a very similar level to CAM D9K in phosphorylation of PLC-β3. On the other hand, two single mutant receptors (E198A and D199A) showed the same with untransfected NIH3T3. These indicate that the mutant receptors except for E198A and D199A induce activation of PLC-β3 like wild-type CXCR2, but showed some differences in PLC-β3 activation levels.

To study whether the activation of PLC-β3 by combinatorial mutant receptors leads to cellular transformation like CAM D9K, foci formation assays were performed. All the transfectants except for E198A and D199A formed foci,

but the number and size of foci were significantly smaller than CAM D9K (Fig. 18). Furthermore, treatment with U-73122, an inhibitor of PLC-β signaling, prevented the formation of foci derived from all the combinatorial mutant receptors (Fig. 19). Therefore, the change of PLC-β3 activation levels might result in a partial reduction of the cellular transformation activity.

A novel constitutively active mutant with double alanine mutations in CXCR2

A novel CAM was identified among the mutations in EC2 of CXCR2. A double mutation E198A/D199A had cellular transformation activity, whereas the individual single mutations of negatively charged residues (E198A and D199A) did not (Fig. 16). Interestingly, the triple combinatorial mutant (D9K/E198A/D199A) consisting of two CAMs (D9K and E198A/D199A) rarely produced foci.

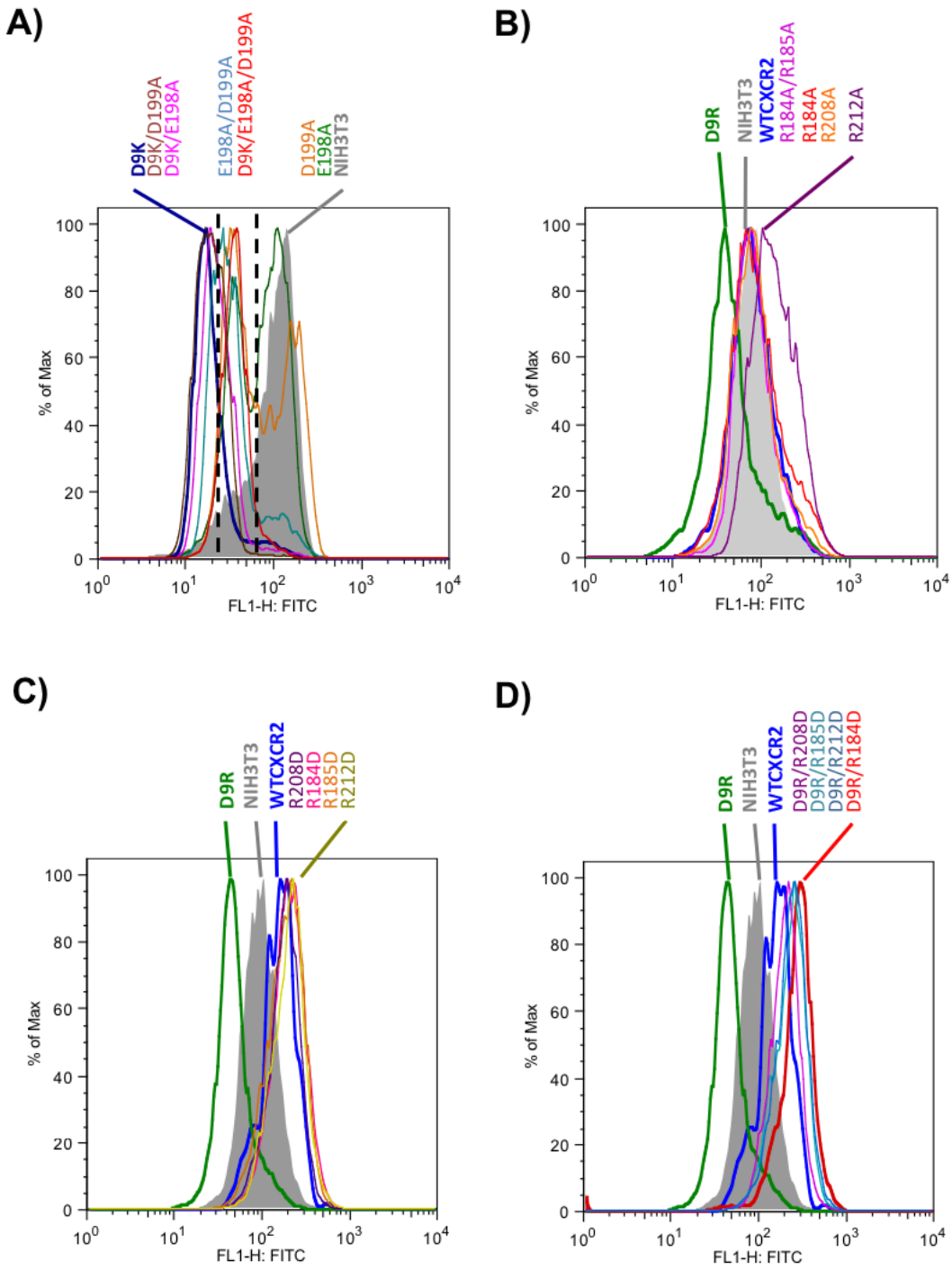

Figure 16. Phosphorylation of PLC-β3 in wild-type and mutant CXCR2 receptors.
These figures showed phosphorylation of PLC-β3 of CAM D9K and mutant receptors for the attraction model **(A)**, CAM D9R and mutant receptors for the repulsion model **(B, C, and D)**.

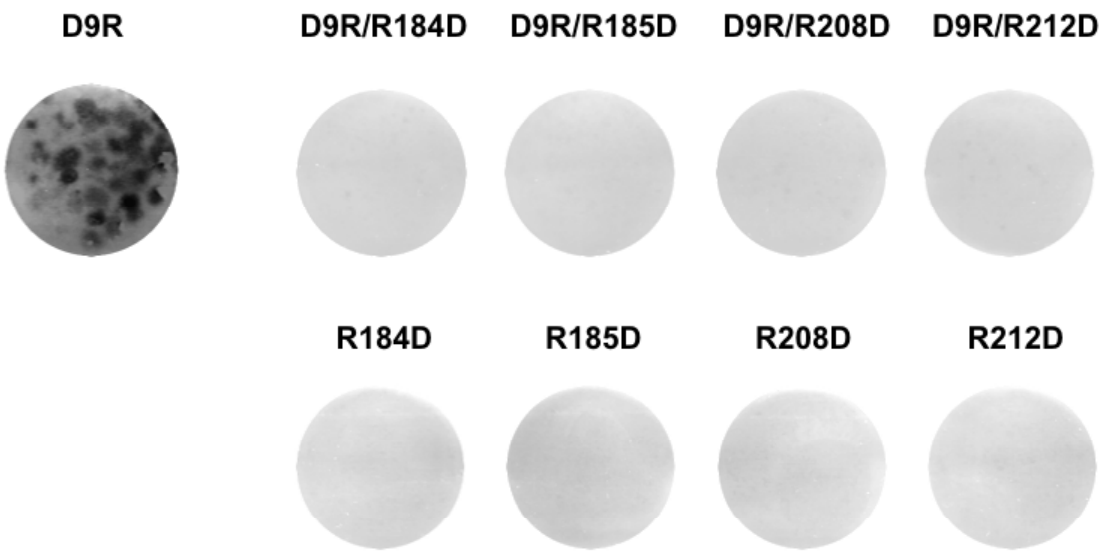

Figure 17. Foci formation assay with NIH3T3 transfectants stably expressing charge-reversal complementary mutant receptors derived from the repulsion model.

Constitutively active mutant D9R was used for positive control. None of all the mutant transfectants showed foci formation.

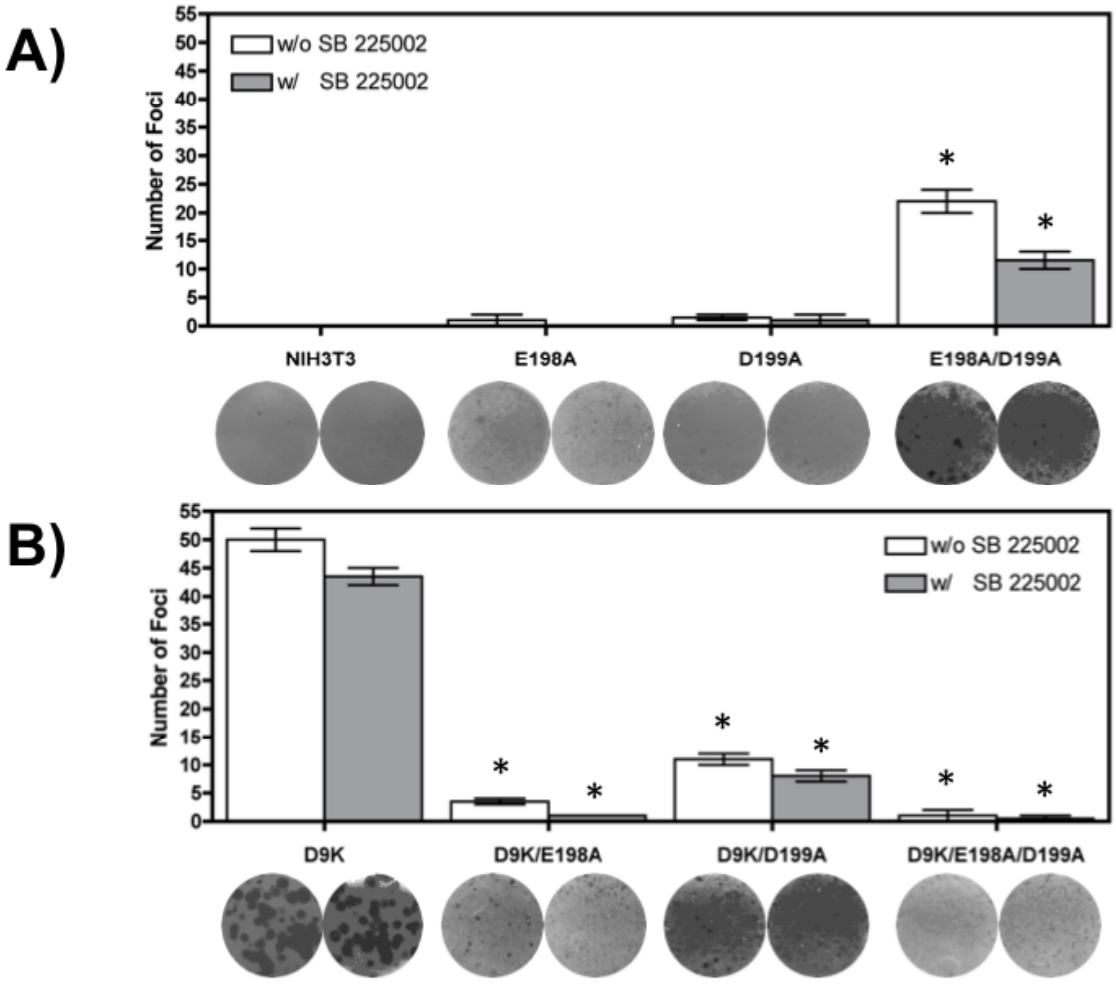

Figure 18. Foci formation assay with NIH3T3 transfectants stably expressing combinatorial mutant receptors derived from the attraction model.

A) Untransfected NIH3T3 cells were used as the negative control. E198A/D199A formed foci, whereas none of E198A and D199A showed a difference in background. **B)** Constitutively active mutant D9K was used as the positive control. All the combinatorial mutants showed a smaller number of foci compared to D9K. Especially, triple mutant D9K/E198A/D199A rarely formed foci. Statistical analysis was calculated by student t-test with statistical significance set at $P<0.05$ (*). Numbers of foci derived from E198A/D199A and all the combinatorial mutants were compared with that of untransfected NIH3T3 cells and D9K, respectively.

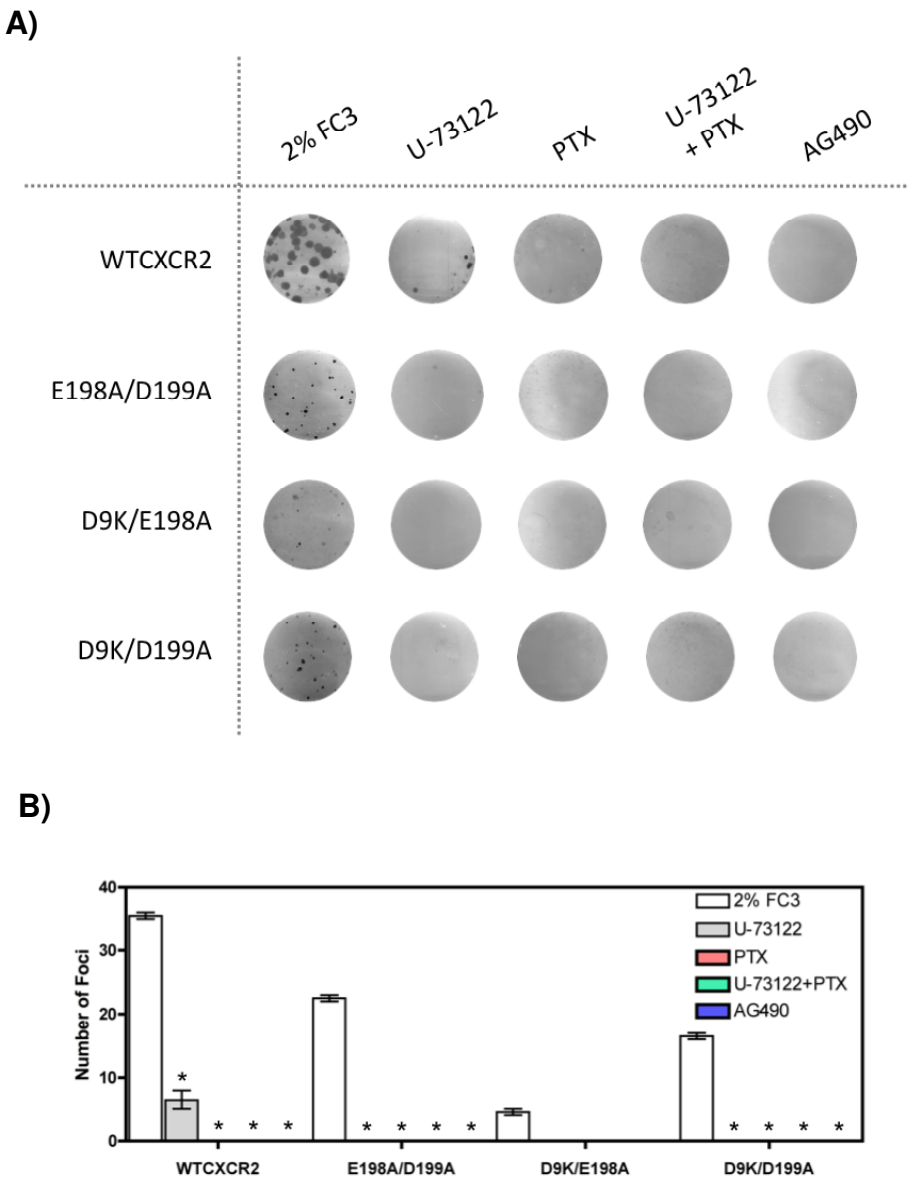

Figure 19. Foci formation assay in the presence of inhibitors of intracellular signaling.

A) There are no foci in the presence of all the inhibitors. 25 μM U-73122 was used for inhibition of $G\alpha_q$-mediated PLC-β signaling, 100 μg/ml pertussis toxin (PTX) was for $G\alpha_i$, and 50 μM AG490 was for Janus kinases-mediated signal transducer and activator of transcription 3 (STAT3) pathway. **B)** T-test showed that inhibitor-mediated reductions of constitutively activation of E198A/D199A and D9K/D199A mutant receptors are statistically significant ($p < 0.05$, *).

Chapter 5 Discussion

An increasing number of studies have focused on the mechanism of receptor activation of GPCRs due to its importance as pharmacological targets (*45, 132*). Two major mechanisms for receptor activation including the ionic lock and toggle switch were found in rhodopsin and β_2AR, whereas most of class A GPCRs do not contain these residues necessary for these mechanisms (*38, 133*). Some including rhodopsin and β_2AR showed the conservation of a Glu residue in the boundary of IC3 and TM6 to interact with the (D/E)R(Y/W) motif for receptor stabilization in the inactive state. CXCR2 also does not contain a conserved Glu residue for the ionic lock, suggesting CXCR2 undergoes an unknown mechanism for receptor activation.

It has been shown that the amino terminus and second extracellular loop of CXCR2 is crucial for ligand recognition and receptor activation (*80, 81, 83-88, 124*). Interestingly, a previous study of the EC2 of CXCR2 showed that a negatively charged residue, Asp199 is crucial to manage internalization speed of the receptor (*84*). Furthermore, another current investigation showed that single mutations (e.g. D9K and D9R) of Asp9 in the amino terminus of CXCR2 lead to constitutive activation (Park et al., unpublished). These observations suggest that charged residues in the second extracellular loop of GPCRs may play a role in receptor stabilization and activation.

To study a role for EC2 in ligand binding, we generated single mutations in EC2, including the substitution of negatively charged residues including Glu198

and/or Asp199 and positively charged residues such as Arg184, Arg185, Arg208, and Arg212 to Ala residue to neutralize their charges. The Arg residues are also mutated to a charge-reversal residue, Asp residue. Like wild-type CXCR2, the mutant receptors were well expressed at the cell surface. However, all the mutant receptors except for D199A demonstrated no binding affinity for CXCL8. This result suggests that charged residues in EC2 of CXCR2 are crucial for ligand recognition, but do not affect cell surface expression.

Furthermore, we designed two concepts, the attraction and repulsion models, to understand CXCR2 activation (Fig. 15). To end that, we constructed two different combinatorial mutation sets consisting of CAMs (D9K and D9R) and the substitutions in EC2. All the combinatorial mutant receptors were well expressed at the cell surface but had no CXCL8 binding affinity similar to most of the single mutations in EC2 of CXCR2. Interestingly, all the complementary charge-reversal mutants to prove the repulsion model (D9R/R184D, D9R/R185D, D9R/R208D, and D9R/R212D) showed no ligand binding affinity, inactivation of PLC-β3 and inhibition of cellular transformation. The mutants were expected to function like wild-type CXCR2 because some studies have generated charge-reversal mutations to mimic the structural constraints of their wild-type receptors (*135*). However, unexpectedly, their structural constraints would not be the same with wild-type CXCR2, even though there is no problem in the protein folding of the mutant receptors (Table 4). Therefore, the mutant receptors would be constitutively inactive mutants (CIM) or dead receptors. On the other hand, another set of the combinatorial mutants (D9K/E198A, D9K/E198A, and

D9K/E198A/D199A) retained their constitutive activity via PLC-β3 signaling even though the mutants were unable to bind CXCL8.

Interestingly, similar results were observed with charged residues in the extracellular loops of neurohyphophysical hormone receptors including vasopressin and oxytocin receptors (*137*). Using Ala mutations and charge-reversal substitutions, some of the charged residues showed a significant reduction of ligand binding affinity, regardless of surface expression. The study also generated two complementary mutants including R46D/D204R and R125D/D204R to prove interaction between the mutated residues. However, the cell surface expression level of the combinatorial mutants was very low (≤20% fold over wild-type) and the binding affinities for their cognate ligands were significantly reduced or undetectable.

Consistent with our result, it has been previously shown that Asp199 in EC2 of CXCR2 is not related to ligand binding (*84*). D199N showed a similar CXCL8 binding affinity to wild-type CXCR2 but D199V has a higher CXCL8 binding affinity than wild-type CXCR2. Furthermore, the mutant receptors (D199N and D199V) had no effect on Ca^{2+} mobilization by CXCL1 or CXCL8 stimulation. Similarly, in this study, D199A showed no difference in PLC-β3 signaling, whereas E198A/D199A induced activation of PLC-β3. Previously, it was shown that negatively charged residues in EC2 of FFAR1 are important for receptor activation for constructing ionic locks to positively charged residues on distinct transmembranes (*134*).

Interestingly, E198A/D199A was identified as a novel constitutively active mutant via foci formation assays. Since many investigations have tried to construct site-directed or random mutagenesis of the EC2 of GPCRs (*36*), it would be the first CAM derived from double mutations of residues in EC2. The double mutant receptor might have structural constraints for CXCR2 activation, whereas the single mutations, E198A and D199A, allow themselves to have inactive forms. The negatively charged residues are very close to a highly conserved disulfide bond (Cys119-Cys196) linking EC2 and TM3. The special location of the two residues in EC2 might explain how the double mutation leads to constitutive activation. The neutralization (with Ala residue) of the residues might induce a structural change in TM3 through the disulfide bond. Furthermore, the substitution with Ala in combinatorial mutant receptors derived from the attraction models might promote breakdown of the structural constraints of CAM D9K.

Unlike rhodopsin and β_2AR, most of class A GPCRs including CXCR2 lack possible residues in IC3 for an ionic lock, pointing to the need to study possible other mechanisms for activation of GPCRs. Our observations might provide new insight to understand a role of extracellular regions (especially, amino terminus and EC2) in ligand binding and receptor activation.

PART IV CONCLUSIONS

Most chemokine receptors can be activated by more than one chemokine (*77*). CXC chemokine receptor 2 (CXCR2) binds multiple CXC chemokines including CXCL1 (GRO-α), CXCL2 (GRO-β), CXCL3 (GRO-γ), CXCL5 (ENA78), CXCL6 (GCP2), CXCL7 (NAP2), and CXCL8 (*78, 79*). Although CXCR1 and CXCR2 show over 75% amino acid identity, only CXCL6 and CXCL8 activate CXCR1, suggesting that the two chemokine receptors have different mechanisms for chemokine ligand binding (*80*). It has been shown that the amino terminus and second extracellular loop of CXCR2 is crucial for ligand recognition and receptor activation (*80, 81, 83-88, 124*). Interestingly, a previous study of the EC2 of CXCR2 showed that a negatively charged residue, Asp199, is crucial to manage internalization speed of the receptor (*84*). Furthermore, another current investigation showed that single mutations (e.g. D9K and D9R) of Asp9 in the amino terminus of CXCR2 led to constitutive activation (Park et al., unpublished). These observations suggest that charged residues in the second extracellular loop of GPCRs may play a role in receptor stabilization and activation. However, the mechanism of the ligand binding and receptor activation is still unknown.

First, in our study, a CXCR2 structure is predicted on the basis of crystal GPCR structures including rhodopsin, β_2AR, and CXCR4 by homology modeling (Fig. 10). The highly conserved motifs ((D/E)R(Y/W), NPXXY, toggle switch, and disulfide bonds found in sequence alignments of the template GPCRs were helpful to generate CXCR2 models (Fig. 7,8,9). Using Cα RMSDs, structural alignments of seven transmembrane domains showed individual models tend to be similar to their templates (Fig, 11). Modeling results indicated that the crystal

structure of CXCR4 might be the best template for CXCR2 prediction due to the relatively high identity (33.3% identity for CXCR4) in sequence alignments and the lowest RMSD values (0.78Å). Site Finder was used to predict ligand binding sites of b2AR-CXCR2 and CXCR4 (Fig. 12). The prediction suggests that residues in all the extracellular loops are highly associated with ligand binding. Residues in some of the transmembranes domains showed involvement in ligand binding as well. The second extracellular loop of the CXCR4-based homology modeled CXCR2 provided two β-strands like rhodopsin and CXCR4 and the prediction is very similar with results of the predictions from two web-based prediction programs, NPS@SOPMA and NetSurfP (Fig. 13). Superimposition of the second extracellular loops of CXCR4 and CXCR4-based CXCR2 suggested that the second extracellular loop of CXCR2 is structurally very similar with that of CXCR4 with below 2.0 Å RMSD.

Furthermore, we studied solvent accessibility of residues in the second extracellular loop of CXCR2, a key region for ligand binding and receptor activation, in the inactive state of the receptor. MTSEA-biotin accessibility of substituted cysteine residues in the second extracellular loop was measured by immunostaining of FITC-streptavidin using flow cytometric analysis. The normalization of the accessibility was determined based on the cell surface expression level of the substituted cysteine mutant receptors (Fig. 14). Most of the residues in the second extracellular loop were found to be solvent accessible in the inactive state of CXCR2, indicating that the residues might be involved in ligand recognition. The results showed that all the charged residues except for

Arg208 in second extracellular loop also have solvent accessibility, pointing to possibility of ligand binding. However, ^{204}TANWR^{208} residues showed no solvent accessibility, suggesting that they might be involved in the interaction with the amino terminus or other extracellular loops. Our finding of ligand binding sites for CXCR2 models also suggests that the most of the residues in the region could form a ligand binding pocket to contact its cognate ligands.

Second, we studied the role of charged residues in EC2 of CXCR2 in ligand binding and receptor activation. Using constitutively active CXCR2 mutants, D9K and D9R, a potential role of charged residues in the second extracellular loop of CXCR2 was investigated.

Combinatorial mutations consisting of the constitutively active mutants in the amino terminus and single mutations of charged residues in the second extracellular loop were generated to study two concepts including “attraction” and “repulsion” model (Fig. 15). The mutant receptors were used to test their effects on cell surface expression, ligand binding, receptor activation through PLC-β3, and cellular transformation. All of the mutations in the repulsion model result in CXCR2 receptors that are unable to bind ligand, suggesting that all the Arg residues (Arg184, Arg185, Arg208, and Arg212) in the second extracellular loop are important for ligand recognition. Although charge-reversal complementary mutations in the repulsion model were expected to retain structural constraints of CXCR2, none of the mutant receptors function as wild-type CXCR2 in the inactive and active state (Fig. 16, 17). Interestingly, mutations in the attraction model partially inhibited receptor activation of constitutively active mutant D9K,

suggesting that Glu198 and Asp199 residues in the second extracellular loop are associated with receptor activation (Fig. 16, 18). Furthermore, a novel constitutively active mutant, E198A/D199A, was identified in this study (Fig. 16, 18). These negatively charged residues are very close to a disulfide bond (Cys119-Cys196) linking the second extracellular loop and the third transmembrane.

In Part II, the discoveries about the structural basis of CXCR2 and interdisciplinary approaches would provide new insights to investigate unknown mechanisms of interaction with its cognate ligands and receptor activation. These observations in Part III suggest the interaction between the amino terminus and EC2 of CXCR2 for ligand binding and receptor activation. Although crystallization studies of the amino terminus are limited for homology modeling and dynamic simulation (e.g. ligand docking), several groups have resolved the structures of the amino terminus in GPCRs using NMR, indicating that this approach with NMR would be effective and accurate to understand unknown amino terminus structures (*138-140*). Furthermore, some biochemical approaches including disulfide cross-linking, disulfide trapping, and protein digestion, would be helpful to discover unknown mechanism of ligand binding and receptor activation in GPCRs including CXCR2 (*11, 139, 141, 142*).

REFERENCES

1. Fredriksson, R., Lagerstrom, M. C., Lundin, L. G., and Schioth, H. B. (2003) The G-protein-coupled receptors in the human genome form five main families. Phylogenetic analysis, paralogon groups, and fingerprints, *Mol Pharmacol 63*, 1256-1272.
2. Pierce, K. L., Premont, R. T., and Lefkowitz, R. J. (2002) Seven-transmembrane receptors, *Nat Rev Mol Cell Biol 3*, 639-650.
3. Insel, P. A., Tang, C. M., Hahntow, I., and Michel, M. C. (2007) Impact of GPCRs in clinical medicine: monogenic diseases, genetic variants and drug targets, *Biochim Biophys Acta 1768*, 994-1005.
4. Gether, U. (2000) Uncovering molecular mechanisms involved in activation of G protein-coupled receptors, *Endocr Rev 21*, 90-113.
5. Tsao, P., Cao, T., and von Zastrow, M. (2001) Role of endocytosis in mediating downregulation of G-protein-coupled receptors, *Trends Pharmacol Sci 22*, 91-96.
6. Kohout, T. A., and Lefkowitz, R. J. (2003) Regulation of G protein-coupled receptor kinases and arrestins during receptor desensitization, *Mol Pharmacol 63*, 9-18.
7. Rosenbaum, D. M., Rasmussen, S. G., and Kobilka, B. K. (2009) The structure and function of G-protein-coupled receptors, *Nature 459*, 356-363.
8. Wu, B., Chien, E. Y., Mol, C. D., Fenalti, G., Liu, W., Katritch, V., Abagyan, R., Brooun, A., Wells, P., Bi, F. C., Hamel, D. J., Kuhn, P., Handel, T. M., Cherezov, V., and Stevens, R. C. (2010) Structures of the CXCR4 Chemokine GPCR with Small-Molecule and Cyclic Peptide Antagonists, *Science*.
9. Hauser, M., Kauffman, S., Lee, B. K., Naider, F., and Becker, J. M. (2007) The first extracellular loop of the Saccharomyces cerevisiae G protein-coupled receptor Ste2p undergoes a conformational change upon ligand binding, *J Biol Chem 282*, 10387-10397.
10. Day, P. W., Rasmussen, S. G., Parnot, C., Fung, J. J., Masood, A., Kobilka, T. S., Yao, X. J., Choi, H. J., Weis, W. I., Rohrer, D. K., and Kobilka, B. K. (2007) A monoclonal antibody for G protein-coupled receptor crystallography, *Nat Methods 4*, 927-929.
11. Wess, J., Han, S. J., Kim, S. K., Jacobson, K. A., and Li, J. H. (2008) Conformational changes involved in G-protein-coupled-receptor activation, *Trends Pharmacol Sci 29*, 616-625.
12. George, S. R., O'Dowd, B. F., and Lee, S. P. (2002) G-protein-coupled receptor oligomerization and its potential for drug discovery, *Nat Rev Drug Discov 1*, 808-820.
13. Palczewski, K., Kumasaka, T., Hori, T., Behnke, C. A., Motoshima, H., Fox, B. A., Le Trong, I., Teller, D. C., Okada, T., Stenkamp, R. E., Yamamoto, M., and Miyano, M. (2000) Crystal structure of rhodopsin: A G protein-coupled receptor, *Science 289*, 739-745.

14. Lodowski, D. T., and Palczewski, K. (2009) Chemokine receptors and other G protein-coupled receptors, *Curr Opin HIV AIDS 4*, 88-95.
15. Ludeke, S., Mahalingam, M., and Vogel, R. (2009) Rhodopsin activation switches in a native membrane environment, *Photochem Photobiol 85*, 437-441.
16. Neumann, J. M., Couvineau, A., Murail, S., Lacapere, J. J., Jamin, N., and Laburthe, M. (2008) Class-B GPCR activation: is ligand helix-capping the key?, *Trends Biochem Sci 33*, 314-319.
17. Kunishima, N., Shimada, Y., Tsuji, Y., Sato, T., Yamamoto, M., Kumasaka, T., Nakanishi, S., Jingami, H., and Morikawa, K. (2000) Structural basis of glutamate recognition by a dimeric metabotropic glutamate receptor, *Nature 407*, 971-977.
18. Klabunde, T., and Hessler, G. (2002) Drug design strategies for targeting G-protein-coupled receptors, *Chembiochem 3*, 928-944.
19. Pebay-Peyroula, E., Rummel, G., Rosenbusch, J. P., and Landau, E. M. (1997) X-ray structure of bacteriorhodopsin at 2.5 angstroms from microcrystals grown in lipidic cubic phases, *Science 277*, 1676-1681.
20. Arshava, B., Taran, I., Xie, H., Becker, J. M., and Naider, F. (2002) High resolution NMR analysis of the seven transmembrane domains of a heptahelical receptor in organic-aqueous medium, *Biopolymers 64*, 161-176.
21. Unger, V. M., and Schertler, G. F. (1995) Low resolution structure of bovine rhodopsin determined by electron cryo-microscopy, *Biophys J 68*, 1776-1786.
22. Cherezov, V., Rosenbaum, D. M., Hanson, M. A., Rasmussen, S. G., Thian, F. S., Kobilka, T. S., Choi, H. J., Kuhn, P., Weis, W. I., Kobilka, B. K., and Stevens, R. C. (2007) High-resolution crystal structure of an engineered human beta2-adrenergic G protein-coupled receptor, *Science 318*, 1258-1265.
23. Rosenbaum, D. M., Cherezov, V., Hanson, M. A., Rasmussen, S. G., Thian, F. S., Kobilka, T. S., Choi, H. J., Yao, X. J., Weis, W. I., Stevens, R. C., and Kobilka, B. K. (2007) GPCR engineering yields high-resolution structural insights into beta2-adrenergic receptor function, *Science 318*, 1266-1273.
24. Warne, T., Serrano-Vega, M. J., Baker, J. G., Moukhametzianov, R., Edwards, P. C., Henderson, R., Leslie, A. G., Tate, C. G., and Schertler, G. F. (2008) Structure of a beta1-adrenergic G-protein-coupled receptor, *Nature 454*, 486-491.
25. Park, J. H., Scheerer, P., Hofmann, K. P., Choe, H. W., and Ernst, O. P. (2008) Crystal structure of the ligand-free G-protein-coupled receptor opsin, *Nature 454*, 183-187.
26. Jaakola, V. P., Griffith, M. T., Hanson, M. A., Cherezov, V., Chien, E. Y., Lane, J. R., Ijzerman, A. P., and Stevens, R. C. (2008) The 2.6 angstrom crystal structure of a human A2A adenosine receptor bound to an antagonist, *Science 322*, 1211-1217.
27. Teller, D. C., Okada, T., Behnke, C. A., Palczewski, K., and Stenkamp, R. E. (2001) Advances in determination of a high-resolution three-dimensional structure of rhodopsin, a model of G-protein-coupled receptors (GPCRs), *Biochemistry 40*, 7761-7772.

28. Sansom, M. S., and Weinstein, H. (2000) Hinges, swivels and switches: the role of prolines in signalling via transmembrane alpha-helices, *Trends Pharmacol Sci 21*, 445-451.
29. Shi, L., Liapakis, G., Xu, R., Guarnieri, F., Ballesteros, J. A., and Javitch, J. A. (2002) Beta2 adrenergic receptor activation. Modulation of the proline kink in transmembrane 6 by a rotamer toggle switch, *J Biol Chem 277*, 40989-40996.
30. Altenbach, C., Kusnetzow, A. K., Ernst, O. P., Hofmann, K. P., and Hubbell, W. L. (2008) High-resolution distance mapping in rhodopsin reveals the pattern of helix movement due to activation, *Proc Natl Acad Sci U S A 105*, 7439-7444.
31. Horn, F., Vriend, G., and Cohen, F. E. (2001) Collecting and harvesting biological data: the GPCRDB and NucleaRDB information systems, *Nucleic Acids Res 29*, 346-349.
32. Filipek, S., Teller, D. C., Palczewski, K., and Stenkamp, R. (2003) The crystallographic model of rhodopsin and its use in studies of other G protein-coupled receptors, *Annu Rev Biophys Biomol Struct 32*, 375-397.
33. Palczewski, K. (2006) G protein-coupled receptor rhodopsin, *Annu Rev Biochem 75*, 743-767.
34. Kaushal, S., Ridge, K. D., and Khorana, H. G. (1994) Structure and function in rhodopsin: the role of asparagine-linked glycosylation, *Proc Natl Acad Sci U S A 91*, 4024-4028.
35. Murray, A. R., Fliesler, S. J., and Al-Ubaidi, M. R. (2009) Rhodopsin: the functional significance of asn-linked glycosylation and other post-translational modifications, *Ophthalmic Genet 30*, 109-120.
36. Klco, J. M., Wiegand, C. B., Narzinski, K., and Baranski, T. J. (2005) Essential role for the second extracellular loop in C5a receptor activation, *Nat Struct Mol Biol 12*, 320-326.
37. Massotte, D., and Kieffer, B. L. (2005) The second extracellular loop: a damper for G protein-coupled receptors?, *Nat Struct Mol Biol 12*, 287-288.
38. Audet, M., and Bouvier, M. (2008) Insights into signaling from the beta2-adrenergic receptor structure, *Nat Chem Biol 4*, 397-403.
39. Ballesteros, J. A., Jensen, A. D., Liapakis, G., Rasmussen, S. G., Shi, L., Gether, U., and Javitch, J. A. (2001) Activation of the beta 2-adrenergic receptor involves disruption of an ionic lock between the cytoplasmic ends of transmembrane segments 3 and 6, *J Biol Chem 276*, 29171-29177.
40. Hanson, M. A., Cherezov, V., Griffith, M. T., Roth, C. B., Jaakola, V. P., Chien, E. Y., Velasquez, J., Kuhn, P., and Stevens, R. C. (2008) A specific cholesterol binding site is established by the 2.8 A structure of the human beta2-adrenergic receptor, *Structure 16*, 897-905.
41. Zhang, Y., Devries, M. E., and Skolnick, J. (2006) Structure modeling of all identified G protein-coupled receptors in the human genome, *PLoS Comput Biol 2*, e13.
42. Costanzi, S. (2008) On the applicability of GPCR homology models to computer-aided drug discovery: a comparison between in silico and crystal structures of the beta2-adrenergic receptor, *J Med Chem 51*, 2907-2914.

43. Mirzadegan, T., Benko, G., Filipek, S., and Palczewski, K. (2003) Sequence analyses of G-protein-coupled receptors: similarities to rhodopsin, *Biochemistry 42*, 2759-2767.
44. Mobarec, J. C., Sanchez, R., and Filizola, M. (2009) Modern homology modeling of G-protein coupled receptors: which structural template to use?, *J Med Chem 52*, 5207-5216.
45. Kristiansen, K. (2004) Molecular mechanisms of ligand binding, signaling, and regulation within the superfamily of G-protein-coupled receptors: molecular modeling and mutagenesis approaches to receptor structure and function, *Pharmacol Ther 103*, 21-80.
46. Vaidehi, N., Floriano, W. B., Trabanino, R., Hall, S. E., Freddolino, P., Choi, E. J., Zamanakos, G., and Goddard, W. A., 3rd. (2002) Prediction of structure and function of G protein-coupled receptors, *Proc Natl Acad Sci U S A 99*, 12622-12627.
47. Eglen, R. M., and Reisine, T. (2009) New insights into GPCR function: implications for HTS, *Methods Mol Biol 552*, 1-13.
48. Hall, D. A. (2000) Modeling the functional effects of allosteric modulators at pharmacological receptors: an extension of the two-state model of receptor activation, *Mol Pharmacol 58*, 1412-1423.
49. Kobilka, B. (2004) Agonist binding: a multistep process, *Mol Pharmacol 65*, 1060-1062.
50. Schwartz, T. W., Frimurer, T. M., Holst, B., Rosenkilde, M. M., and Elling, C. E. (2006) Molecular mechanism of 7TM receptor activation--a global toggle switch model, *Annu Rev Pharmacol Toxicol 46*, 481-519.
51. Hu, J., Wang, Y., Zhang, X., Lloyd, J. R., Li, J. H., Karpiak, J., Costanzi, S., and Wess, J. (2010) Structural basis of G protein-coupled receptor-G protein interactions, *Nat Chem Biol 6*, 541-548.
52. Liang, W., Hoang, Q., Clark, R. B., and Fishman, P. H. (2008) Accelerated dephosphorylation of the beta2-adrenergic receptor by mutation of the C-terminal lysines: effects on ubiquitination, intracellular trafficking, and degradation, *Biochemistry 47*, 11750-11762.
53. Dorsam, R. T., and Gutkind, J. S. (2007) G-protein-coupled receptors and cancer, *Nat Rev Cancer 7*, 79-94.
54. Oldham, W. M., and Hamm, H. E. (2008) Heterotrimeric G protein activation by G-protein-coupled receptors, *Nat Rev Mol Cell Biol 9*, 60-71.
55. Hermans, E. (2003) Biochemical and pharmacological control of the multiplicity of coupling at G-protein-coupled receptors, *Pharmacol Ther 99*, 25-44.
56. Wong, S. K. (2003) G protein selectivity is regulated by multiple intracellular regions of GPCRs, *Neurosignals 12*, 1-12.
57. Rebecchi, M. J., and Pentyala, S. N. (2000) Structure, function, and control of phosphoinositide-specific phospholipase C, *Physiol Rev 80*, 1291-1335.
58. Strathmann, M. P., and Simon, M. I. (1991) G alpha 12 and G alpha 13 subunits define a fourth class of G protein alpha subunits, *Proc Natl Acad Sci U S A 88*, 5582-5586.

59. Dhanasekaran, N., and Dermott, J. M. (1996) Signaling by the G12 class of G proteins, *Cell Signal 8*, 235-245.
60. Clapham, D. E., and Neer, E. J. (1997) G protein beta gamma subunits, *Annu Rev Pharmacol Toxicol 37*, 167-203.
61. Schwindinger, W. F., and Robishaw, J. D. (2001) Heterotrimeric G-protein betagamma-dimers in growth and differentiation, *Oncogene 20*, 1653-1660.
62. Pitcher, J. A., Hall, R. A., Daaka, Y., Zhang, J., Ferguson, S. S., Hester, S., Miller, S., Caron, M. G., Lefkowitz, R. J., and Barak, L. S. (1998) The G protein-coupled receptor kinase 2 is a microtubule-associated protein kinase that phosphorylates tubulin, *J Biol Chem 273*, 12316-12324.
63. Ferguson, S. S. (2001) Evolving concepts in G protein-coupled receptor endocytosis: the role in receptor desensitization and signaling, *Pharmacol Rev 53*, 1-24.
64. Ross, E. M., and Wilkie, T. M. (2000) GTPase-activating proteins for heterotrimeric G proteins: regulators of G protein signaling (RGS) and RGS-like proteins, *Annu Rev Biochem 69*, 795-827.
65. Miller, W. E., and Lefkowitz, R. J. (2001) Expanding roles for beta-arrestins as scaffolds and adapters in GPCR signaling and trafficking, *Curr Opin Cell Biol 13*, 139-145.
66. Perry, S. J., Baillie, G. S., Kohout, T. A., McPhee, I., Magiera, M. M., Ang, K. L., Miller, W. E., McLean, A. J., Conti, M., Houslay, M. D., and Lefkowitz, R. J. (2002) Targeting of cyclic AMP degradation to beta 2-adrenergic receptors by beta-arrestins, *Science 298*, 834-836.
67. Baggiolini, M. (1998) Chemokines and leukocyte traffic, *Nature 392*, 565-568.
68. Rossi, D., and Zlotnik, A. (2000) The biology of chemokines and their receptors, *Annu Rev Immunol 18*, 217-242.
69. Locati, M., and Murphy, P. M. (1999) Chemokines and chemokine receptors: biology and clinical relevance in inflammation and AIDS, *Annu Rev Med 50*, 425-440.
70. Strieter, R. M., Polverini, P. J., Kunkel, S. L., Arenberg, D. A., Burdick, M. D., Kasper, J., Dzuiba, J., Van Damme, J., Walz, A., Marriott, D., and et al. (1995) The functional role of the ELR motif in CXC chemokine-mediated angiogenesis, *J Biol Chem 270*, 27348-27357.
71. Phillips, R. J., Burdick, M. D., Lutz, M., Belperio, J. A., Keane, M. P., and Strieter, R. M. (2003) The stromal derived factor-1/CXCL12-CXC chemokine receptor 4 biological axis in non-small cell lung cancer metastases, *Am J Respir Crit Care Med 167*, 1676-1686.
72. Holmes, W. E., Lee, J., Kuang, W. J., Rice, G. C., and Wood, W. I. (1991) Structure and functional expression of a human interleukin-8 receptor, *Science 253*, 1278-1280.
73. Murphy, P. M., and Tiffany, H. L. (1991) Cloning of complementary DNA encoding a functional human interleukin-8 receptor, *Science 253*, 1280-1283.
74. Murphy, P. M. (2002) International Union of Pharmacology. XXX. Update on chemokine receptor nomenclature, *Pharmacol Rev 54*, 227-229.

75. (2001) Chemokine/chemokine receptor nomenclature, *J Leukoc Biol 70*, 465-466.
76. Zlotnik, A., Yoshie, O., and Nomiyama, H. (2006) The chemokine and chemokine receptor superfamilies and their molecular evolution, *Genome Biol 7*, 243.
77. Rot, A., and von Andrian, U. H. (2004) Chemokines in innate and adaptive host defense: basic chemokinese grammar for immune cells, *Annu Rev Immunol 22*, 891-928.
78. Addison, C. L., Daniel, T. O., Burdick, M. D., Liu, H., Ehlert, J. E., Xue, Y. Y., Buechi, L., Walz, A., Richmond, A., and Strieter, R. M. (2000) The CXC chemokine receptor 2, CXCR2, is the putative receptor for ELR+ CXC chemokine-induced angiogenic activity, *J Immunol 165*, 5269-5277.
79. Strieter, R. M., Gomperts, B. N., and Keane, M. P. (2007) The role of CXC chemokines in pulmonary fibrosis, *J Clin Invest 117*, 549-556.
80. Murphy, P. M. (1994) The molecular biology of leukocyte chemoattractant receptors, *Annu Rev Immunol 12*, 593-633.
81. Ben-Baruch, A., Bengali, K. M., Biragyn, A., Johnston, J. J., Wang, J. M., Kim, J., Chuntharapai, A., Michiel, D. F., Oppenheim, J. J., and Kelvin, D. J. (1995) Interleukin-8 receptor beta. The role of the carboxyl terminus in signal transduction, *J Biol Chem 270*, 9121-9128.
82. Catusse, J., Faye, P., Loillier, B., Cremers, B., Franck, R. M., Luccarini, J. M., Pruneau, D., and Paquet, J. L. (2003) Cloning and characterization of guinea pig interleukin-8 receptor, *Biochem Pharmacol 66*, 1171-1180.
83. Ahuja, S. K., Lee, J. C., and Murphy, P. M. (1996) CXC chemokines bind to unique sets of selectivity determinants that can function independently and are broadly distributed on multiple domains of human interleukin-8 receptor B. Determinants of high affinity binding and receptor activation are distinct, *J Biol Chem 271*, 225-232.
84. Nasser, M. W., Raghuwanshi, S. K., Malloy, K. M., Gangavarapu, P., Shim, J. Y., Rajarathnam, K., and Richardson, R. M. (2007) CXCR1 and CXCR2 activation and regulation. Role of aspartate 199 of the second extracellular loop of CXCR2 in CXCL8-mediated rapid receptor internalization, *J Biol Chem 282*, 6906-6915.
85. Katancik, J. A., Sharma, A., Radel, S. J., and De Nardin, E. (1997) Mapping of the extracellular binding regions of the human interleukin-8 type B receptor, *Biochem Biophys Res Commun 232*, 663-668.
86. Katancik, J. A., Sharma, A., and de Nardin, E. (2000) Interleukin 8, neutrophil-activating peptide-2 and GRO-alpha bind to and elicit cell activation via specific and different amino acid residues of CXCR2, *Cytokine 12*, 1480-1488.
87. Catusse, J., Liotard, A., Loillier, B., Pruneau, D., and Paquet, J. L. (2003) Characterization of the molecular interactions of interleukin-8 (CXCL8), growth related oncogen alpha (CXCL1) and a non-peptide antagonist (SB 225002) with the human CXCR2, *Biochem Pharmacol 65*, 813-821.

88. Houimel, M., and Mazzucchelli, L. (2009) Identification of biologically active peptides that inhibit binding of human CXCL8 to its receptors from a random phage-epitope library, *J Leukoc Biol 85*, 728-738.
89. Limatola, C., Di Bartolomeo, S., Catalano, M., Trettel, F., Fucile, S., Castellani, L., and Eusebi, F. (2005) Cysteine residues are critical for chemokine receptor CXCR2 functional properties, *Exp Cell Res 307*, 65-75.
90. Suzuki, H., Prado, G. N., Wilkinson, N., and Navarro, J. (1994) The N terminus of interleukin-8 (IL-8) receptor confers high affinity binding to human IL-8, *J Biol Chem 269*, 18263-18266.
91. Schraufstatter, I. U., Ma, M., Oades, Z. G., Barritt, D. S., and Cochrane, C. G. (1995) The role of Tyr13 and Lys15 of interleukin-8 in the high affinity interaction with the interleukin-8 receptor type A, *J Biol Chem 270*, 10428-10431.
92. Li, F., and Gordon, J. R. (2001) Il-8((3-73))K11R is a high affinity agonist of the neutrophil CXCR1 and CXCR2, *Biochem Biophys Res Commun 286*, 595-600.
93. Li, F., Zhang, X., and Gordon, J. R. (2002) CXCL8((3-73))K11R/G31P antagonizes ligand binding to the neutrophil CXCR1 and CXCR2 receptors and cellular responses to CXCL8/IL-8, *Biochem Biophys Res Commun 293*, 939-944.
94. Zhao, X., Li, F., Town, J. R., Zhang, X., Wang, W., and Gordon, J. R. (2007) Humanized forms of the CXCR1/CXCR2 antagonist, bovine CXCL8((3-74))K11R/G31P, effectively block ELR-CXC chemokine activity and airway endotoxemia pathology, *Int Immunopharmacol 7*, 1723-1731.
95. Ludwig, A., Ehlert, J. E., Flad, H. D., and Brandt, E. (2000) Identification of distinct surface-expressed and intracellular CXC-chemokine receptor 2 glycoforms in neutrophils: N-glycosylation is essential for maintenance of receptor surface expression, *J Immunol 165*, 1044-1052.
96. Miller, L. J., Kurtzman, S. H., Wang, Y., Anderson, K. H., Lindquist, R. R., and Kreutzer, D. L. (1998) Expression of interleukin-8 receptors on tumor cells and vascular endothelial cells in human breast cancer tissue, *Anticancer Res 18*, 77-81.
97. Richards, B. L., Eisma, R. J., Spiro, J. D., Lindquist, R. L., and Kreutzer, D. L. (1997) Coexpression of interleukin-8 receptors in head and neck squamous cell carcinoma, *Am J Surg 174*, 507-512.
98. Norgauer, J., Metzner, B., and Schraufstatter, I. (1996) Expression and growth-promoting function of the IL-8 receptor beta in human melanoma cells, *J Immunol 156*, 1132-1137.
99. Takamori, H., Oades, Z. G., Hoch, O. C., Burger, M., and Schraufstatter, I. U. (2000) Autocrine growth effect of IL-8 and GROalpha on a human pancreatic cancer cell line, Capan-1, *Pancreas 21*, 52-56.
100. Venkatakrishnan, G., Salgia, R., and Groopman, J. E. (2000) Chemokine receptors CXCR-1/2 activate mitogen-activated protein kinase via the epidermal growth factor receptor in ovarian cancer cells, *J Biol Chem 275*, 6868-6875.

101. Waugh, D. J., and Wilson, C. (2008) The interleukin-8 pathway in cancer, *Clin Cancer Res 14*, 6735-6741.
102. Nicholls, D. J., Tomkinson, N. P., Wiley, K. E., Brammall, A., Bowers, L., Grahames, C., Gaw, A., Meghani, P., Shelton, P., Wright, T. J., and Mallinder, P. R. (2008) Identification of a putative intracellular allosteric antagonist binding-site in the CXC chemokine receptors 1 and 2, *Mol Pharmacol 74*, 1193-1202.
103. Arvanitakis, L., Geras-Raaka, E., Varma, A., Gershengorn, M. C., and Cesarman, E. (1997) Human herpesvirus KSHV encodes a constitutively active G-protein-coupled receptor linked to cell proliferation, *Nature 385*, 347-350.
104. Couty, J. P., Geras-Raaka, E., Weksler, B. B., and Gershengorn, M. C. (2001) Kaposi's sarcoma-associated herpesvirus G protein-coupled receptor signals through multiple pathways in endothelial cells, *J Biol Chem 276*, 33805-33811.
105. Montaner, S., Sodhi, A., Pece, S., Mesri, E. A., and Gutkind, J. S. (2001) The Kaposi's sarcoma-associated herpesvirus G protein-coupled receptor promotes endothelial cell survival through the activation of Akt/protein kinase B, *Cancer Res 61*, 2641-2648.
106. Smit, M. J., Verzijl, D., Casarosa, P., Navis, M., Timmerman, H., and Leurs, R. (2002) Kaposi's sarcoma-associated herpesvirus-encoded G protein-coupled receptor ORF74 constitutively activates p44/p42 MAPK and Akt via G(i) and phospholipase C-dependent signaling pathways, *J Virol 76*, 1744-1752.
107. Cannon, M. L., and Cesarman, E. (2004) The KSHV G protein-coupled receptor signals via multiple pathways to induce transcription factor activation in primary effusion lymphoma cells, *Oncogene 23*, 514-523.
108. Casarosa, P., Bakker, R. A., Verzijl, D., Navis, M., Timmerman, H., Leurs, R., and Smit, M. J. (2001) Constitutive signaling of the human cytomegalovirus-encoded chemokine receptor US28, *J Biol Chem 276*, 1133-1137.
109. McLean, K. A., Holst, P. J., Martini, L., Schwartz, T. W., and Rosenkilde, M. M. (2004) Similar activation of signal transduction pathways by the herpesvirus-encoded chemokine receptors US28 and ORF74, *Virology 325*, 241-251.
110. Sherrill, J. D., and Miller, W. E. (2006) G protein-coupled receptor (GPCR) kinase 2 regulates agonist-independent Gq/11 signaling from the mouse cytomegalovirus GPCR M33, *J Biol Chem 281*, 39796-39805.
111. Stropes, M. P., and Miller, W. E. (2008) Functional analysis of human cytomegalovirus pUS28 mutants in infected cells, *J Gen Virol 89*, 97-105.
112. Sherrill, J. D., Stropes, M. P., Schneider, O. D., Koch, D. E., Bittencourt, F. M., Miller, J. L., and Miller, W. E. (2009) Activation of intracellular signaling pathways by the murine cytomegalovirus G protein-coupled receptor M33 occurs via PLC-{beta}/PKC-dependent and -independent mechanisms, *J Virol 83*, 8141-8152.

113. Casarosa, P., Gruijthuijsen, Y. K., Michel, D., Beisser, P. S., Holl, J., Fitzsimons, C. P., Verzijl, D., Bruggeman, C. A., Mertens, T., Leurs, R., Vink, C., and Smit, M. J. (2003) Constitutive signaling of the human cytomegalovirus-encoded receptor UL33 differs from that of its rat cytomegalovirus homolog R33 by promiscuous activation of G proteins of the Gq, Gi, and Gs classes, *J Biol Chem 278*, 50010-50023.
114. Wu, D., LaRosa, G. J., and Simon, M. I. (1993) G protein-coupled signal transduction pathways for interleukin-8, *Science 261*, 101-103.
115. Fromm, C., Coso, O. A., Montaner, S., Xu, N., and Gutkind, J. S. (1997) The small GTP-binding protein Rho links G protein-coupled receptors and Galpha12 to the serum response element and to cellular transformation, *Proc Natl Acad Sci U S A 94*, 10098-10103.
116. Schraufstatter, I. U., Chung, J., and Burger, M. (2001) IL-8 activates endothelial cell CXCR1 and CXCR2 through Rho and Rac signaling pathways, *Am J Physiol Lung Cell Mol Physiol 280*, L1094-1103.
117. Neel, N. F., Barzik, M., Raman, D., Sobolik-Delmaire, T., Sai, J., Ham, A. J., Mernaugh, R. L., Gertler, F. B., and Richmond, A. (2009) VASP is a CXCR2-interacting protein that regulates CXCR2-mediated polarization and chemotaxis, *J Cell Sci 122*, 1882-1894.
118. Burger, M., Burger, J. A., Hoch, R. C., Oades, Z., Takamori, H., and Schraufstatter, I. U. (1999) Point mutation causing constitutive signaling of CXCR2 leads to transforming activity similar to Kaposi's sarcoma herpesvirus-G protein-coupled receptor, *J Immunol 163*, 2017-2022.
119. Burger, M., Hartmann, T., Burger, J. A., and Schraufstatter, I. (2005) KSHV-GPCR and CXCR2 transforming capacity and angiogenic responses are mediated through a JAK2-STAT3-dependent pathway, *Oncogene 24*, 2067-2075.
120. Sai, J., Fan, G. H., Wang, D., and Richmond, A. (2004) The C-terminal domain LLKIL motif of CXCR2 is required for ligand-mediated polarization of early signals during chemotaxis, *J Cell Sci 117*, 5489-5496.
121. Yang, G., Rosen, D. G., Liu, G., Yang, F., Guo, X., Xiao, X., Xue, F., Mercado-Uribe, I., Huang, J., Lin, S. H., Mills, G. B., and Liu, J. (2010) CXCR2 promotes ovarian cancer growth through dysregulated cell cycle, diminished apoptosis, and enhanced angiogenesis, *Clin Cancer Res 16*, 3875-3886.
122. Bolitho, C., Hahn, M. A., Baxter, R. C., and Marsh, D. J. (2010) The chemokine CXCL1 induces proliferation in epithelial ovarian cancer cells by transactivation of the epidermal growth factor receptor, *Endocr Relat Cancer 17*, 929-940.
123. Murphy, P. M., Baggiolini, M., Charo, I. F., Hebert, C. A., Horuk, R., Matsushima, K., Miller, L. H., Oppenheim, J. J., and Power, C. A. (2000) International union of pharmacology. XXII. Nomenclature for chemokine receptors, *Pharmacol Rev 52*, 145-176.
124. Prado, G. N., Suetomi, K., Shumate, D., Maxwell, C., Ravindran, A., Rajarathnam, K., and Navarro, J. (2007) Chemokine signaling specificity: essential role for the N-terminal domain of chemokine receptors, *Biochemistry 46*, 8961-8968.

125. Ahuja, S., Crocker, E., Eilers, M., Hornak, V., Hirshfeld, A., Ziliox, M., Syrett, N., Reeves, P. J., Khorana, H. G., Sheves, M., and Smith, S. O. (2009) Location of the retinal chromophore in the activated state of rhodopsin*, *J Biol Chem 284*, 10190-10201.
126. Holst, B., and Schwartz, T. W. (2003) Molecular mechanism of agonism and inverse agonism in the melanocortin receptors: Zn(2+) as a structural and functional probe, *Ann N Y Acad Sci 994*, 1-11.
127. Scarselli, M., Li, B., Kim, S. K., and Wess, J. (2007) Multiple residues in the second extracellular loop are critical for M3 muscarinic acetylcholine receptor activation, *J Biol Chem 282*, 7385-7396.
128. Geourjon, C., and Deleage, G. (1995) SOPMA: significant improvements in protein secondary structure prediction by consensus prediction from multiple alignments, *Comput Appl Biosci 11*, 681-684.
129. Petersen, B., Petersen, T. N., Andersen, P., Nielsen, M., and Lundegaard, C. (2009) A generic method for assignment of reliability scores applied to solvent accessibility predictions, *BMC Struct Biol 9*, 51.
130. Unal, H., Jagannathan, R., Bhat, M. B., and Karnik, S. S. (2010) Ligand-specific conformation of extracellular loop-2 in the angiotensin II type 1 receptor, *J Biol Chem 285*, 16341-16350.
131. Seifert, R., and Wenzel-Seifert, K. (2002) Constitutive activity of G-protein-coupled receptors: cause of disease and common property of wild-type receptors, *Naunyn Schmiedebergs Arch Pharmacol 366*, 381-416.
132. Smit, M. J., Vischer, H. F., Bakker, R. A., Jongejan, A., Timmerman, H., Pardo, L., and Leurs, R. (2007) Pharmacogenomic and structural analysis of constitutive g protein-coupled receptor activity, *Annu Rev Pharmacol Toxicol 47*, 53-87.
133. Rovati, G. E., Capra, V., and Neubig, R. R. (2007) The highly conserved DRY motif of class A G protein-coupled receptors: beyond the ground state, *Mol Pharmacol 71*, 959-964.
134. Sum, C. S., Tikhonova, I. G., Costanzi, S., and Gershengorn, M. C. (2009) Two arginine-glutamate ionic locks near the extracellular surface of FFAR1 gate receptor activation, *J Biol Chem 284*, 3529-3536.
135. Rana, S., and Baranski, T. J. (2010) Third extracellular loop (EC3)-N terminus interaction is important for seven-transmembrane domain receptor function: implications for an activation microswitch region, *J Biol Chem 285*, 31472-31483.
136. Bakker, R. A., Casarosa, P., Timmerman, H., Smit, M. J., and Leurs, R. (2004) Constitutively active Gq/11-coupled receptors enable signaling by co-expressed G(i/o)-coupled receptors, *J Biol Chem 279*, 5152-5161.
137. Hawtin, S. R., Simms, J., Conner, M., Lawson, Z., Parslow, R. A., Trim, J., Sheppard, A., and Wheatley, M. (2006) Charged extracellular residues, conserved throughout a G-protein-coupled receptor family, are required for ligand binding, receptor activation, and cell-surface expression, *J Biol Chem 281*, 38478-38488.

138. Pellegrini, M., and Mierke, D. F. (1999) Molecular complex of cholecystokinin-8 and N-terminus of the cholecystokinin A receptor by NMR spectroscopy, *Biochemistry 38*, 14775-14783.
139. Veldkamp, C. T., Seibert, C., Peterson, F. C., De la Cruz, N. B., Haugner, J. C., 3rd, Basnet, H., Sakmar, T. P., and Volkman, B. F. (2008) Structural basis of CXCR4 sulfotyrosine recognition by the chemokine SDF-1/CXCL12, *Sci Signal 1*, ra4.
140. Tikhonova, I. G., and Costanzi, S. (2009) Unraveling the structure and function of G protein-coupled receptors through NMR spectroscopy, *Curr Pharm Des 15*, 4003-4016.
141. Buck, E., and Wells, J. A. (2005) Disulfide trapping to localize small-molecule agonists and antagonists for a G protein-coupled receptor, *Proc Natl Acad Sci U S A 102*, 2719-2724.
142. Umanah, G. K., Son, C., Ding, F., Naider, F., and Becker, J. M. (2009) Cross-linking of a DOPA-containing peptide ligand into its G protein-coupled receptor, *Biochemistry 48*, 2033-2044.

VITA

Hae Ryong Kwon was born in January 30, 1981 in South Korea. He attended the Chungbuk National University in Cheongju, South Korea where he received the degree of Bachelor of Science in Life Sciences (concentration: Microbiology) in February 2003. Afterwards, he continued his master studies at the same university where he received the degree of Master of Science in Microbiology in February 2005. In August 2007, Hae Ryong started his Master's degree of Life Sciences (concentration: the Genome Science and Technology) at the University of Tennessee, Knoxville. Upon completion of his studies, his diploma (Master of Science in Life Sciences) was awarded in December 2010.